Defining influences on packaging and reassortment of the segmented reovirus genome

By

Timothy Wade Thoner Jr.

Dissertation

Submitted to the Faculty of the

Graduate School of Vanderbilt University

in partial fulfillment of the requirements

for the degree of

DOCTOR OF PHILOSOPHY

in

Microbe-Host Interactions

December 17th, 2022

Nashville, Tennessee

Approved:

John Karijolich, PhD (Chair)

Mark R. Denison, MD

Irina N. Kaverina, PhD

Kristen M. Ogden, PhD

Ann T. Tate, PhD

To my family, without whom none of this is possible.

ACKNOWLEDGMENTS

The work in this dissertation would not have been possible without financial support from the National Institutes of Health (1R01AI155646), the Vanderbilt Institute for Clinical and Translational Research (UL1 TR002243), and the Vanderbilt Digestive Disease Research Consortium through National Institutes of Health grant P30DK058404.

To my mentor, Kristen Ogden, I am sincerely grateful. You entrusted me to assume the role of first graduate student in your lab, and it has been an incredible journey to grow alongside you. Even in your busiest moments, you always made time for me and other trainees, and I hope to emulate this as I grow in my career. If there is something I have learned under your mentorship, it is to take that extra step – to think a just a bit deeper, to go all out on that experiment, or to invest more time into that draft manuscript – to always put forward the best science possible. I owe so much of my scientific and professional success to your mentorship.

I consider myself incredibly fortunate to have had the opportunity to carry out my thesis work in a lab filled with bright and supportive friends and colleagues. Our scientific discussions are always exciting and have contributed innumerably to this work. Beyond that, though, the Ogden lab has provided me a source of sanity and camaraderie, even in what have been uniquely challenging times. I hope I can find a group half as supportive as the Ogden lab in the next stage of my career.

I would like to thank all members of my thesis Committee – Drs. Ann Tate, Irina Kaverina, John Karijolich, and Mark Denison. Your diverse and insightful scientific perspectives have contributed greatly to my success and growth as a scientist. I would also like to thank the members of the Karijolich lab for lending their experimental expertise to our collaborative work and the Denison lab for keen scientific discussions and for occasionally adopting us into their ranks. Many thanks also to Dr. Terence Dermody and the Dermody lab for providing valuable knowledge and resources to our collaborative efforts.

I also want to thank my family, those who have always been with me and those I have acquired. The path to a PhD is often described as a marathon. You instilled in me the perseverance to continue and reminded me of my purpose when I needed it most. No matter where my passions have taken me, you have always provided me with a constant source of encouragement and support.

Most importantly, I want to thank my loving and supportive wife, Katie, and my incredible son, Lincoln. It is an understatement to say that the journey to acquiring a PhD presents many challenges. Katie, through it all, you have been my biggest cheerleader. Whether you were making the leap to leave your family to follow me to Nashville, or were tagging along for weekend trips into the lab, you did whatever you could to make my dream a reality. When I published a paper, you were the loudest and proudest supporter. When experiments were failing or grants were falling through, you gave me a home to come back to. For all of this, I am forever grateful. Lincoln, you are, and will always be, my greatest accomplishment. You make every hard moment worth it.

TABLE OF CONTENTS

Page

LIST OF FIGURES

Figure **Page**

LIST OF TABLES

Table **Page**

CHAPTER 1

INTRODUCTION AND LITERATURE REVIEW

1.1. Reassortment is an important process that enhances genetic diversity and provides opportunity for novel functionality.

Viruses with multi-segmented genomes are unique in their capacity to readily exchange large amounts of genetic information via a process known as reassortment. Reassortment occurs when genome segments from multiple parent viruses are simultaneously packaged by a progeny virus, and reassortment events can have dramatic consequences, as reassortment has generated pandemic viruses, enabled zoonotic transmission events, and has led to the development of antiviral resistance (Simonsen et al., 2007). Live-attenuated vaccines have also been shown to occasionally reassort genome segments with circulating strains, sometimes leading to disease (Nomikou et al., 2015; Weyer et al., 2016; Donato et al., 2012). Exchange of genome segments encoding surface-exposed viral proteins can also generate antigenically-novel progeny capable of evading immune recognition (Kim, Webster, and Webby, 2018). While reassortment occurs frequently in nature, it does require coordination of various complex processes. For instance, two viruses must replicate within the same host cell at the same time to undergo reassortment. Beyond this, many multi-segmented genomes utilize highly coordinated packaging strategies that necessitate a significant amount of genetic conservation. For coinfecting viruses to exchange genome segments, then, both viruses must be similar enough for genome segments from both viruses to be recognized for packaging into progeny virions.

Furthermore, to successfully replicate their genomes and synthesize new progeny, viruses use complex strategies to hijack and concentrate host resources while simultaneously evading recognition and degradation by the host. These processes often result in compartmentalization of viral mRNA transcription, genome replication, and assembly. In this Chapter, I will detail what is known about shared processes in the replication cycle of viruses with segmented genomes that must be coordinated to package, assort, and reassort genome segments.

1.1.1. Reassortment occurs for all viruses with segmented genomes.

Reassortment can lead to rapid acquisition of genetic diversity for viruses with segmented genomes. This process has been especially well-studied for influenza A virus, as reassortment has contributed to the generation of multiple pandemic influenza A viruses, such as those that emerged in 1957, 1968, and 2009 (Kawaoka, Krauss, and Webster, 1989; Fang et al., 1981; Garten et al., 2009). Different strains of influenza viruses are uniquely primed to undergo reassortment events based on differences in receptor usage. For instance, human influenza A viruses bind to α2,6-linked sialic acids, while avian influenza A binds α2,3-linked sialic acids (Ito et al., 1998). While the difference in receptor usage imparts tropism biases on the part of these viruses, porcine hosts express both α2,3-linked and α2,6-linked sialic acids, providing a “mixing vessel” wherein human, avian, and porcine influenza viruses readily coinfect the same host and reassort genome segments (Scholtissek, 1996). Reassortment also occurs frequently in seasonal influenza strains, which in combination with mutation of surface-exposed glycoproteins can impart novel antigenic structures that are less efficiently detected by

the immune system of previously infected hosts (Kim, Webster, and Webby, 2018). Thus, significant genetic shifts in response to reassortment can be advantageous for viruses with segmented genomes.

While reassortment has been especially well-characterized among influenza A viruses, evidence for reassortment exists in all virus families with segmented genomes. For instance, viruses of all serogroups in the *Bunyaviridae* family regularly undergo reassortment events (Briese, Calisher, and Higgs, 2013). Many viruses in this family replicate both within vertebrate and arthropod hosts, and the high feeding frequency of the arthropod host may provide unique opportunity for frequent coinfection and reassortment (Briese, Calisher, and Higgs, 2013). Viruses of the *Reoviridae* family also regularly reassort genome segments. In fact, recent evidence suggests that nearly all circulating bluetongue virus isolates are reassortant viruses and that these viruses readily exchange all ten genome segments during natural infection (Nomikou et al., 2015). Other *Reoviridae* family viruses, including rotavirus and mammalian orthoreovirus, frequently undergo reassortment. In fact, the G9P[8] and G12P[8] rotaviruses that began circulating in humans in the 1990's and 2000's are likely to be reassortant viruses that acquired VP7 genes of animal origin (Matthijnssens et al., 2010; Teodoroff et al., 2005; Santos et al., 1999; Midgley et al., 2012). Occasional multi-host reassortment events occur for rotaviruses wherein genome segments from viruses that frequently infect different host species are assorted into a single genome (Dóró et al., 2015). For example, whole genome sequencing and subsequent phylogenetic analysis revealed that one rotavirus strain, isolated from a child with acute dehydrating gastroenteritis, had genome segments that were most closely related to animal rotavirus

strains, including genome segments of feline, ovine, and buffalo origin (Bányai et al., 2009). Reassortant mammalian orthoreoviruses are also frequently detected in nature in a variety of mammalian hosts, including swine, bats, and humans (Qin et al., 2017; Zhang et al., 2016; Naglič et al., 2018; Wang et al., 2015; Mikuletič et al., 2019).

1.1.2. Reassortment has consequences for progeny viruses.

Although reassortment occurs frequently in nature, reassortment is not always beneficial for the virus, and reassortment generally yields one of three possible consequences (McDonald et al., 2016). The reassortment event can be advantageous, allowing for enhanced replication or broader tropism of the reassortant virus (Garten et al., 2009) (**Fig. 1-1A**). Reassortment events can also be disadvantageous; in these situations, introduction of the novel genome segments can decrease the fitness of progeny viruses or may even yield non-functional progeny (Li et al., 2008) (**Fig. 1-1B**). Lastly, reassortment events can introduce mismatch in cognate RNA or proteins, leading to compensatory mutations that restore functionality in a genotypically unique progeny virus (Roner et al., 1990; Joklik and Roner, 1995) (**Fig. 1-1C**). While reassortment does occur frequently in nature, most evidence suggests that reassortment events are generally selected against, and this negative selection bias is stronger when viruses are more distantly related (Villa and Lässig, 2017). In fact, while co-circulating rotavirus strains can reassort their genes, over time these reassortant viruses are replaced by viruses with preferred genome constellations (McDonald et al. 2009). Much of this can be attributed to what is known as segment mismatch – that is, incompatibility between parent viruses that renders would-be reassortant progeny non-

viable or functionally deficient. Thus, genetic compatibility of parent viruses is a critical determinant of successful reassortment events. However, some viruses, such as those in the *Cystoviridae* family, readily reassort genome segments even when viruses are highly genetically divergent. This may be a result of the genome organization strategy; cystoviruses often encode cognate proteins on the same gene, eliminating the issue of segment mismatch (McDonald et al., 2016).

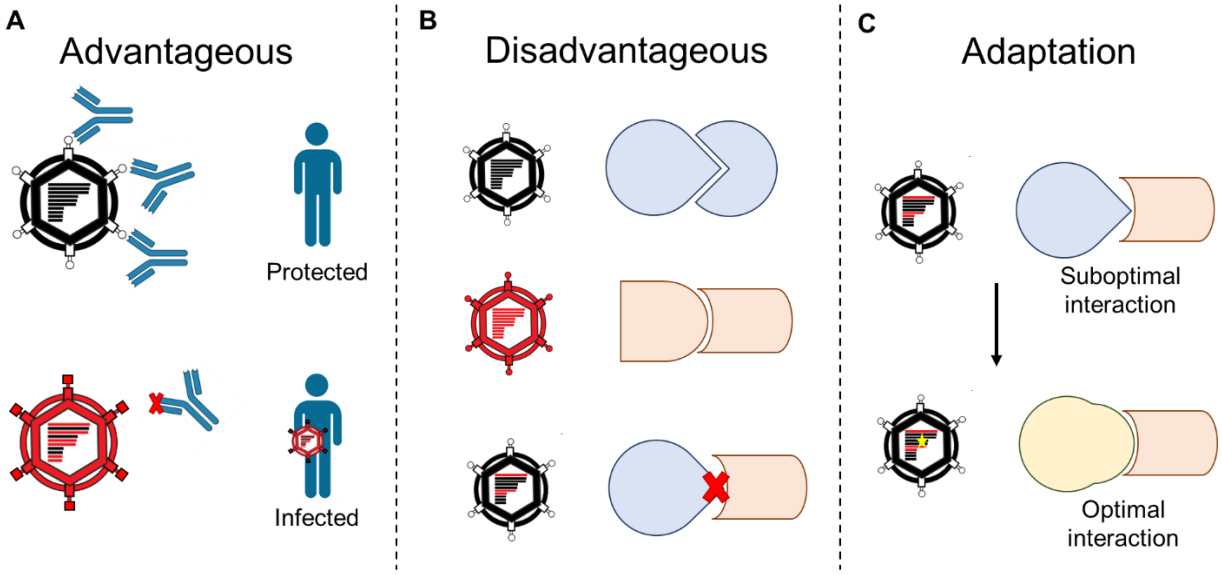

Figure 1-1. Reassortment events have immediate and evolutionary consequences for reassortant virus progeny. (A) Reassortment events can benefit reassortant progeny. For example, reassortment can introduce novel antigenic structures that may not be recognized by host immunity. (B) However, reassortment can also disrupt critical RNA and protein interactions that are vital for replication, leading to unfit virus progeny. (C) Adaptive mutations can restore functionality following reassortment events that lead to suboptimal RNA and protein interactions.

1.1.3. Segment mismatch influences reassortment.

If two viruses coinfect the same host but are highly genetically divergent, reassortment cannot occur or may be limited, as these two viruses will not share the appropriate cognate RNA and proteins. In the absence of segment mismatch, influenza A virus readily reassorts its genome segments in cell culture and animal models (Marshall et al., 2013; Tao et al., 2014). However, coinfection with some influenza strains allows for frequent reassortment events, but reassortant progeny suffer from reduced fitness (Phipps et al., 2015). Similarly, interactions between bunyavirus small and large genome segments are often conserved such that most reassortant viruses exchange only the medium genome segment of the tripartite genome (Briese, Calisher, and Higgs, 2013). Segment mismatch also limits reassortment among viruses of the *Reoviridae* family. Early studies of reovirus reassortment determined that type 1 and type 3 reovirus crosses yielded only a select few reassortant progeny, while the majority of progeny had parental genotypes (Wenske et al., 1985), suggesting that type 1 x type 3 reovirus reassortants are less fit than parental viruses. Later studies sought to further understand the mechanism of this limitation and observed that nonrandom associations exist between genome segments in reassortant viruses. Specifically, type 1 x type 3 reassortants were much more likely to have genome segments L1–L2, L1–M1, L1–S1, and L3–S1 from the same parental virus (Nibert, Margraf, and Coombs, 1996), suggesting that maintaining interactions between those segments is critical for viral replication. Similar observations have been made for other viruses with multi-segmented genomes, including influenza A virus (Lubeck, Palese, and Schulman,

1979), rotavirus (Gombold and Ramig, 1986), and some bunyaviruses (Urquidi and Bishop, 1992).

1.1.4. Viruses of the *Reoviridae* family have segmented genomes and are medically and economically important.

Mammalian orthoreovirus (reovirus) was first identified in the 1950s and is so named because it infects the respiratory and intestinal tracts but is generally not associated with disease (*r*espiratory, *e*nteric, *o*rphan virus) (Sabin, 1959). Reovirus particles are composed of a non-enveloped, double-layered protein shell that encapsidates a genome of ten double-stranded RNA (dsRNA) genome segments (Bellamy et al., 1967; Gomatos and Tamm, 1963). The reovirus outer capsid is composed of the σ1 attachment protein overlying heterohexamers of the μ1 and σ3 structural proteins (Liemann et al., 2002) (**Fig. 1-2A**). Upon penetration through host endosomes, the outer capsid is shed to reveal transcriptionally-active core particles made up of structural proteins λ1 and σ2, as well as the viral RNA-dependent RNA polymerase λ3, and the polymerase cofactor μ2 (Reinisch, Nibert, and Harrison, 2000; Coombs, 1998; Zhang et al., 2003). λ2 forms turrets in core particles from which nascent viral mRNAs synthesized by λ3 exit the core (Dryden et al., 1993). All ten reovirus genome segments are monocistronic with the exception of the S1 gene, which encodes σ1 and σ1s in overlapping reading frames, and the M3 genome segment, which encodes μNS and μNSC in the same open reading frame (Ernst and Shatkin, 1985; McCutcheon, Broering, and Nibert, 1999). The size of genome segments ranges from approximately 1200 – 3900 nucleotides, giving a total genome length of about 23.5 kilobases. Genome

segments are named based on their size; there are four small genome segments (S1, S2, S3, and S4), three medium genome segments (M1, M2, and M3), and three large genome segments (L1, L2, and L3) (Shatkin, Sipe, and Loh, 1968). The 5’ and 3’ untranslated regions of each genome segment are highly conserved (McCutcheon, Broering, and Nibert, 1999) and contain 5’-GCUA and 3’-UCAUC nucleotide sequences (Antczak et al., 1982) (**Fig. 1-2B**). 5’ and 3’ termini of viral mRNA are predicted to form a partial duplex interrupted by stem loops, referred to as a panhandle structure (Chappell et al., 1994) (**Fig. 1-2C**).

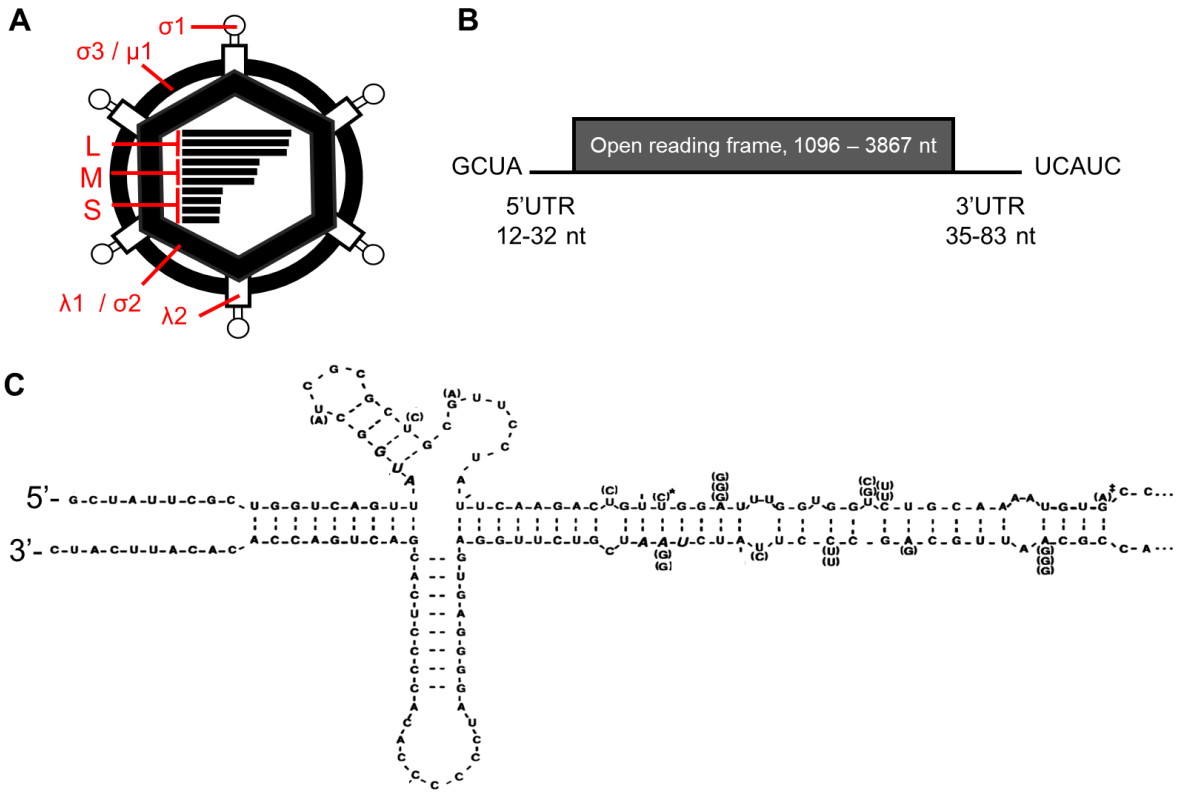

Figure 1-2. Reovirus is composed of double-layered particles that encapsidate ten double-stranded RNA genome segments. (A) The outer capsid of reovirus particles is made up of σ3 and μ1 heterohexamers. The attachment protein σ1 is imbedded in λ2 turrets. The outer capsid surrounds an inner capsid composed of λ1 and σ2. The viral genome is ten segments of double-stranded RNA, three large segments (L), three medium segments (M), and four small segments (S). (B) Each genome segment is approximately 1200-3900 nucleotides in length. The 5' and 3' termini are highly conserved and contain short untranslated regions (UTRs). All except for the S1 and M3 genome segments encode only a single protein. (C) Reovirus +RNA transcripts are predicted form terminal panhandle structures. The predicted secondary structure of S2 is shown (adapted from Chappell et al., 1994. *J Virol* 750-756, with permission from the American Society for Microbiology.)

Reovirus consists of three major serotypes, Type 1 Lang (T1L), Type 2 Jones (T2J), and Type 3 Dearing (T3D) (Rosen, 1960), with T1L and T3D being the most heavily studied. These viruses differ in various aspects of their replication that makes them

useful tools for the study of reovirus biology. For instance, T3D reovirus is susceptible to trypsin cleavage of the attachment protein σ1 in the mouse gut, while T1L is resistant to cleavage, resulting in a diminished ability for T3D to infect the mouse intestine (Chappell et al., 1998). Further, the enhanced capacity of T1L, relative to T3D, to replicate and be isolated from intestinal tissue is associated with differences in the S1, S2, and L2 genome segments (Bodkin and Fields, 1989). T3D also induces stronger antiviral responses and more cell death *in vivo* and *in vitro* than does T1L. Differences in interferon induction between the two strains can be mapped to the M1 genome segment, encoding polymerase cofactor μ2, while differences in cell death associate with the S1 and M2 genome segments (Irvin et al., 2012; Tyler et al., 1996; Hoyt et al., 2005). In the brain, T3D reovirus infect neurons and causes a lethal meningoencephalitis, while T1L infects ependymal cells and results in ependymitis and hydrocephalus (Weiner et al., 1977). Within infected cells, reovirus of all strains establish proteinaceous virus replication factories (VFs). T1L replicates within filamentous VFs that track along microtubules, while T3D established globular VFs (Parker et al., 2002). The morphology of factories is attributed to association of the μ2 protein from each strain with microtubules (Parker et al., 2002). The capacity of μ2 to associate with host cytoskeleton also determines packaging efficiency, and as a result, T1L packages the viral genome much more efficiently than T3D (Shah et al., 2017).

Reovirus has a broad host tropism, and commonly infects humans, swine, cattle, felines, canines, and other mammals (Dermody, Parker, and Sherry, 2013). Seroprevalence studies suggest that the majority of humans are exposed to reovirus before adulthood, with most infections occurring within the first 5 years of life (Tai et al.,

2005). Studies of reovirus have been pivotal in the understanding of processes critical to the replication of many viruses, including mRNA capping (Furuichi, Muthukrishnan, and Shatkin, 1975), transcytosis of microfold (M) cells in the gut by enteric viruses (Wolf et al., 1981), and endosomal proteolytic processing of viruses during entry (Ebert et al., 2002). Reovirus is a genetically-tractable virus that shares many characteristics with other medically and economically-important members of the *Reoviridae* family, including rotavirus and bluetongue virus. Prior to vaccine introduction, rotavirus was the leading cause of severe gastroenteritis in children <5 years of age (Parashar et al., 2003). Even in the post-vaccine era, rotavirus is a significant cause of morbidity and mortality globally, causing over 100,000 deaths each year (Crawford et al., 2017). BTV is an insect-borne virus in the *Reoviridae* family that causes significant disease and mortality in ruminants, leading to substantial production losses and economic impact in affected countries (Gethmann, Probst, and Conraths, 2020). More recent studies suggest that while reovirus infection only rarely causes symptoms in humans, it is still relevant to human health. For instance, reovirus infection may be associated with the loss of tolerance to gluten in celiac disease (Bouziat et al., 2017), and some reovirus strains are being considered as oncolytics (Twigger et al., 2008; Karapangiotou et al., 2012).

1.2. Packaging a segmented viral genome is a complex process.

For viruses with segmented genomes to reassort genome segments, coinfecting viruses must be similar enough to allow for simultaneous packaging of genome segments from both parent viruses. Viruses of many families, including the *Arenaviridae*, *Birnaviridae*, *Bromoviridae*, *Bunyaviridae*, *Chrysoviridae*, *Closteroviridae*, *Cystoviridae*,

Orthomyxoviridae, *Partitiviridae*, *Picobirnaviridae*, and the *Reoviridae* families, encapsidate a segmented genome (McDonald et al., 2016). Segmented viral genomes vary significantly in the number of genome segments they package, the total size of the viral genome, and the requirements for packaging. As such, viruses accomplish the task of packaging a segmented genome through different mechanisms.

1.2.1. Packaging of segmented viral genomes often occurs through a core-filling or concerted model.

Packaging of multi-segmented viral genomes often occurs through a “core-filling” model and a “concerted” model (McDonald et al., 2016). In the core-filling model, genome segments are sequentially introduced into a pre-existing viral capsid. Evidence supports a core-filling packaging model for bacteriophages of the *Cystoviridae* family and for bunyaviruses (Gottlieb et al., 1991; Gottlieb et al., 1990; Shreur, Kormelink, and Kortekaas, 2018). Viruses that package their genomes via the core-filling model frequently package incomplete sets of genome segments. For example, single molecule fluorescent *in situ* hybridization experiments revealed that cells infected with Rift Valley fever virus at a low infection multiplicity do not always contain all three genome segments (Wicgeurs Shreur and Kortekaas, 2016), and mature Rift Valley fever virus virions have been shown to package unequal ratios of the three genomic segments (Gauliard et al., 2006). These viruses are able to maintain infectivity through genetic complementation; cells are infected with multiple virus particles, and collectively these particles package a full complement of the genome. However, as the number of total genome segments increases, the likelihood of genetic complementation via this strategy

is reduced. If packaging of a given genome segment is random, then the number of particles required to provide a full complement of the genome can become too high to maintain infectivity as the number of genome segments increases. Thus, viruses with greater numbers of genome segments are predicted to utilize a concerted packaging model.

In the concerted genome packaging model, independent genome segments interact to form a supramolecular RNA complex that can be encapsidated by viral structural proteins. Recent studies on packaging for viruses of the *Reoviridae* family, which package 9-12 dsRNA genome segments, suggest that these viruses utilize a concerted packaging model. For example, bluetongue virus ssRNA must be present for capsid assembly to occur, suggesting that genome segments are not being introduced into pre-formed capsids (Lourenco and Roy, 2011). Packaging of bluetongue virus genome segments requires specific secondary structure motifs formed by interactions of the 5' and 3' end of the genome segments (Burkhardt et al., 2014). Similarly, the 5' and 3' termini of reovirus +RNAs are predicted to interact to form panhandle structures (Chapell et al., 1994) (**Fig. 1-3A**), and the 5' and 3' terminal sequences of reovirus genome segments are highly conserved and are required for genome packaging (Chappell et al., 1994; Kedl, Schmechel, and Schiff, 1995). Although the minimum sequence required for packaging all ten reovirus genome segments has yet to be precisely defined, deletion mutants of the shortest reovirus genome segment, S4, can be rescued, with transcomplementation of the encoded protein, after replacing all but the 5'- and 3- terminal 1-149 nucleotides and 769-1196 nucleotides with sequence encoding green fluorescent protein (Kobayashi et al., 2007). Similarly, single-stranded

RNA containing only the 5’ terminal 96 nucleotides and 3’ terminal 284 nucleotides from the S2 genome segment can be incorporated into progeny virions and converted into dsRNA (Roner, Bassett, and Roehr, 2004). Together, these findings provide evidence that highly conserved sequence and structural features of the 5’ and 3’ termini of genome segments of many *Reoviridae* family viruses are required for efficient genome packaging.

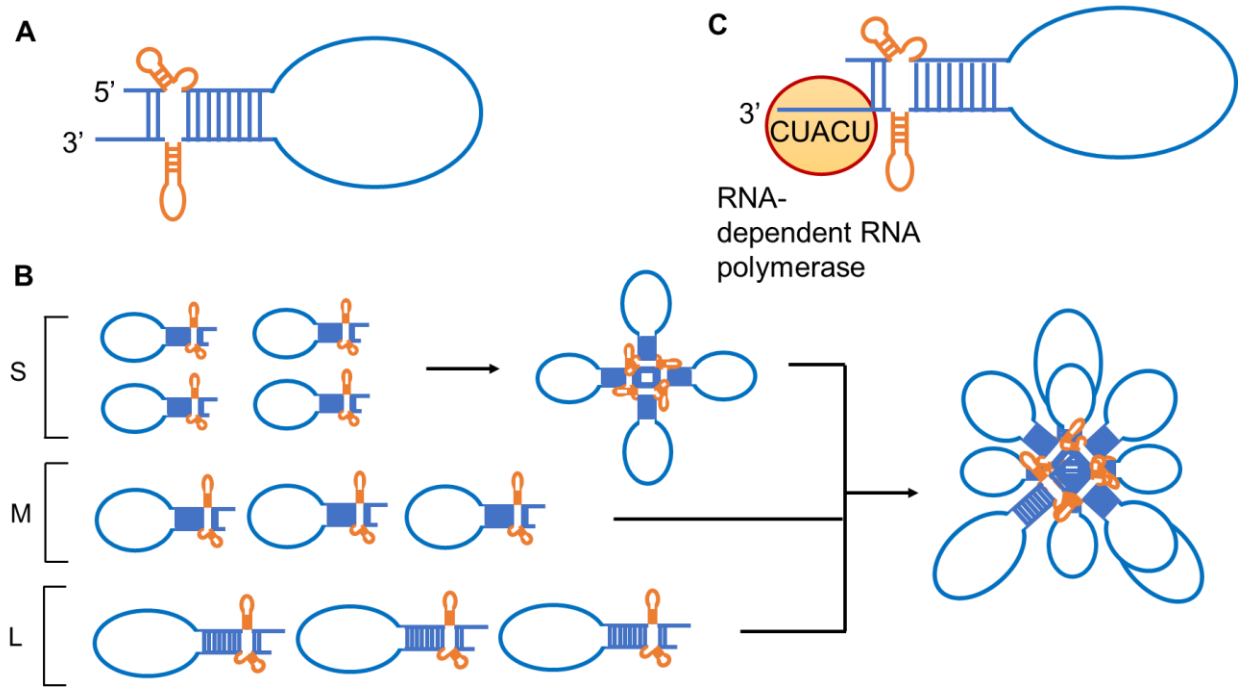

Figure 1-3. Packaging of the multi-segmented *Reoviridae* family virus genomes requires *cis*-segment and *trans*-segment RNA-RNA interactions, as well as association with viral proteins. (A) 5’- and 3’- untranslated regions of +RNA transcripts are predicted to form stem loop structures that contribute to the overall panhandle structure of individual transcripts. (B) Reovirus and rotavirus RNA-dependent RNA polymerase are predicted to associate with 5’ cap and 3’ overhang before using +RNA as a template for synthesis of the minus-strand of the dsRNA genome segments. (C) Reovirus packages four small (S), three medium (M), and three large (L) genome segments. Evidence from *in vitro* studies of bluetongue virus and rotavirus genome packaging suggest that

Reoviridae family viruses rely on *trans*-segment interactions, initiated by small genome segments, to form a packageable supramolecular RNA complex.

1.2.2. Packaging for viruses of the *Reoviridae* family requires RNA-RNA interactions.

The order of genome segment association and RNA complex formation is also highly regulated for viruses of the *Reoviridae* family. *In* vitro reconstitution assays of bluetongue virus RNA complex assembly indicate that the absence of any genome segments results in inefficient packaging of all other genome segments (Sung and Roy, 2014). The smallest genome segments are especially important in this process, and disruption of interactions between small genome segments prevents the formation of a complete genome complex (Fajardo, Sung, and Roy, 2015) (**Fig. 1-3B**). Rotavirus genome segments similarly rely on *trans*-segment interactions to form a packageable RNA complex (Fajardo et al., 2017). The precise location of *trans*-segment interactions has yet to be directly identified for most *Reoviridae* family viruses. However, computational predictions of *trans*-segment interaction sites have identified specific nucleotide sequences at the 5'- and 3'- termini, as well as in the interior, of the five smallest BTV genome segments. Mutation of these sequences inhibits RNA complex formation and prevents virus rescue, indicating that these sequences are essential for packaging and assembly (Alshaikhahmed et al., 2018). Direct evidence for this packaging pattern does not exist for reovirus; however, these studies represent a growing body of evidence suggesting that genome packaging by viruses of the *Reoviridae* family is highly coordinated and requires genetic conservation at specific sites.

1.2.3. Packaging for viruses of the *Reoviridae* family requires RNA-protein interactions.

Viruses of the *Reoviridae* family package a full complement of +RNA genome segments and use +RNA as template for synthesizing the negative strand of the dsRNA genome. These viruses encode an RNA-dependent RNA polymerase that recognizes 3' terminal sequences on +RNA transcripts before replicating the transcript to form dsRNA (Tao et al., 2002; Lu et al., 2008) (**Fig. 1-3C**). Rotavirus phylogenetically separates into distinct clades, which differ in 3' terminal sequences that are recognized by the viral polymerase, potentially acting as a limiting factor in reassortment (Ogden, Johne, and Patton, 2012; McDonald et al., 2016). In addition to the viral polymerase, the reovirus polymerase cofactor μ2 also has ssRNA and dsRNA binding activity, and efficient catalysis by the viral polymerase relies on the polymerase cofactor (Brentano et al., 1998; Kim et al., 2004). Furthermore, reovirus +RNA transcripts are often 5'-capped, and it has been proposed that the polymerase might associate with the 5' cap to facilitate insertion of the 3' end of the negative strand into the template channel of the polymerase (Tao et al., 2002). As such, association with viral structural protein λ2, which displays guanylyltransferase and methyltransferase activity (Cleveland, Zarbl, and Millward, 1986; Tao et al., 2002), may be critical for synthesis of packageable viral transcripts. Finally, nonstructural proteins are responsible for recruiting transcriptionally active core particles and +RNA to sites of genome assembly (Lee et al., 2021; Antczak and Joklik, 1992; Miller et al., 2010). Thus, *cis*- and *trans*-segment interactions, as well

as interaction between viral RNA and structural and nonstructural proteins, are critical for efficient reovirus genome packaging.

1.2.4. *Reoviridae* family viruses are hypothesized to use an "all-or-nothing" packaging model.

During infection, reovirus generates particles that are identical in their polypeptide components but differ in their capacity to package the viral genome (Smith, Zweerink, and Joklik, 1969). These particles can be differentiated by buoyant density and in electron micrographs, where top component particles appear empty, in contrast to virions, which appear to contain the viral genome (Lai, Werenne, and Joklik, 1973). The abundance of virions and top component during infection exhibits strain specificity; type 3 reovirus generates a higher ratio of top component:virions throughout infection relative to type 1 reovirus, and this difference relies on the association of VFs with the host cytoskeleton (Shah et al., 2017). The presence of distinct "full" and "empty" particle species has led to the hypothesis that reovirus uses an all-or-nothing packaging mechanism; however, this hypothesis has not been formally tested. Influenza A virus, which like viruses of the *Reoviridae* family seems to follow a concerted packaging model (Gerber et al., 2014), has been shown to uptake multiple copies of a single genome segment (Enami et al., 1991). Furthermore, next-generation sequencing analyses of other viruses with segmented genomes, such as Flock House virus and brome mosaic virus, suggest that these viruses are capable of packaging a variety of host RNA species in addition to the viral genome (Routh, Domitrovic, and Johnson, 2012; Shrestha et al., 2018). However, it is unclear whether the residual volume in

some reovirus particles allows for packaging of multiple copies of a singular genome segment or of host transcripts, similar to what has been observed for other viruses with segmented genomes.

1.3. Assembly requires the coordination of multiple processes, including transcription, translation, and packaging.

In addition to the physical coordination and compatibility of +RNA and viral proteins for efficient packaging and reassortment of multi-segmented genomes, coordination of other processes in the virus replication cycle are also required. To successfully assort and package the viral genome, +RNA and viral proteins involved in nascent particle assembly must be colocalized within the cell. To reassort genome segments, viruses must have +RNA from both coinfecting viruses present in the same physical space at the time of nascent particle assembly. Viruses often compartmentalize replication within membrane-bound or proteinaceous VFs. These structures serve to concentrate components required for viral transcription, translation, and new particle assembly, and may prevent recognition or degradation of the virus by host antiviral machinery.

1.3.1. Viruses with segmented genomes use various strategies to replicate within host cells.

Viruses with segmented genomes can be quite varied in the strategies they use to replicate within host cells. For instance, influenza virus first traffics to the nucleus, where viral replication and mRNA transcription occur (Neumann, Noda, and Kawaoka, 2009). Viral ribonucleoprotein complexes are exported from the nucleus late in the replication

cycle, and assembly and budding of progeny viruses takes place at the plasma membrane (Neumann, Noda, and Kawoaka, 2009). Unlike influenza viruses, many viruses with segmented genomes primarily replicate within the host cytoplasm. For instance, bunyaviruses, as well as Flock House virus, replicate within membraneous spherules (Novoa et al., 2005; Kopek et al., 2007). These spherules are single membrane invaginations formed within various host membranes that harbor viral RNA and polymerase, act as sites for genome transcription and replication, and preclude access to undesired proteins (Fernández de Castro, Volonté, and Risco, 2013). Viruses of the *Reoviridae* family establish and replicate within proteinaceous VFs that are assembled by viral non-structural proteins (**Fig. 1-4**).

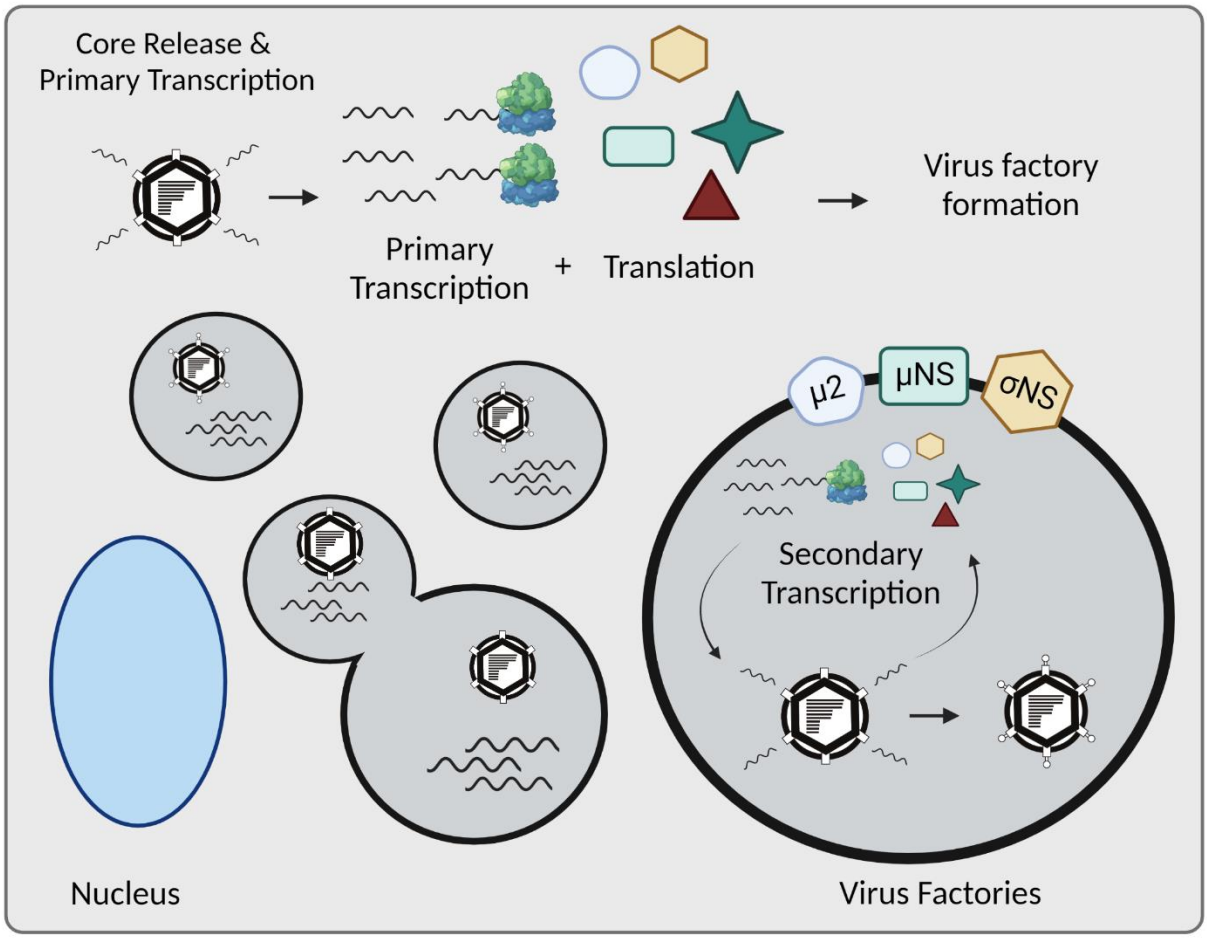

Figure 1-4. Reovirus replicates within cytoplasmic virus factories. Transcriptionally-active core particles are released from the endosome into the cytoplasm following entry into the host cell. Here, viral transcripts are translated and nonstructural proteins form VFs and recruit viral proteins and cores. Secondary transcription and new particle assembly occur within VFs, and addition of outer capsid proteins halts transcription. VFs from type 3 reoviruses exhibit globular morphology and grow in size as replication progresses. VFs also undergo fusion events, potentially contributing to increased VF size later in infection.

1.3.2. Reovirus undergoes transcription, translation, packaging, and assembly within cytoplasmic virus factories.

Reovirus sheds its outer capsid layer during penetration through the endosome, and transcriptionally-active core particles are deposited into the cytoplasm (Chandran et al., 2003; Morgan and Zweerink, 1975). These “primary transcriptase” particles generate +RNA transcripts that are used for initial rounds of viral protein translation. Early transcripts associate with viral nonstructural proteins μNS and σNS, as well as outer capsid protein σ3, in single stranded RNA-containing complexes (Antczak and Joklik, 1992). These same viral proteins go on to establish VFs, in the case of μNS and σNS (Broering et al., 2005; Becker, Peters, and Dermody, 2003), while σ3 suppresses host responses to infection (Roebke et al., 2020). Core particles are recruited to nascent VFs, and bromodeoxyuridine labelling of viral transcription has provided direct evidence that reovirus transcription is localized to VFs (Miller et al., 2010). VFs also incorporate components of the host translation machinery to enable the synthesis of new viral proteins without the need to expose viral +RNA to the host cytoplasm (Desmet, Anguish, and Parker, 2014). With viral +RNA and structural proteins present within VFs, +RNA complexes will then be packaged within assembling particles inside VFs (Shah et al., 2017). These particles use +RNA as a template to form negative strands, which are then used as a template to further transcribe +RNA. These “secondary transcriptase” particles are thought to synthesize the majority of +RNA from within VFs (Miller et al., 2010). Addition of the outer capsid inhibits transcription, and results in the formation of infectious virions (Farsetta, Chandran, and Nibert, 2000).

1.3.3. *Reoviridae* family VFs are established by viral nonstructural proteins and associate with host cytoskeleton.

Reovirus VFs are primarily established by non-structural proteins µNS and σNS. Virus factory-like structures can be formed by transfecting cells with plasmids encoding µNS alone (Broering et al., 2005). In the absence of µNS, nonstructural protein σNS is freely dispersed throughout the cytoplasm (Becker, Peters, and Dermody, 2003). Following transfection of µNS, σNS then associates with factory-like structures, indicating that µNS is responsible for localization of σNS to VFs (Becker, Peters, and Dermody, 2003). Deletion mutants of µNS suggest that this protein is also responsible for recruitment of other viral proteins and transcriptionally-active core particles to VFs (Miller et al., 2010). While µNS is primarily responsible for recruitment of viral proteins to VFs, σNS has recently been appreciated to increase the half-life of viral RNA and is responsible for incorporating viral RNA into VFs (Zamora et al., 2018; Lee et al., 2021). Specifically, mutations in the RNA-binding domain of σNS preclude +RNA access into VFs (Lee et al., 2021). VF association with microtubules is an important determinant of VF morphology and packaging efficiency (Parker et al., 2002; Shah et al., 2017), and reovirus polymerase co-factor µ2 is responsible for VF association with microtubules (Parker et al., 2002). Amino acid identity at residue 208 of µ2 determines VF morphology, and VFs generated with reovirus strain T1L form filamentous VFs that track alongside microtubules, while those generated by T3D are globular in morphology (Parker et al., 2002; **Fig. 1-5**). Rotavirus VFs, often referred to as viroplasms, share many characteristics with reovirus VFs. These structures are assembled by nonstructural proteins NSP2 and NSP5 and appropriate perinuclear localization of

viroplasms relies on stabilized microtubules (Eichwald et al., 2004; Cabral-Romero and Padilla-Noriega, 2006; Eichwald et al., 2012). NSP5 localization to viroplasms also requires an additional phosphorylation step, as unphosphorylated NSP5 is dispersed throughout the cytoplasm, while phosphorylated NSP5 localizes to factories (Criglar et al., 2017). Like reovirus, rotavirus transcription and replication are compartmentalized within viroplasms (Silvestri, Taraporewala, and Patton, 2004).

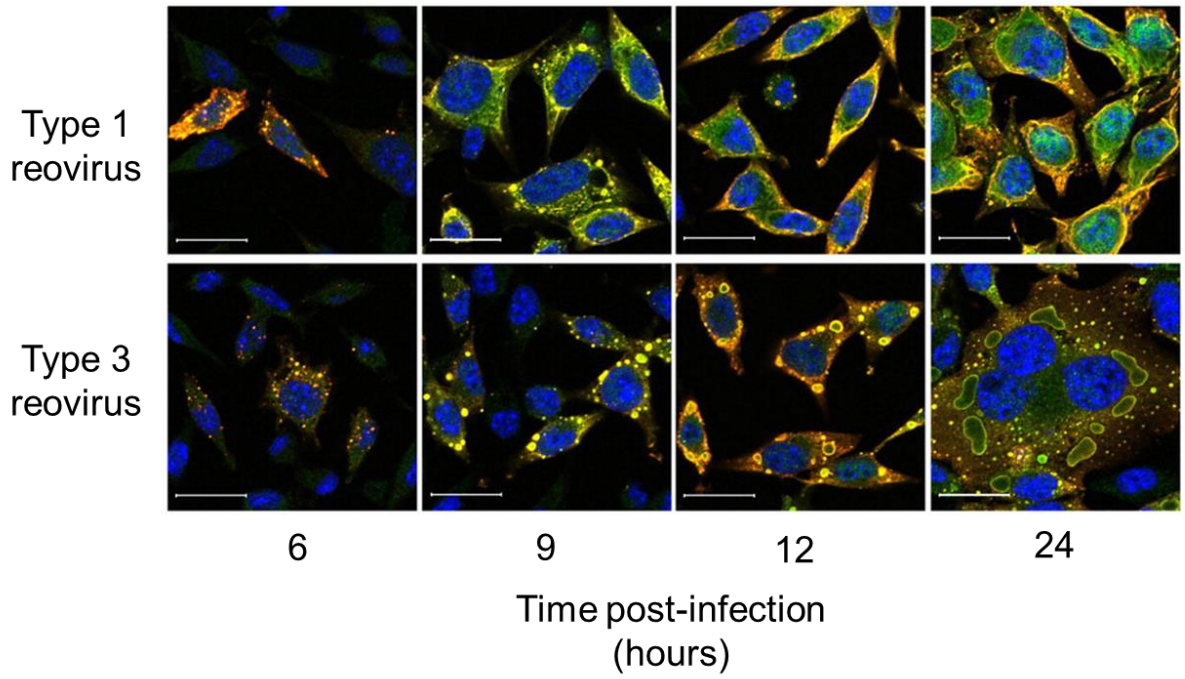

Figure 1-5. VFs of different reovirus serotypes display distinct morphology. Type 1 reovirus factories exhibit filamentous morphology while type 3 reovirus VFs exhibit globular morphology. Type 3 reovirus VFs initially present as small, punctate structures in the cytoplasm and become larger as infection progresses. VF morphology corresponds to amino acid differences in μ2 (figure adapted from Ooms et al., 2010. *JBC* 285:41604-41613, with permission from the American Society for Microbiology.)

1.3.4. *Reoviridae* family virus factories are motile and display liquid-like properties.

VFs made by viruses of the *Reoviridae* family often first present as small, punctate structures in the cytoplasm early in infection that become larger as replication progresses (Ooms et al., 2010; Eichwald et al., 2004) (**Fig. 1-5**). Live-cell imaging of reovirus nonstructural proteins during infection revealed that reovirus VFs are motile and undergo fusion and fission events, which may contribute to the growth of VFs over time (Bussiere et al., 2017). Treatment of cells with microtubule destabilizing drugs disrupts and prevents fusion of VFs and inhibits reovirus and rotavirus replication, indicating that motility and fusion of reovirus VFs and rotavirus viroplasms require stabilized microtubules (Eichwald et al., 2012; Eichwald, Ackermann, and Nibert, 2018). It has recently been appreciated that VFs for many viruses are motile and display liquid-like properties, such that VFs are spherical, fuse to form larger structures, and dissolve in the presence of aliphatic diols (Nikolic et al., 2017; Heinrich et al., 2018). Rotavirus viroplasms were also recently shown to display properties of phase separated condensates. These viroplasms undergo fusion and fission events and are readily dissolved by aliphatic diols (Geiger et al., 2021). However, a liquid-to-solid transition occurs later in the replication cycle whereby viroplasms are no longer dissolved and replication is no longer inhibited by propylene glycol (Geiger et al., 2021). Thus, reovirus and rotavirus compartmentalize processes important for genome packaging and reassortment within cytoplasmic VFs, and these VFs readily undergo fusion and fission events. How compartmentalization of replication and motility of replication compartments influences reassortment is an open question (**Fig. 1-6**).

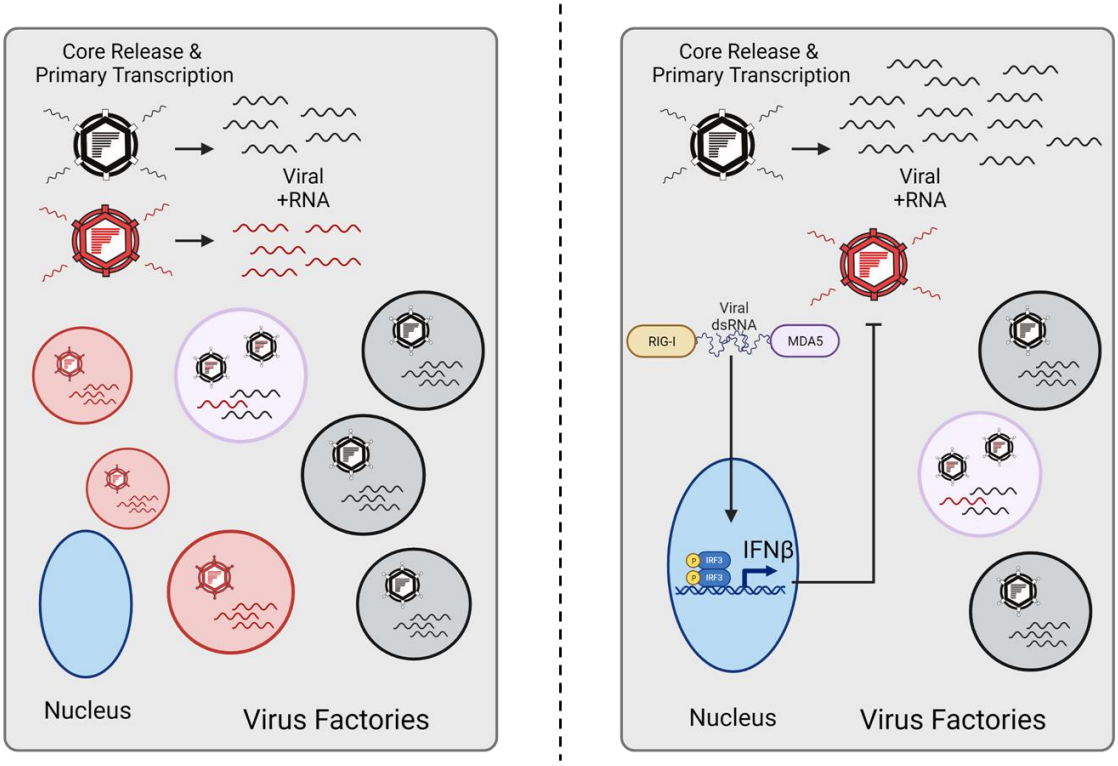

Figure 1-6: The reovirus replication strategy and host responses to infection may influence reassortment potential. (Left panel) Reovirus generates new +RNA transcripts and packages its genome within VFs. However, how this process is mediated during coinfection is not understood. Coinfecting viruses may establish distinct VFs, potentially imposing a physical barrier to RNA-RNA interactions that are critical for packaging +RNA from both viruses into progeny particles. (Right panel) Host sensors RIG-I and MDA5 recognize reovirus dsRNA and produce type I interferon in response. Whether this limits secondary infection by reovirus has yet to be ascertained; however, if secondary infection is restricted, this could severely limit the ability of two viruses to reassort genome segments.

1.4. The host responses to infection and virus-virus interactions may influence packaging and reassortment.

Coinfection dynamics play an important role in determining reassortment frequency, and virus-virus and virus-host interactions can influence the frequency of coinfection. In the absence of segment mismatch, coinfecting influenza A viruses readily reassort genome segments (Marshall et al., 2013). However, even in the absence of segment mismatch, influenza does not reassort genome segments when the host is inoculated with coinfecting viruses via distinct routes (Richard et al., 2018), highlighting the importance of cellular coinfection and spatial compartmentalization within the host in determining reassortment frequency. All viruses must contend with host antiviral responses to successfully infect and replicate within the host, and the ability of viruses to counteract these responses may be an important determinant of coinfection. Furthermore, many viruses interfere the ability of other viruses to replicate simultaneously within the same host.

1.4.1. Host responses to infection can determine success of viral infection.

Reovirus replicates first within the host intestine and gains access to the basolateral membrane of host enterocytes by transcytosing across microfold cells in the villus crypt (Wolf et al., 1981; Gonzalez-Hernandez et al., 2014). After transcytosis of the intestinal epithelium, reovirus can replicate within intestinal epithelial cells (Rubin, Kornstein, and Anderson, 1985) and can subsequently disseminate hematogenously to secondary sites of infection, including the liver, heart, and brain (Tyler, 1991; Johnson et al., 2009),

perhaps through binding to B and T lymphocytes (Epstein, Powers, and Weiner, 1981). Reovirus can then cause significant pathogenesis at secondary sites of replication in newborn mice (Forrest and Dermody, 2003).

Antiviral host responses can suppress viral replication, leading to less spread within the host and fewer chances for coinfection. Host cells recognize short and long reovirus dsRNA to initiate antiviral responses via retinoic acid-inducible gene I (RIG-I) and melanoma differentiation-associated protein 5 (MDA5), resulting in the production and secretion of interferon and other antiviral factors (Kato et al., 2008; Loo et al., 2008; Kell and Gale Jr, 2015). Type I interferon signaling initiated as a consequence of this recognition is responsible for limiting virus replication and spread at secondary sites of replication (Dionne et al., 2011; Sherry, Torres, and Blum, 1998; Phillips et al., 2020) and contributes to pathology in the brain (Dionne et al., 2011). Importantly, though, type I interferon signaling is dispensable for protection of the host against reovirus infection at mucosal sites of infection, such as the intestine (Mahlakoiv et al., 2015). Instead, type III interferons are responsible for protecting mucosal sites from infection by reovirus, as well as other enteric viruses (Mahlakõiv et al., 2015; Baldridge et al., 2018; Lazear et al., 2015). At the cellular level, natural killer cells and neutrophils are early responders at the site of reovirus infection (Taterka, Cebra, and Rubin, 1995; Morin et al., 1996). Additionally, reovirus readily replicates and causes disease in neonatal mice but requires much higher titers to establish infection in adult mice than in neonates (George et al., 1990). However, reovirus replicates to high titers in adult SCID mice, which lack T and B cells, and SCID mice subsequently succumb to disease (George et al., 1990). Suppression of viral replication by host responses can also limit coinfection and

reassortment. For instance, rotavirus reassortment is significantly reduced in passively immune suckling mice relative to nonimmune mice (Gombold and Ramig, 1989). However, the influence of host antiviral responses on reovirus replication during coinfection, and by extension the influence of these responses on reassortment, has yet to be determined (**Fig. 1-6**).

1.4.2. Virus-virus interactions can influence coinfection potential.

Virus-virus interactions can also be important in determining the frequency of coinfection and reassortment. Virus interference occurs when infection with one virus limits or prevents infection by another. This interference is considered homologous when viruses of the same family compete, or heterologous when a virus interferes with replication of another virus outside of its family. In a specific case of interference called superinfection exclusion, previous infection with one virus may restrict replication of a second virus, even though interference may not occur when these viruses enter a host at the same time (Laureti et al., 2020). The mechanism of viral interference can vary, depending on the initiating virus. Interference and superinfection exclusion can be mediated by either a viral effector, such as a viral protein that directly degrades the viral receptor (Wildum et al., 2006), or a host effector, such as a host antiviral response that broadly inhibits subsequent infection (Isaacs and Lindenmann, 1957; Huang, Dai, and Ke, 2019). Viruses of nearly every family have been shown to interfere with the replication of other viruses (Kumar et al., 2018), and in addition to suppressing viral replication, virus interference and superinfection exclusion can also prevent reassortment for some viruses (Ramig et al., 1989). Whether other viruses of the

Reoviridae family limit superinfection, and what influence this might have on reassortment for these viruses, are open questions.

1.5. Summary

Viruses of the *Reoviridae* family, like many other viruses with segmented genomes, undergo highly coordinated packaging and assembly processes that could influence the potential of these viruses to reassort genome segments. While much work has been done to understand how viruses of the *Reoviridae* family package their multi-segmented genome, the strict requirements for packaging of the reovirus genome have yet to be elucidated. In Chapter 2, I describe next-generation RNA sequencing analyses of reovirus virions and TC particles to assess the specificity of reovirus packaging. In support of an all-or-nothing packaging mechanism, I show that reovirus virions strictly package viral genome segments in an equimolar fashion. However, in the absence of genome, reovirus particles uptake host RNAs sharing some characteristics with reovirus transcripts, stressing the importance of these features in packaging.

In the context of coinfection, viruses with segmented genomes can exchange genome segments through a process called reassortment. Although it is well-established that incompatibility between parent viruses can prevent reassortment or limit the fitness of reassortant progeny, less is known about whether there are influences on reassortment frequency outside of parental incompatibility. In Chapter 3, I describe the use of post-PCR genotyping methods to quantify reassortment frequency in the absence of segment mismatch. In these analyses, I determine that reovirus efficiently reassorts genome segments during coinfection and superinfection. I provide evidence to suggest

that the reovirus replication strategy does not restrict reassortment. I also show that, given sufficient time, reovirus might limit superinfection. In Chapter 4, I describe preliminary work to determine the mechanism of reovirus superinfection exclusion and its impact on reassortment frequency in mice. Through this, I provide evidence that the mechanism of reovirus superinfection exclusion is likely to differ in cell culture and in mouse models and that type I and type III signaling have little to no effect on reovirus reassortment *in* vivo. Collectively, this work provides a more thorough understanding of packaging and reassortment of the reovirus genome. More broadly, the findings described in this dissertation detail how viruses manage to reassort genome segments despite compartmentalized replication and may have important implications for determining the likelihood of reassortment during natural infection.

CHAPTER 2

REOVIRUS LOW-DENSITY PARTICLES PACKAGE CELLULAR RNA

This chapter was adapted from Thoner et al. 2021. Reovirus low-density particles package cellular RNA. *Viruses* 13:1096.

2.1. Introduction

Packaging of segmented, double-stranded RNA (dsRNA) genomes by eukaryotic viruses is an incompletely understood process that requires the coordination of up to 12 viral RNA species as well as structural and non-structural proteins (Borodavka, Desselberger, and Patton, 2018; McDonald and Patton, 2011; Roy, 2017; Taraporewala and Patton, 2004). Two major packaging models have been proposed: (i) a concerted model in which *trans*-interactions between plus-strand (+) RNA species of each segment promote formation of a packageable supramolecular complex that is subsequently encapsidated by viral structural proteins, and (ii) a core-filling model wherein each segment is individually packaged into a preformed core particle (Borodavka, Desslerberger, and Patton, 2018; McDonald and Patton, 2011). Viral nonstructural proteins may act as chaperones and facilitate RNA-RNA interactions that aid in selective RNA packaging (Borodavka et al., 2015; Bravo et al., 2018). Following viral +RNA packaging, minus-strand RNA is synthesized to form dsRNA genome segments, which are present in particles in equimolar proportions. Evidence suggests that members of the *Reoviridae* family of viruses with segmented, dsRNA genomes

employ concerted packaging. However, many questions about how these viruses package their multi-partite genomes remain unanswered.

Mammalian orthoreovirus (reovirus) is a useful model for studies of RNA packaging by viruses belonging to the *Reoviridae* family. Reovirus has a broad host range, has been implicated in the loss of oral tolerance to gluten associated with celiac disease, and is under investigation for its oncolytic therapeutic potential (Bouziat et al., 2017; Twigger et al., 2008; Karapangiotou et al., 2012). Prototype strains that represent two of the major reovirus serotypes include Type 1 Lang (T1L) and Type 3 Dearing (T3D) (Rosen, 1960). These viruses differ in cell tropism, induction of cell responses, including innate immune signaling and cell death pathways, and pathogenesis in mouse models of disease. Robust reverse genetics systems permit genetic manipulation of T1L and T3D reoviruses (Kobayashi et al., 2007; Kobayashi et al., 2010). Reovirus particles exhibit icosahedral symmetry and are organized into two concentric capsid layers that encapsidate a genome composed of ten dsRNA genome segments, three large (L1-L3), three medium (M1-M3), and four small (S1-S4), that are present in equimolar amounts in purified particles (Shatkin, Sipe, and Loh, 1968). Following host cell entry and escape from the endosome, transcriptionally-active reovirus core particles release viral +RNA into the cytoplasm, where newly translated viral structural and non-structural proteins associate with one another and the host cell cytoskeleton to establish inclusions termed virus factories, which serve as sites of progeny virus assembly. Reovirus +RNAs are capped, non-polyadenylated, and typically contain a single open reading frame (ORF) flanked by 5′ and 3′ untranslated regions (UTRs). Within virus factories, assembling reovirus cores package viral +RNAs and an estimated 12 copies of the viral RNA-

dependent RNA polymerase (RdRp) and synthesize minus-strand RNA to form the dsRNA genome (Coombs, 1998). Newly assembled core particles undergo secondary transcription, synthesizing additional viral +RNA within virus factories (Miller et al., 2010).

While studies of reovirus RNAs, proteins, and particles have yielded insights into packaging, many facets of this complex problem remain incompletely understood. Reovirus RNA packaging signals are thought to reside in the 5′ and 3′ UTRs and extend into the adjacent ORF, with a sequence element in the 5′ end and structural elements in the 3′ end potentially contributing to packaging (Kobayashi et al., 2007; Demidenko et al., 2013; Roner, Bassett, and Roehr, 2004; Roner and Reohr, 2006; Roner and Steele, 2007; Zou and Brown, 1992). Rotavirus non-structural protein NSP2 binds viral +RNA, influences its structure, and is predicted to help nucleate virus assembly (Borodavka, Desselberger, and Patton, 2018; Borodavka et al., 2017). Reovirus non-structural proteins μNS and σNS, which is a predicted rotavirus NSP2 homolog, associate with reovirus +RNA and are components of assembling reovirus particles (Taraporewala and Patton, 2004; Antczak and Joklik, 1992). The reovirus RdRp, λ3, is thought to associate with +RNA at each of the five-fold icosahedral vertices, interacting preferentially with molecules containing G or U in the penultimate position (McDonald, Tao, and Patton, 2009; Tao et al., 2002; Zhang et al., 2003). Thus, non-structural proteins and λ3 may play important roles in packaging the reovirus genome. Finally, reovirus primarily generates two species of particles that can be separated based on differences in density (Smith, Zweerink, and Joklik, 1969). Higher-density virions appear “full” of RNA by negative-stain electron microscopy (EM) analysis and contain the complete viral

genome. Lower density top component (TC) particles have indistinguishable protein composition to virions but appear “empty” of RNA by negative-stain EM and cryo-EM (Smith, Zweerink, and Joklik, 1969; Dryden et al., 1998; Lai, Wérenne, and Joklik, 1973). Together, these characteristics suggest reovirus packaging is a highly regulated process resulting in encapsidation of either a complete set of viral genome segments or no segments at all (Borodavka, Desselberger, and Patton, 2018; McDonald and Patton, 2011). However, TC particles are reported to retain a level of infectivity, albeit a low level, even after multiple sequential rounds of purification, which is inconsistent with the complete lack of packaged viral RNA (Lai, Wérenne, and Joklik, 1973).

In addition to packaging the viral genome, many viruses package host cell RNA species. Host RNA packaging is especially common for retroviruses, including Rous sarcoma virus, Moloney murine leukemia virus, and human immunodeficiency virus, as well as for some bipartite and tripartite single-stranded RNA viruses such as brome mosaic virus and Flock House virus (FHV) (Bishop et al., 1970; Eckwahl et al., 2015; Huang et al., 1994; Routh, Domitrovic, and Johnson, 2012; Shrestha et al., 2018). There is tremendous variability in the amount of host RNA packaged by different viruses, with host RNA constituting up to 30% of total RNA in retrovirus virions but only about 1% in FHV virions (Routh, Domitrovic, and Johnson, 2012; Linial and Miller, 1990; Telesnitsky and Wolin, 2016). Many different types of host RNA can be packaged by viruses, including non-coding RNA (ncRNA), messenger RNA (mRNA), and endogenous retroelement RNAs (Telesnitsky and Wolin, 2016). FHV virus-like particles, which are formed from expressed viral proteins in the absence of viral nucleic acids, package significantly more host RNA than do virions (Routh, Domitrovic, and Johnson,

2012). The presence of equimolar ratios of packaged segments and an apparent “all-or-none” packaging strategy suggest that reovirus assortment and packaging are exquisitely specific and that host RNA is unlikely to be packaged. Studies of bluetongue virus (BTV) suggest that the smallest genome segments form *trans*-segment interactions that nucleate assembly of RNA complexes containing a full complement of genomic segments (AlShaikhahmed et al., 2018; Sung and Roy, 2014; Fajardo et al., 2017). There also is evidence for stable, sequence-specific interactions between rotavirus +RNAs (Borodavka et al., 2017). These studies further underscore the orderly nature of RNA packaging by viruses in the *Reoviridae* family. However, the detection of rotaviruses with segments containing duplications that have arisen following natural infection or laboratory passage and the recovery of recombinant rotaviruses engineered to contain duplicated or exogenous sequences up to 900 bp in length suggest there is at least some available space for packaging of additional RNA (Hundley et al., 1985; Ballard, McCrae, and Desselberger, 1992; Kojima et al., 2000; Komoto et al., 2018; Philip et al., 2019). Reovirus TC particles presumably have even more space available inside the particle. However, whether viruses in the *Reoviridae* family package host RNA is currently unknown.

In this Chapter, I sought to gain insight into RNA packaging by viruses in the *Reoviridae* family using reovirus as a model system. Reovirus virions and TC particles served as tools to elucidate reovirus packaging potential. I enriched for reovirus virions and TC particles and defined their RNA content using next-generation RNA-sequencing (NGS). As anticipated, reovirus virions almost exclusively packaged viral dsRNA, with enrichment of very few host-derived RNAs. In contrast, reovirus TC particles were

selectively enriched for numerous host RNA species, which constituted a substantial percent of overall RNA content. Host RNA selection by TC particles was not dependent on RNA abundance in the cell, and specifically enriched host RNAs varied for two reovirus strains independent of the viral RdRp. While the precise features of host RNA that facilitate packaging into TC particles remain to be elucidated, these findings suggest that genome packaging into reovirus virions is exquisitely selective, while RNA packaging into reovirus TC particles is more promiscuous than that of virions, yet selective nonetheless.

2.2. Coauthor Contributions

I generated all viruses by reverse genetics, purified virion and top component preparations, titrated viruses, extracted RNA for bioanalyzer, performed RT-qPCR, and prepared libraries for next-generation sequencing. Analysis of RNA by Bioanalyzer was performed by the Vanderbilt Technologies for Advanced Genomics (VANTAGE) core. Next-generation sequencing analysis was performed by Xiang Ye. Preparation of samples for negative-stain electron microscopy and imaging were conducted by Evan Krystofiak.

2.3. Results

2.3.1. Reovirus top component particles are less infectious than virions.

Reovirus TC particles are reported to retain a low level of infectivity, despite ostensibly lacking viral genomic RNA (Lai, Wérenne, and Joklik, 1973). To verify that TC particles are infectious, I enriched for recombinant strain (rs) T1L reovirus virions and TC particles by organic extraction and cesium chloride gradient ultracentrifugation from infected L cells. rsT1L TC could be cleanly separated from virions based on density (**Fig. 2-1A**). I also processed mock-infected L cells using the same organic extraction and cesium chloride gradient ultracentrifugation approach and collected samples migrating at identical locations in the gradient as virions and TC particles (mock virions and mock TC). To compare the protein composition of TC particles and virions, I resolved the enriched particles by SDS-PAGE, stained the proteins with colloidal Coomassie, and quantified protein band intensity. Using this approach, I was able to normalize for protein content between virions and TC particles based on protein band intensity per volume of loaded sample. After normalizing, I found that the relative proportions of reovirus proteins were approximately equal for virions and TC particles, although a few additional proteins, including bands migrating slightly below λ1 and μ1, were detected more prominently in TC than virion preparations (**Fig. 2-1B**). This normalization process was used in subsequent experiments to obtain equivalent amounts of virions and TC particles. By negative-stain electron microscopy (EM), enriched virions presented as electron-lucent particles, while most enriched TC particles had a dark, electron-dense interior, suggesting the absence of genomic RNA, as anticipated (**Fig. 2-1C**) (Smith, Zweerink, and Joklik, 1969; Lai, Wérenne, and Joklik,

1973). Some TC particles had a partially obscured or electron-lucent interior, though it was usually at least partially dark. Both virions and TC particles were about 80 nm in diameter. A noteworthy observation made using negative-stain EM was the detection of proteins that appeared as stacked ring-like structures. Far more of these structures were present in TC than virion preparations. However, they also were present at higher concentrations in mock-TC than mock-virion preparations, suggesting they are cellular protein complexes that migrate with a similar density to reovirus particles. To better assess the types of particles present, I quantified at least 100 particles in each of three independent preparations of rsT1L virions and TC particles based on appearance by negative-stain EM. I found that ~ 1% of particles in virion preparations appeared completely electron dense in the center, suggesting a low level of TC particle contamination (**Fig. 2-1D**). About 3% of particles in TC preparations appeared completely electron lucent, suggesting low-level virion contamination. Additionally, 22% of particles in TC preparations were partially dark and partially lucent in the center; these “indeterminate” particles might have packaged some viral or host RNA but not a complete reovirus genome. These observations suggest that our gradient centrifugation and manual fractionation approach permitted strong enrichment but not absolute purification of T1L TC particles, which are similar in protein composition to virions but appear to lack all or most of the viral genome.

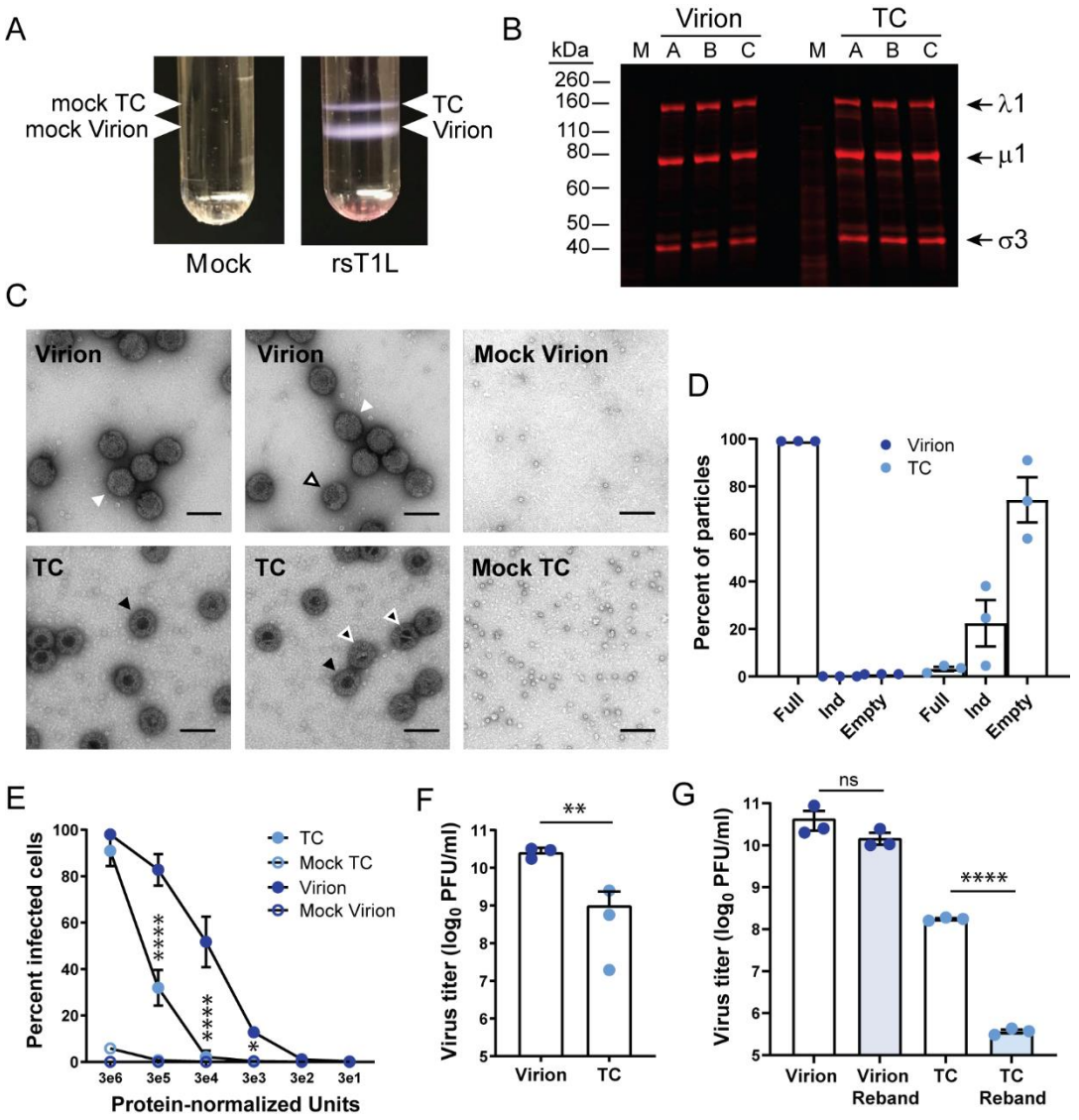

Figure 2-1. Low-density rsT1L reovirus TC particles have similar protein composition but are less infectious than virions. (A) L cells were adsorbed with medium (mock) or rsT1L reovirus at a MOI of 10 PFU/cell and incubated in suspension culture for 48 h prior to pelleting, sonication, and organic extraction. Ultracentrifugation in a cesium chloride density gradient was used to separate low-density TC particles from higher-density virions, as shown. Bands collected from the same positions in the gradient from processed mock-infected L cells are referred to as “mock virions” and “mock TC.” (B) Coomassie-stained SDS polyacrylamide gel on which equivalent protein concentrations of rsT1L reovirus virions and TC from three independently purified particle preparations were resolved by electrophoresis and imaged. Presumptive major viral structural proteins are indicated. (C) Negative-stain electron micrographs of density gradient-purified virions, TC particles, mock virions, and mock TC particles. Scale bar = 100 nm. White arrowheads indicate “full” virions. A white arrowhead with black outline indicates a partially uncoated virion. Black arrowheads indicate “empty” TC particles. Black

arrowheads with white outline indicate partially filled, indeterminate particles. (D) Quantitation of rsT1L virions and TC particles in EM images based on visual assessment as full, empty, or indeterminate. n = 3 independently purified preparations, at least 100 particles per preparation. (E) Monolayers of L cells were adsorbed with serial ten-fold dilutions of equivalent protein concentrations of rsT1L reovirus virions, TC particles, or mock preparations thereof for 1 h. Unbound particles were washed away, and cells were incubated for 16-20 h prior to fixation and staining to detect nuclei and reovirus proteins in virus factories. Percent infected cells were detected in four fields of view and averaged. Error bars represent standard deviation. n = 3 independently purified preparations. **, $p < 0.01$; ***, $p < 0.001$ for TC compared to virion by Sidak's multiple comparison test. (F) Monolayers of L cells were adsorbed with equivalent protein concentrations of rsT1L reovirus virions, TC particles, or mock preparations thereof for 1 h. Cells were overlaid with a medium agar mixture and incubated for one week, with an intermittent feed, prior to staining to detect live cells. Error bars represent standard deviation. Plaque titers for individual samples are shown. n = 3 independently purified preparations. **, $p < 0.01$ compared to virion by unpaired t test. (G) Virions and TC particles enriched by cesium chloride gradient ultracentrifugation were collected and re-banded by cesium chloride gradient ultracentrifugation. Monolayers of L cells were adsorbed with equivalent protein concentrations of rsT1L reovirus virions and TC particles derived from initial enrichment or rebanding for 1 h. Cells were overlaid with a medium agar mixture and incubated for one week, with an intermittent feed, prior to staining to detect live cells. Error bars represent standard deviation. Plaque titers were determined in triplicate. ****, $p < 0.0001$ by unpaired t test.

To quantify infectivity of the two enriched particle types, I adsorbed L cells with serial dilutions of protein-normalized rsT1L virions and TC particles and quantified infected cells after a single infectious cycle using a fluorescent focus assay. At the lowest dilution tested, both virions and TC particles could achieve high levels of infectivity (**Fig. 2-1E**). However, with non-saturating concentrations of particles, virions were ~2.5 to 25 times more infectious than TC particles, and TC required ~100 times more particles than virions to infect at least 1% of cells. Titration of virions and TC particles by plaque assay indicated that virions contained an average of ~ 30 times more infectious PFU per protein-normalized unit than TC particles, though the range was broad, from ~10-1,300 times more infectious units for the three independent preparations (**Fig. 2-1F**). There was no gross visible difference in plaque size between virions and TC particles (not

shown). To further assess the effects of contaminating virions on TC particle infectivity, I enriched a preparation of virions and TC particles with two sequential rounds of organic extraction and cesium chloride gradient ultracentrifugation. I collected and determined the titer of protein-normalized virion and TC particle samples following each round of enrichment (**Fig. 2-1G**). In the initial enriched preparations, protein-normalized virions contained ~ 250 times as many infectious units per volume as TC particles. The titer of virions decreased slightly but not significantly per protein-normalized unit following rebanding. However, the titer of TC particles decreased to nearly 1/500th the infectivity of the initial enriched TC preparation per protein-normalized unit following rebanding. Together, these findings suggest that enriched virion preparations are far more infectious than TC particle preparations, but much of the residual infectivity detected in enriched TC particle preparations likely derives from low levels of contaminating virions.

2.3.2. Reovirus particles contain viral double-stranded RNA.

To visualize the RNA content of enriched rsT1L virion and TC particle preparations based on electrophoretic mobility, I used Bioanalyzer analysis. Particles were mock-treated or treated with benzonase to remove extra-particle nucleic acids. Then, RNA was extracted and resolved. RNA concentration and electrophoretic profiles differed markedly between mock-treated and benzonase-treated particles and between virions and TC particles. In the absence of benzonase treatment, strong signals from rsT1L virion-extracted RNA were detected at a small size between 25 and 200 nt and then from ~ 1,000 to nearly 4,000 nt, with distinct signals from ~1,000 to 2,000 nt, which may represent reovirus +RNAs (**Fig. 2-2A**). Following benzonase treatment, RNA

concentration was reduced to less than 1/100th the untreated level. Signal for the smallest RNAs largely disappeared, and RNA molecules packaged within rsT1L virions exhibited a distinct laddering pattern between ~ 2,000 and 3,000 nt, which may represent reovirus dsRNA genome segments. Overall RNA concentrations for protein-normalized TC particle equivalents were substantially lower than those of virions. In the absence of benzonase treatment, RNA extracted from TC particle preparations detectably contained only small RNAs between 25 and 200 nt. Following benzonase treatment of TC particles, RNA concentration was reduced to ~1/10th the untreated level. Small RNAs were still detected in TC-extracted RNA, as were many other bands, including two that were similar in size to 18s and 28s ribosomal RNA (rRNA). These findings suggest that TC particles encapsidate RNA, perhaps including small RNAs, but they do not encapsidate similar levels of viral genomic RNA as do virions.

To determine whether TC particles encapsidate viral RNA, I isolated RNA from protein-normalized equivalents of enriched rsT1L virions and TC particles, or equal volumes of contemporaneously purified mock preparations thereof. I generated cDNA by reverse transcription with random hexamers and quantified the relative abundance of S4 transcripts using primers specific for reovirus T1L S4 +RNA. I found that purified TC particles contain significantly more S4 +RNA than mock TC preparations (**Fig. 2-2B**). However, consistent with Bioanalyzer results and their enhanced infectivity, virions contained significantly more S4 +RNA than TC particles (**Figs. 2-1D-E and 2-2A-B**).

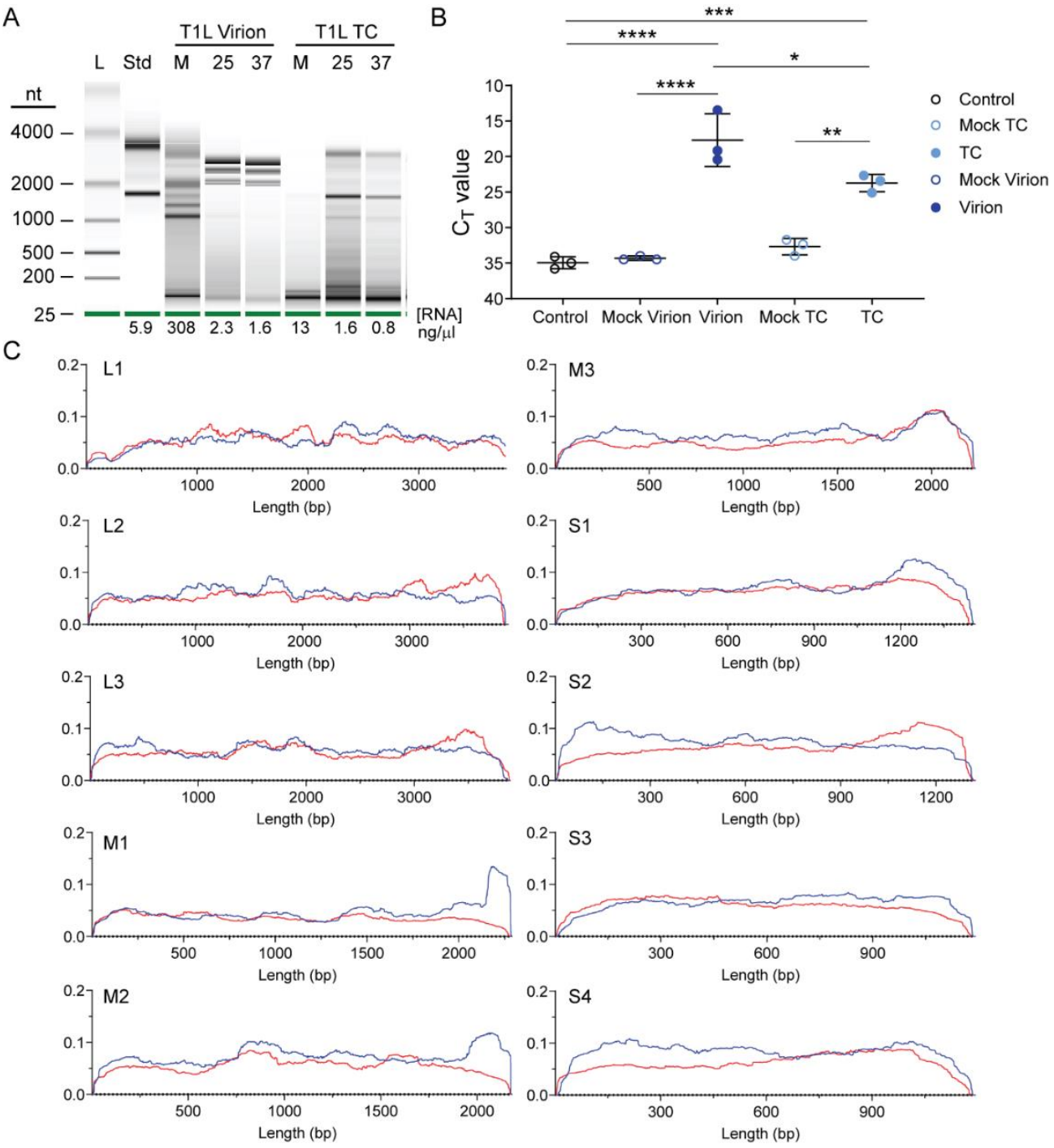

Figure 2-2. Enriched reovirus rsT1L TC particles package viral RNA. (A) Enriched rsT1L virions and TC particles were mock treated at 25°C (M) or treated with benzonase at 25°C (25) or 37°C (37) to remove extra-particle nucleic acids. RNA was extracted, quantified, and resolved on a pico RNA chip using an Agilent Bioanalyzer. Shown are electrophoresis results, with the size of the ladder (L) in nucleotides indicated. A standard (Std) indicates eukaryotic 18s and 28s rRNA peaks. RNA concentration is indicated below each lane. (B) S4 RT-qPCR analysis of virions and TC particles. RNA

was extracted from three independent, protein normalized rsT1L virion and TC particle preparations and equal volumes of a contemporaneously purified mock virion or TC preparation. cDNA was reverse transcribed using random hexamers, and qPCR reactions were conducted in the presence of primers specific for T1L S4. Nuclease-free water was added to control reactions in the place of template RNA. Shown are raw C_T values for the three independent rsT1L particle preparations or single mock preparations in triplicate. *, $p < 0.05$; **, $p < 0.01$; ***, $p < 0.001$; ****, $p < 0.0001$ by Sidak's multiple comparison test. (C) Scaled Illumina read counts at each site for each segment in a representative rsT1L TC particle preparation. Segment identity and length (x-axis) in bases are shown. Multiplication of the scaled y-axis factor by 1,000,000 will reveal coverage at each site in CPM for plus-strand and minus-strand reads, which are indicated by red and blue lines, respectively.

To quantify and determine the strandedness of packaged rsT1L TC RNA compared with that of virions, I used NGS. To minimize the influence of extra-particle nucleic acids on sequencing results, I treated virions and TC particles with benzonase prior to RNA extraction. I generated randomly primed, directional libraries using RNA extracted from three independent preparations of rsT1L TC, two independent preparations each of rsT1L virions and total RNA from rsT1L-infected L cells, the cell type from which the particles had been purified, or from mock-virion and mock-TC preparations, and I sequenced them using Illumina technology. Both rsT1L virions and TC particles contained reads mapping to the full length of both strands for all ten T1L reovirus genome segments, although there were fewer viral reads in TC particles than in virions (**Table 2-1**). On average, rsT1L particles contained slightly more reads mapping to the plus-strand, 57.6% and 62.2% of total viral reads for virions and TC, respectively, than reads mapping to the minus-strand, 42.4% and 37.8% of total viral reads for virions and TC, respectively. These percentages are relatively consistent with the packaging of dsRNA, though slightly skewed towards +RNA. In contrast, for rsT1L-infected L cells, an average of 91% of reads mapped to the plus-strand, while 9% of reads mapped to the

minus-strand, consistent with the presence of an abundance of +RNA transcripts in cells (**Table 2-1**). To determine if enriched TC particles package full-length segments, I analyzed read coverage for the plus- and minus-strands of all ten genome segments. For TC particles, read coverage was relatively uniform across the plus- and minus-strand of all genome segments, with the clearest exceptions in the minus-strands of the M1 and M2 genome segments, which exhibited denser coverage at the 5′ end (**Fig. 2-2C**). Based on the assumption that each reovirus RNA segment should be represented equivalently, I adjusted the percent of anticipated NGS reads based on segment length and determined whether the observed percent of viral reads mapping to each segment matched our expectation (**Fig. 2-3A**). For rsT1L-infected L cells, the observed percent of reads mapping to L1 and M1 were lower and those mapping to M3 and S3 were higher than expected, suggesting that differences in +RNA stability or transcription efficiency may result in deviation from the anticipated RNA read ratios. However, only the percent of reads mapping to M3 in rsT1L virions differed significantly from the segment's percent of total viral genome length, and no rsT1L TC segments differed in observed versus expected percentages of mapped reads based on segment length. Together, these findings suggest rsT1L TC particles encapsidate all ten reovirus dsRNA genome segments in the expected ratios for complete genomes but at reduced overall levels compared to virions. It is possible that some TC particles encapsidate incomplete reovirus genomes. However, considering the presence of a small percentage of "full" particles in TC preparations and the significant decrease in infectivity observed following TC rebanding, much of the detected viral RNA content may be derived from contaminating virions (**Figs. 2-1D,G**). When using rsT1L virions as reference, rsT1L TC

samples were positively correlated with the mock virion layer; the Pearson correlation coefficient is ~ 0.37, which is consistent with, but fails to definitively indicate, possible contamination between the layers.

Table 2-1. Viral reads from rsT1L-infected L cells and rsT1L or rsT3D^{I}T1L1 TC or virions.

Segm	**Number and percent of total viral reads**									
	Inf-A[a]	**Inf-B**	**%**	**T1L**	**T1L**	**T1L**	**%**	**T1L V-**	**T1L**	**%**
T1L	1,038,	1,06	1	1,129,7	177,57	1,423,8	1	3,447,	2,877,	1
T1L	1,940,	2,05	1	1,259,8	217,04	1,638,2	1	4,181,	3,428,	1
T1L	1,410,	1,56	1	1,243,1	211,30	1,611,8	1	3,809,	3,704,	1
T1L	828,7	888,	8	860,79	457,74	754,08	1	2,229,	2,057,	7
T1L	880,2	987,	9	1,079,9	386,97	1,047,8	1	3,286,	3,834,	1
T1L	1,580,	1,57	1	829,20	257,31	990,19	1	3,435,	4,379,	1
T1L	742,2	659,	6	705,96	76,568	722,03	6	2,210,	2,136,	8
T1L	650,8	621,	6	663,15	211,49	695,39	8	2,020,	2,187,	7
T1L	922,9	900,	8	622,47	169,08	554,90	7	2,109,	2,326,	8
T1L	799,8	752,	7	663,23	220,08	638,50	8	2,158,	2,495,	8
				T3D^{I}	**T3D^{I}**	**T3D^{I}**	**%**	**T3D^{I}**	**T3D^{I}**	**%**
T1L				765,38	755,87	841,39	6	4,508,	2,323,	1
T3D				1,607,5	1,377,4	1,876,7	1	3,165,	3,399,	1
T3D				1,902,6	2,076,9	3,083,1	1	4,751,	4,271,	1
T3D				825,55	652,10	620,49	6	4,088,	1,424,	1
T3D				1,756,6	2,928,3	2,766,2	1	4,041,	4,738,	1
T3D				2,218,4	2,812,8	3,649,3	2	5,792,	4,661,	1
T3D				526,48	684,41	619,58	5	347,90	1,347,	3
T3D				378,20	403,54	313,40	3	137,27	835,8	2
T3D				685,21	691,05	1,147,2	6	261,88	1,439,	3
T3D				378,87	527,15	514,22	4	2,156,	1,105,	6
Segm	**Number and percent of plus-strand viral reads per segment[c]**									
	Inf-A	**Inf-B**	**%**	**T1L**	**T1L**	**T1L**	**%**	**T1L V-**	**T1L**	
T1L	967,4	926,	9	559,48	72,257	716,91	4	1,478,	1,239,	4
T1L	1,715,	1,68	8	600,38	76,108	831,88	4	1,778,	1,542,	4
T1L	1,318,	1,38	9	643,64	136,57	824,85	5	1,947,	2,259,	5
T1L	776,8	756,	9	592,36	407,33	451,15	7	1,247,	1,246,	5
T1L	842,0	877,	9	676,67	357,04	610,16	7	2,086,	2,948,	7
T1L	1,524,	1,46	9	499,05	214,59	550,53	6	2,069,	3,280,	6
T1L	642,1	543,	8	385,85	48,236	392,04	5	1,144,	1,105,	5
T1L	631,3	568,	9	413,15	190,92	379,51	6	1,099,	1,249,	5

T1L	884,7	829,	9	371,08	146,71	299,73	6	1,238,	1,588,	6
T1L	765,5	705,	9	411,37	206,93	369,63	7	1,331,	1,754,	6
				T3D^{I}	**T3D^{I}**	**T3D^{I}**	**%**	**T3D^{I}**	**T3D^{I}**	**%**
T1L				420,93	444,64	462,29	5	2,284,	1,284,	5
T3D				1,176,8	1,101,9	1,632,3	8	1,614,	2,418,	6
T3D				1,625,2	1,809,9	2,809,0	8	2,431,	3,306,	6
T3D				496,59	436,26	424,14	6	2,036,	878,3	5
T3D				1,600,3	2,775,4	2,623,8	9	2,195,	4,406,	7
T3D				2,035,1	2,626,6	3,547,8	9	3,120,	4,304,	7
T3D				421,81	604,23	561,39	8	198,14	1,167,	7
T3D				257,66	299,37	250,12	7	71,453	620,8	6
T3D				617,93	619,14	1,122,1	9	134,51	1,292,	7
T3D				296,97	417,18	449,19	8	1,113,	889,5	6

[a] Inf, total RNA from infected cells; A, B, and C refer to independent particle, RNA, and library preparations.

[b] V, virions

[c] Remaining viral reads totaling 100% and the number from the top portion of the table are minus-strand reads.

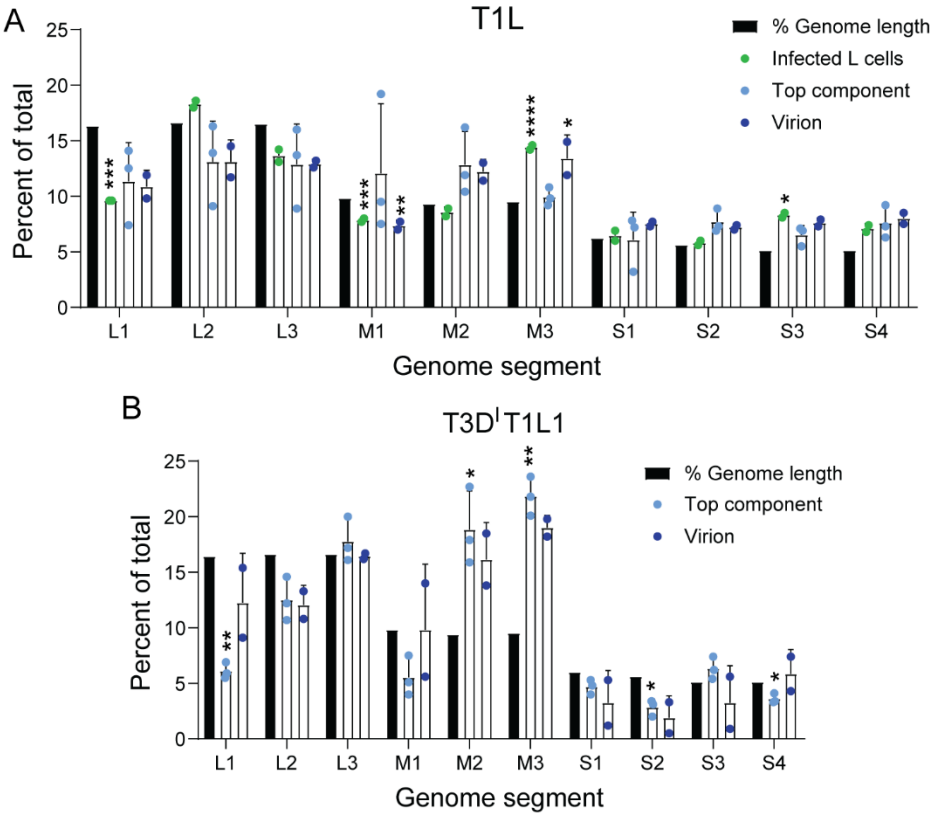

Figure 2-3. Percent of packaged viral reads for each reovirus segment. The percent of total T1L reference genome length was calculated for each genome segment and is indicated with a black bar. Numbers of viral reads from Illumina-ready libraries mapping to each segment were identified by alignment with the reference sequence. The percent of total viral reads was calculated for each particle type. Shown are percentages calculated for TC (light blue), virions (dark blue), or infected L cells (green) for rsT1L (A) or rsT3D^{I}T1L1 (B). Error bars represent standard deviation. n = 2 or 3 independent library preparations. *, $p < 0.05$; **, $p < 0.01$; ***, $p < 0.001$ compared to percent of total T1L reference genome length by one-sample t test.

2.3.3. Top component particles contain host RNA.

NGS can identify non-viral RNA species, as well as viral RNA species, contained within virions and TC particles. While more than 99.9% of reads from RNA in rsT1L virions aligned with viral sequences, only ~ 18-74% of reads from RNA in rsT1L TC particles were viral, with remaining reads mapping to host transcripts (**Table 2-2**). To determine whether any cellular RNAs were preferentially packaged in rsT1L virions and TC particles, I compared read counts mapping to genes of the *Mus musculus* genome from virions and TC particles to mock particle preparations. I set stringent cutoffs of a *p* value < 0.01 and a greater than eight-fold change over mock to identify limited sets of host genes that were significantly enhanced in the data sets (**Fig. 2-4A and Table 2-3**). All ten T1L reovirus genes were identified for both virions and TC and, unsurprisingly, exhibited the highest fold change over mock. rsT1L TC showed a significant increase in reads mapping to 34 host genes relative to mock TC preparations, while virions did not show a significant increase in read count for any host gene relative to mock virion preparations. Of note, about three quarters of all genes that were significantly enriched for rsT1L TC were histone-encoding genes (**Table 2-3**). Many reads aligning with 18s rRNA were detected in TC preparations, in accordance with Bioanalyzer results, but they were not significant when compared with mock TC preparations (**Fig. 2-2A and**

Table 2-3). Gene set over-representation analyses indicated significant enrichment of host genes involved in ribonucleoprotein complex biogenesis, non-coding RNA processing, DNA conformation changes, and several other processes (**Fig. 2-4D**). I used RT-qPCR to validate the presence of transcripts encoding host genes HIST1H1E and HIST1H2AI, which were significantly enriched by our standards, and HIST2H3C2, which was significant by p-value but just missed our significance cutoff for CPM. Though differences were modest, as expected based on low numbers of mapped reads, two of these genes had significantly lower C_T values in TC than mock TC preparations, suggesting they are enriched in rsT1L TC particles, and the third gene trended towards lower C_T values in TC particles (**Fig. 2-4C**). These observations suggest that rsT1L virions specifically package viral transcripts to the exclusion of host transcripts, but numerous host transcripts are enriched in rsT1L TC particles.

Table 2-2. Percent of viral and cellular reads from rsT1L-infected L cells and rsT1L or rsT3D^{l}T1L1 TC particles or virions.

Sample	Viral	Host	Percent	Percent
Mock Inf-A[a]	413	999,58	<0.1	>99.9
Mock Inf-B	332	999,66	<0.1	>99.9
T1L Inf-A	762,352	237,64	76	24
T1L Inf-B	798,981	201,01	80	20
Mock TC	387	999,61	<0.1	>99.9
T1L TC-A	587,065	412,93	59	41
T1L TC-B	178,652	821,34	18	82
T1L TC-C	742,350	257,65	74	26
T3D^{l}T1L1 TC-	663,806	336,19	66	34
T3D^{l}T1L1 TC-	700,570	299,43	70	30
T3D^{l}T1L1 TC-	763,056	236,94	76	24
Mock Virion	697	999,30	<0.1	>99.9
T1L Virion-A	999,792	208	>99.9	<0.1
T1L Virion-B	999,609	391	>99.9	<0.1
T3D^{l}T1L1	999,901	99	>99.9	<0.1
T3D^{l}T1L1	998,510	1,490	99.9	0.1

[a] Inf, total RNA from mock-infected or T1L reovirus-infected cells; A, B, and C refer to independent sample and library preparations.

It is possible that TC packaging of host RNAs is due to the abundance of RNA species within the cell and that increased expression of host genes in response to infection may drive non-specific packaging of host RNA. Therefore, I also conducted NGS analysis on total RNA extracted from mock-infected and rsT1L-infected L cells. Viral reads accounted for a significant portion (~ 76-80%) of total reads for RNA extracted from rsT1L-infected L cells. However, relative to mock-infected cells, rsT1L-infected cells displayed a significant increase in 105 host genes (**Fig. 2-4B**). Of the 34 host genes significantly enhanced in rsT1L TC particles over mock TC particles, none were significantly increased in expression in rsT1L-infected cells compared to mock-infected cells (**Fig. 2-4A-B**). Consistent with these findings, gene set over-representation analyses indicate distinct biological functions for genes upregulated in rsT1L TC and rsT1L-infected cells, with transcripts involved in cell-cycle regulation, the response to virus infection, RNA catabolic processes, and regulation of mRNA metabolic processes enriched in infected L cells (**Fig. 2-4E**). Accordingly, the Pearson correlation coefficient between mock-virion versus mock-TC preparations compared to rsT1L virion versus TC preparations is ~ 0.007, which suggests that RNA associated with particles differs from host RNA in the mock corresponding layer. Together, these observations suggest that increased expression of host genes in response to infection is not the primary determinant of host gene packaging by rsT1L TC particles.

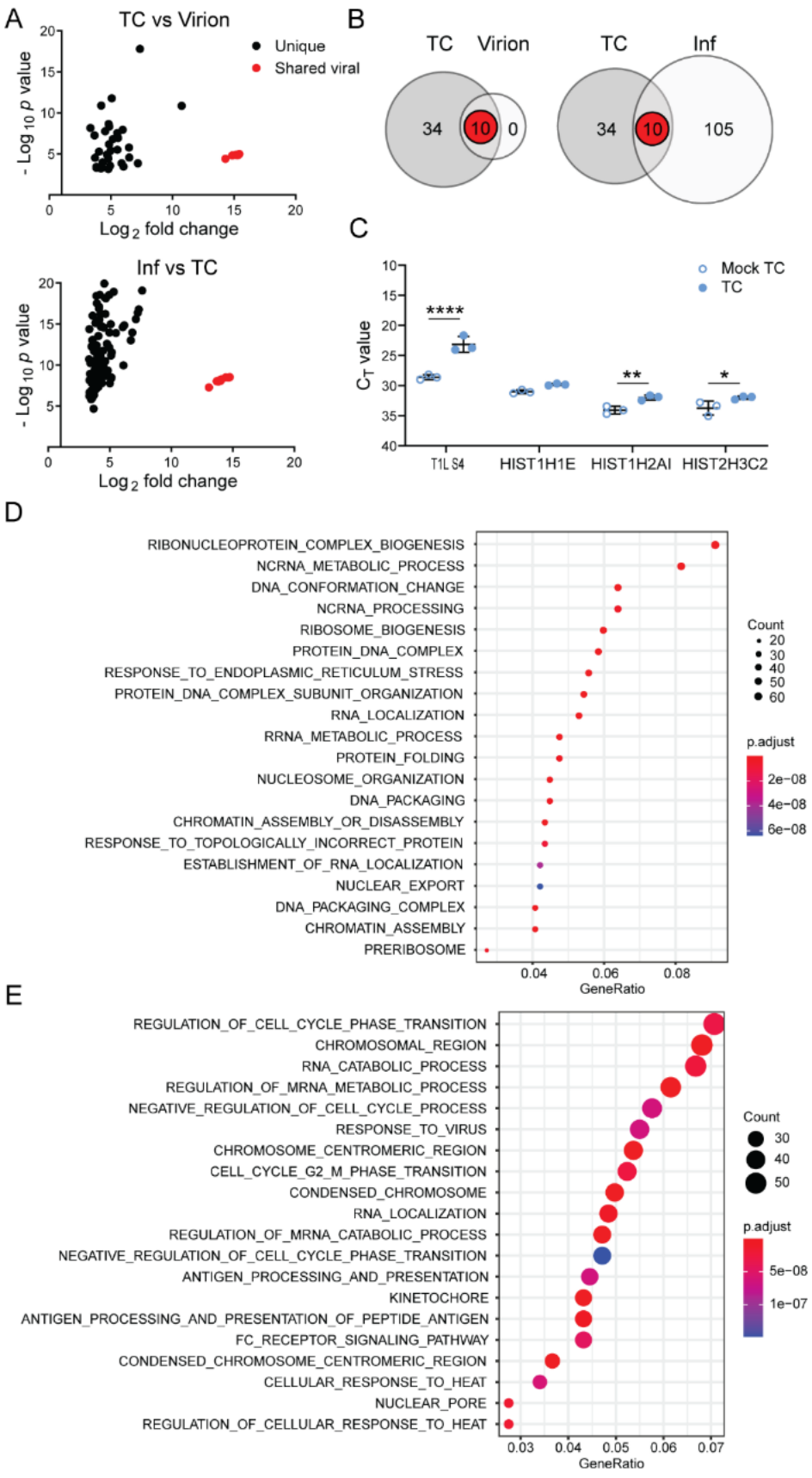
A
TC vs Virion
Unique
Shared viral
- Log 10 p value
Log 2 fold change
Inf vs TC
B
TC
Virion
34
10
0
TC
Inf
34
10
105
C
Mock TC
TC
****
**
*
C T value
T1L S4
HIST1H1E
HIST1H2AI
HIST2H3C2
D
RIBONUCLEOPROTEIN_COMPLEX_BIOGENESIS
NCRNA_METABOLIC_PROCESS
DNA_CONFORMATION_CHANGE
NCRNA_PROCESSING
RIBOSOME_BIOGENESIS
PROTEIN_DNA_COMPLEX
RESPONSE_TO_ENDOPLASMIC_RETICULUM_STRESS
PROTEIN_DNA_COMPLEX_SUBUNIT_ORGANIZATION
RNA_LOCALIZATION
RRNA_METABOLIC_PROCESS
PROTEIN_FOLDING
NUCLEOSOME_ORGANIZATION
DNA_PACKAGING
CHROMATIN_ASSEMBLY_OR_DISASSEMBLY
RESPONSE_TO_TOPOLOGICALLY_INCORRECT_PROTEIN
ESTABLISHMENT_OF_RNA_LOCALIZATION
NUCLEAR_EXPORT
DNA_PACKAGING_COMPLEX
CHROMATIN_ASSEMBLY
PRERIBOSOME
GeneRatio
Count
p.adjust
E
REGULATION_OF_CELL_CYCLE_PHASE_TRANSITION
CHROMOSOMAL_REGION
RNA_CATABOLIC_PROCESS
REGULATION_OF_MRNA_METABOLIC_PROCESS
NEGATIVE_REGULATION_OF_CELL_CYCLE_PROCESS
RESPONSE_TO_VIRUS
CHROMOSOME_CENTROMERIC_REGION
CELL_CYCLE_G2_M_PHASE_TRANSITION
CONDENSED_CHROMOSOME
RNA_LOCALIZATION
REGULATION_OF_MRNA_CATABOLIC_PROCESS
NEGATIVE_REGULATION_OF_CELL_CYCLE_PHASE_TRANSITION
ANTIGEN_PROCESSING_AND_PRESENTATION
KINETOCHORE
ANTIGEN_PROCESSING_AND_PRESENTATION_OF_PEPTIDE_ANTIGEN
FC_RECEPTOR_SIGNALING_PATHWAY
CONDENSED_CHROMOSOME_CENTROMERIC_REGION
CELLULAR_RESPONSE_TO_HEAT
NUCLEAR_PORE
REGULATION_OF_CELLULAR_RESPONSE_TO_HEAT
GeneRatio
Count
p.adjust

Figure 2-4. Reovirus rsT1L TC particles package host RNA. (A) Graphs showing host genes packaged by rsT1L TC that have a p value < 0.01 and fold change > eight compared to mock TC. Red and pink indicate shared viral and host genes, respectively, between rsT1L TC and virions (upper) or rsT1L-infected L cells (lower). (B) Venn diagrams showing overlap in host genes with a p value < 0.01 and fold change > eight between rsT1L TC and virions (left) or between rsT1L TC and rsT1L-infected L cells (right). Red indicates shared viral genes, and pink indicates shared host genes. (C) RT-qPCR validation of significant viral and host genes in TC compared to mock TC. RNA was extracted from three independent, protein normalized rsT1L TC particle preparations and equal volumes of contemporaneously purified mock TC preparations. cDNA was reverse transcribed using random hexamers, and qPCR reactions were conducted in the presence of primers specific for the indicated target gene. Shown are raw C_T values. *, $p < 0.05$; **, $p < 0.01$; ****, $p < 0.0001$ by Sidak's multiple comparison test. (D-E) Gene set over-representation analyses with GO terms. The p value is indicated by circle color, and transcript count is indicated by circle size, as shown in the legend. (D) Analysis of host genes packaged by rsT1L TC. (E) Analysis of host genes significantly upregulated in rsT1L-infected L cells.

Table 2-3. Viral and host transcripts packaged by rsT1L and rsT3D^{I}T1L1 particles.

Gene Identifier	Log_2F	*p* Value	SYMBOL
rsT1L Virions Significant Genes[b]			
gb|M24734.1|	16.8	7.3E-06	T1L L1
gb|AF378003.1|	17.4	3.4E-06	T1L L2
gb|AF129820.1|	17.2	3.7E-06	T1L L3
gb|AF461682.1|	17.8	2.9E-06	T1L M1
gb|AF490617.1|	17.7	2.5E-06	T1L M2
gb|AF174382.1|	17.8	2.5E-06	T1L M3
gb|EF494445.1|	17.5	2.4E-06	T1L S1
gb|L19774.1|	17.6	2.3E-06	T1L S2
gb|M18389.1|	17.6	2.3E-06	T1L S3
gb|M13139.1|	17.5	2.4E-06	T1L S4
rsT1L TC Significant Genes			
gb|M24734.1|	14.3	3.9E-05	T1L L1
gb|AF378003.1|	15.3	1.4E-05	T1L L2
gb|AF129820.1|	15.3	1.4E-05	T1L L3
gb|AF461682.1|	15.4	1.1E-05	T1L M1
gb|AF490617.1|	15.4	1.3E-05	T1L M2
gb|AF174382.1|	15.3	1.4E-05	T1L M3
gb|EF494445.1|	15.2	1.2E-05	T1L S1
gb|L19774.1|	15.4	1.0E-05	T1L S2
gb|M18389.1|	14.9	1.6E-05	T1L S3
gb|M13139.1|	15.1	1.3E-05	T1L S4
ENSMUST000000832	7.2	1.4E-04	Vaultrc5
ENSMUST000000620	6.0	3.5E-04	Hist1h1e
ENSMUST000001475	6.5	2.8E-05	Lmna
ENSMUST000000988	5.9	1.4E-04	Hist2h3b
ENSMUST000000792	4.9	2.8E-04	Hist1h2bg
ENSMUST000001029	4.3	4.1E-04	Hist1h4c
ENSMUST000000747	4.2	5.9E-04	Hist1h2ak
ENSMUST000000453	4.8	6.9E-04	Hist1h1d
ENSMUST000000997	4.3	4.5E-04	Hist1h2bb
ENSMUST000001029	3.8	5.0E-04	Hist1h4n
ENSMUST000001029	4.3	1.1E-04	Hist1h4k
ENSMUST000000701	5.5	3.2E-06	Hist1h2ai
ENSMUST000001029	4.8	3.7E-05	Hist1h2ae

ENSMUST000000917	4.8	2.2E-05	Hist1h3c
ENSMUST000000877	4.7	1.1E-05	Hist1h4j
ENSMUST000000783	5.0	4.1E-06	Hist1h2ab
ENSMUST000000917	6.0	1.2E-08	Hist1h2bn
ENSMUST000001449	4.9	4.7E-09	Pex6
ENSMUST000001711	3.7	2.9E-05	Hist1h2ac
ENSMUST000000917	5.6	1.1E-07	Hist1h3b
ENSMUST000000917	3.8	3.7E-04	Hist1h2al
ENSMUST000001051	4.8	6.5E-07	Hist1h2bf
ENSMUST000001887	4.0	5.3E-06	Hist1h3h
ENSMUST000000917	5.5	2.9E-08	Hist1h2bl
ENSMUST000002246	5.2	1.6E-07	Hist1h2bm
ENSMUST000002243	4.5	1.8E-08	Hist1h2bh
ENSMUST000001362	4.2	1.3E-11	Rpl7a
ENSMUST000001499	5.1	1.6E-12	Ctu2
ENSMUST000000732	10.8	1.4E-11	Hist1h2af
ENSMUST000000907	4.8	2.3E-09	Hist1h2ad
ENSMUST000001812	6.5	1.7E-06	Gm26870
ENSMUST000001596	7.4	1.6E-18	Acat2
ENSMUST000001072	3.3	6.9E-09	Rpl27
ENSMUST000000917	3.7	5.6E-08	Hist1h2an
rsT3D^{l}-T1L1 Virions Significant Genes			
gb|M24734.1|	18.1	2.9E-06	T1L L1
gb|EF494436.1|	17.3	4.2E-06	T3D L2
gb|EF494437.1|	17.6	3.9E-06	T3D L3
gb|EF494438.1|	17.9	2.7E-06	T3D M1
gb|EF494439.1|	18.1	2.8E-06	T3D M2
gb|EF494440.1|	18.1	3.1E-06	T3D M3
gb|EF494441.1|	16.6	4.2E-06	T3D S1
gb|EF494442.1|	15.7	6.3E-06	T3D S2
gb|EF494443.1|	16.7	4.0E-06	T3D S3
gb|EF494444.1|	17.7	2.6E-06	T3D S4
rsT3D^{l}-T1L1 TC Significant Genes			
gb|M24734.1|	14.0	4.6E-05	T1L L1
gb|EF494436.1|	15.6	1.4E-05	T3D L2
gb|EF494437.1|	15.8	1.3E-05	T3D L3
gb|EF494438.1|	14.5	3.0E-05	T3D M1
gb|EF494439.1|	16.1	1.1E-05	T3D M2
gb|EF494440.1|	15.7	1.5E-05	T3D M3
gb|EF494441.1|	15.5	8.7E-06	T3D S1

gb|EF494442.1|	15.4	7.1E-06	T3D S2
gb|EF494443.1|	16.2	5.2E-06	T3D S3
gb|EF494444.1|	14.7	2.1E-05	T3D S4
ENSMUST000000988	5.8	1.5E-04	Hist2h3b
ENSMUST000000455	7.8	1.2E-07	Socs7
ENSMUST000000339	4.7	1.5E-04	Dusp4
ENSMUST000000320	7.4	2.5E-07	Fbxl14
ENSMUST000000469	4.6	7.1E-05	Usp31
ENSMUST000001475	5.8	3.7E-06	Ccdc6
ENSMUST000000798	3.5	4.0E-04	Znrf2
ENSMUST000000500	4.5	1.9E-05	Arf6
ENSMUST000001783	4.1	2.6E-04	Itpripl2
ENSMUST000000528	5.3	5.9E-07	Mib1
ENSMUST000000079	4.0	3.7E-04	Hnrnpa0
ENSMUST000000939	3.9	4.9E-04	Ccnd1
ENSMUST000001061	3.8	5.3E-05	Foxk2
ENSMUST000000731	6.8	4.2E-14	Ctdspl
ENSMUST000000585	5.7	1.9E-08	Ccni
ENSMUST000000352	4.9	2.1E-07	Prkar2a
ENSMUST000000228	4.9	1.8E-06	Ank
ENSMUST000000449	3.4	2.3E-05	Slc30a1
ENSMUST000000691	5.6	4.8E-10	Zcchc24
ENSMUST000001028	11.4	1.6E-15	Ifit1
ENSMUST000000854	7.9	6.8E-12	Isg15
ENSMUST000000701	4.2	1.6E-04	Hist1h2ai
ENSMUST000001499	5.0	3.6E-08	Inafm2
ENSMUST000000504	4.0	9.4E-07	Tob2
ENSMUST000000138	3.6	2.5E-06	Pten
ENSMUST000001028	10.7	2.1E-09	Ifit3
ENSMUST000000783	4.0	1.2E-04	Hist1h2ab
ENSMUST000001812	6.3	3.2E-06	Gm26870
ENSMUST000000085	4.0	2.2E-06	Carhsp1
ENSMUST000000348	5.2	1.0E-10	Ptpn9
ENSMUST000000286	4.0	9.5E-06	Syt13
ENSMUST000002246	4.4	4.4E-06	Hist1h2bm

[a] FC, fold change over mock

[b] Significant genes exhibit at least eight-fold change over matched mock preparations and *p* values < 0.01.

[c] Symbols in gray text initially showed as “NA” but were identified using a manual search at *ensembl.org*.

2.3.4. The viral polymerase fails to confer complete host RNA packaging specificity.

Concurrent with or following encapsidation in assembling virus particles, viral +RNA transcripts associate with the RdRp, λ3, which is encoded by the L1 segment and synthesizes -RNA to form genomic dsRNA from +RNA templates (McDonald, Tao, and Patton, 2009; Tao et al., 2002). Whether λ3 is important for viral RNA packaging is unknown. However, since rsT1L TC particles contain viral dsRNA, λ3 must associate with packaged viral +RNAs to synthesize the minus-strand. To determine if λ3 specifies the host genes packaged within TC particles, I sequenced RNA packaged by virions and TC particles of recombinant strain T3D^{I}T1L1 reovirus. rsT3D^{I}T1L1 is a T3D reovirus into which a T249I mutation has been engineered in the attachment protein that renders it resistant to proteolytic cleavage, and the λ3-encoding T3D L1 gene has been replaced with that of T1L (Kobayashi et al., 2007). rsT3D^{I}T1L1 produced virions and TC particles in L cells. I generated libraries using RNA extracted from multiple preparations of enriched, benzonase-treated rsT3D^{I}T1L1 virions and TC particles and sequenced them using Illumina technology. When using rsT3D^{I}T1L1 virions as reference, rsT3D^{I}T1L1 TC samples were positively correlated with the mock virion layer; the Pearson correlation coefficient is ~ 0.15, which fails to definitively indicate contamination between the layers. rsT3D^{I}T1L1 TC particles contained reads mapping to all ten viral genome segments (**Table 2-1 and Fig. 2-3B**). However, the percent of viral reads mapping to each segment were less consistent with the expected percentages for rsT3D^{I}T1L1 virions and TC particles than those of rsT1L. Whereas nearly all viral reads in rsT1L virions and TC particles mapped to segments in the expected percentages based on length,

significantly more reads than expected mapped to the M2 and M3 segments, and significantly fewer reads mapped to the L1, L2, and S4 segments in rsT3D^{I}T1L1 TC particles (**Table 2-1 and Fig. 2-3B**). While they did not reach the level of statistical significance, similar trends were observed for rsT3D^{I}T1L1 virions. Proportions of plus-strand to minus-strand viral reads for RNA extracted from rsT3D^{I}T1L1 TC particles also differed substantially from the ~ 50% expected for genomic dsRNA (**Table 2-1**). Of all reads mapping to viral genes, on average, rsT3D^{I}T1L1 virions had 65.2% plus-strand and 34.8% minus-strand reads, while rsT3D^{I}T1L1 TC had 81.2% plus-strand and 18.8% minus-strand reads. These findings suggest that rsT3D^{I}T1L1 TC particles package non-equimolar quantities of the ten reovirus genome segments and disproportionately package viral +RNA or fail to consistently synthesize the minus-strand.

Similar to rsT1L virions, more than 99.8% of reads from RNA in rsT3D^{I}T1L1 virions aligned with viral sequences (**Table 2-2**). However, consistently higher percentages of reads from RNA in rsT3D^{I}T1L1 TC particles were viral (~ 66-76%), with remaining reads mapping to host transcripts. To determine whether any host cell RNAs were preferentially packaged within rsT3D^{I}T1L1 virions and TC particles, I compared read counts mapping to genes of the Mus musculus genome from virions and TC particles to mock particle preparations using the same cutoff values applied in rsT1L analyses. The Pearson correlation coefficient between mock-virion versus mock-TC preparations compared to rsT3D^{I}T1L1 virion versus TC preparations is ~ -0.008, which suggests that RNA associated with particles differs from host RNA in the mock corresponding layer. I identified 32 host RNAs that were significantly enriched in rsT3D^{I}T1L1 TC particles relative to mock TC preparations (**Table 2-3 and Fig. 2-5A-B**). No host genes were

significantly enriched in rsT3D^{I}T1L1 virions (**Fig. 2-5A-B**). While five host genes that were enriched in rsT3D^{I}T1L1 TC particles were also enriched in rsT1L TC particles, most significant host transcripts differed between the two groups (**Fig. 2-5A-B**). Only one viral gene, L1, was shared between rsT1L and rsT3D^{I}T1L1 TC. Histone-encoding genes comprised four of the five host genes that were upregulated in both rsT1L and rsT3D^{I}T1L1 TC preparations (**Table 2-3**). The final shared gene was a predicted lincRNA. Gene ontology analysis suggests that rsT3D^{I}T1L1 TC is more enriched in transcripts involved in interferon and host defense responses than rsT1L (**Fig. 2-5C and Table 2-3**). Together, these findings suggest that there is overlap in the host transcripts packaged by rsT1L and rsT3D^{I}T1L1 TC particles, but the viral RdRp is not primarily responsible for host transcript selection, which may differ among reovirus strains.

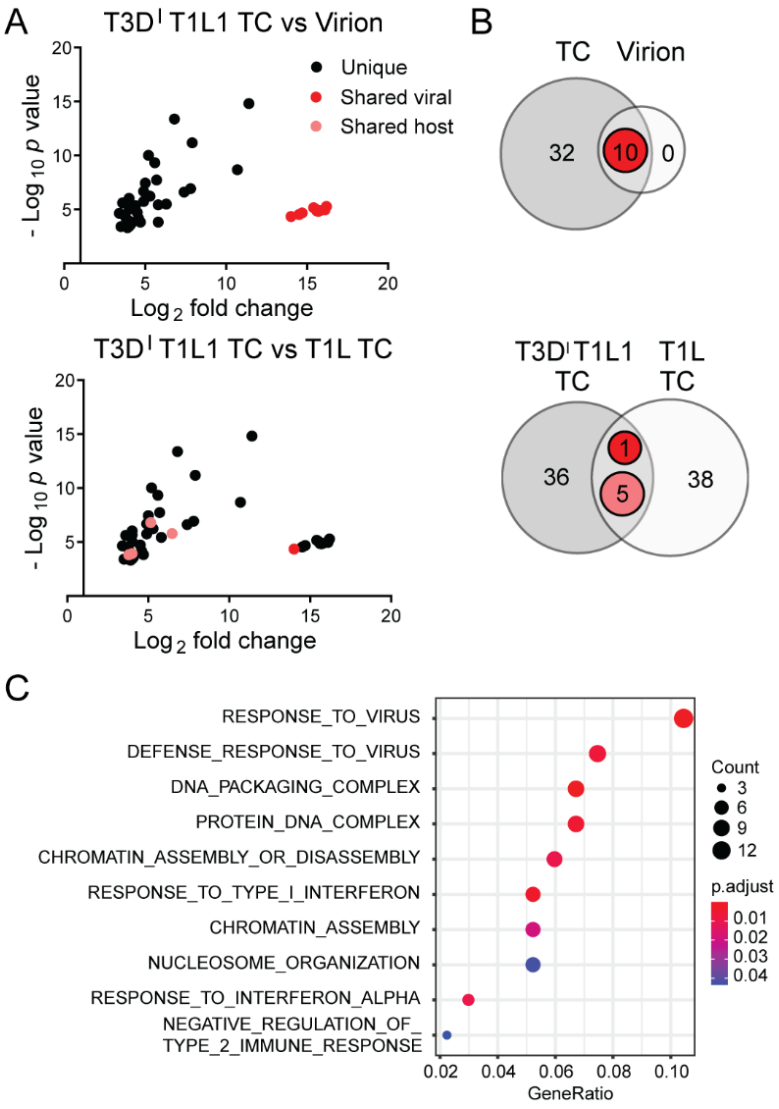

Figure 2-5. rsT1L TC particle host RNA packaging specificity is largely independent of the viral RdRp. (A) Graphs showing host genes packaged by rsT3D^{I}T1L1 TC particles that have a p value < 0.01 and fold change > eight compared to mock TC. Red and pink indicate shared viral and host genes, respectively, between rsT3D^{I}T1L1 TC and virions (upper) or rsT1L TC (lower). (B) Venn diagrams showing overlap in host genes with a p value < 0.01 and fold change > eight between rsT3D^{I}T1L1 TC and virions (upper) or between rsT3D^{I}T1L1 TC and rsT1L TC (lower). Red indicates shared viral genes, and pink indicates shared host genes. (C) Gene set over-representation analysis with GO terms for host genes packaged by rsT3D^{I}T1L1 TC. The p value is indicated by circle color, and transcript count is indicated by circle size, as shown in the legend.

2.4. Discussion

In the current study, I used NGS to elucidate the content of fully infectious reovirus virions and low-density TC particles. Our data support the idea that packaging of the complete reovirus genome into virions is exquisitely specific. NGS analysis indicated that nearly all the RNA contained within cesium chloride gradient-purified reovirus virions is viral RNA. In fact, while TC preparations were significantly enriched in 32-34 host RNAs, no host transcripts were significantly enriched in virions based on our criteria (**Figs. 2-4A-B, 2-5A-B, and Table 2-3**). Reads mapping to host RNA represented < 0.1% of total reads in enriched virions (**Table 2-2**). The proportion of reads corresponding to each of the ten viral genome segments in rsT1L virions was consistent with the expected proportion based on segment length, and encapsidated genome segments were largely double-stranded (**Fig. 2-2A and Table 2-1**). Thus, reovirus virions rarely encapsidate host RNA.

Previous studies have found that despite appearing empty in electron micrographs, reovirus TC particles retain a level of infectivity much lower than that of virions (Lai, Wérenne, and Joklik, 1973). Our analyses of the infectivity of virions and TC particles by plaque assay and fluorescent focus assay suggest a similar result (**Fig. 2-1E-F**). However, virion contamination likely explains the majority of residual infectivity in our TC particle preparations, as much infectivity is lost upon rebanding (**Fig. 2-1G**). Variation in virion contamination could contribute to the variability observed in the percent of rsT1L TC reads that map to viral sequences (**Table 2-2**). While virion contamination likely accounts for a substantial proportion of viral reads and residual TC infectivity, it is possible that some viral RNA is packaged within TC particles. I harvested TC particles

from the top of the gradient and observed only a small percentage of fully electron-lucent particles in TC preparations by negative-stain EM (**Fig. 2-1C-D**). Some level of TC infectivity also may be accomplished through genetic complementation. If many TC particles package one or a small number of viral genome segments, then a complete set of viral +RNA transcripts could be provided when multiple particles are concurrently introduced into the same target cell and permit productive infection. In fluorescent-focus assays, near-saturating levels of infectivity were achieved for protein-normalized virions and TC particles when high particle numbers were used (**Fig. 2-1E**). However, consistent with cooperative interactions among TC particles, ten-fold dilutions of inocula resulted in a much more rapid decrease in infectivity for TC particles than for virions. Thus, both virion contamination and genetic complementation may contribute to TC particle infectivity.

Although genetic complementation could in part explain TC infectivity, it is a poor fit with current packaging models. The observation that reovirus virions and TC particles form distinct bands in cesium chloride gradients and that each reovirus genome segment is packaged in rsT1L TC in the expected proportions based on segment length are consistent with “all-or-none” segment packaging (**Figs. 2-1A and 2-3A**). However, in negative-stain EM images, a significant percent of TC particles contained partially filled centers, which could represent partially packaged viral genomes (**Fig. 2-1C-D**). Based on observations for BTV, one might expect that small, viral RNA complex-nucleating segments would be overrepresented if only a few segments were being packaged within individual TC particles, but relatively increased levels of small segments were not detected in these particles (**Fig. 2-2C and Table 2-1**). If TC infectivity is maintained

through genetic complementation, reovirus RNA packaging may follow a less strict order based on size class than rotavirus and BTV, or RNA packaging may follow less strict guidelines in TC particles than in virions (AlShaikhahmed et al., 2018; Sung and Roy, 2014; Fajardo et al., 2017). Future studies employing dilution and single-cell techniques may be useful in resolving these discordant observations.

It is unclear why TC particles fail to package a complete set of viral genome segments. Since read coverage for RNA packaged in rsT1L TC particles was relatively uniform across segment length, with approximately equal proportions of reads representing plus-strand and minus-strand RNA for nearly all segments, it is unlikely that defective viral genomes contribute significantly to the failure of TC particles to package the complete viral genome (**Fig. 2-2C**) (Vignuzzi and López, 2019). Segments for which read coverage was substantially skewed were M1 and M2, which showed read enrichment localized to the 5′ end of the minus-strand. I hypothesize that these reads reflect abortive minus-strand synthesis, which is unlikely to influence packaging. It is possible that packaging of host transcripts by TC particles somehow precludes packaging of viral +RNA segments or complexes. If this is the case, it does not appear that TC particles become “filled” with host transcripts, based on particle density and appearance by negative-stain EM (**Fig. 2-1A,C**). Therefore, some other mechanism must prevent complete viral RNA packaging into TC particles. Recent detection of collapsed, single-shelled particles in reovirus-infected cells suggests that the inner capsid may be assembled prior to being filled with RNA and RdRps (Sutton et al., 2020). However, TC particles appear to encapsidate the RdRp but not a complete viral

genome. Thus, it is unclear whether these “star-like” single-shelled particles represent assembly intermediates or dead-end particle forms.

Viral and host RNA packaging by rsT1L and rsT3D^{I}T1L1 virions and TC particles exhibited notable differences. While rsT1L virions and TC particles packaged reads mapping to most viral segments in proportion to length, in several instances, rsT3D^{I}T1L1 TC particles deviated from expected proportions (**Fig. 2-3**). Proportions of packaged plus-strand RNA in rsT3D^{I}T1L1 TC particles, but typically not rsT1L TC particles, often were higher than expected for dsRNA (**Table 2-1**). Finally, rsT3D^{I}T1L1 TC particles consistently packaged higher percentages of viral reads, relative to host reads, than rsT1L, though the level of virion contamination in rsT3D^{I}T1L1 TC particle preparations was not quantified (**Table 2-2**). Future analyses of rsT3D^{I} may clarify whether differences in rsT1L and rsT3D^{I}T1L1 viral RNA packaging are strain specific or result from mismatch with the RdRp. Of the 34 host transcripts significantly enriched in rsT1L TC particles, five were enriched in rsT3D^{I}T1L1 TC particles, and rsT3D^{I}T1L1 TC particles were enriched for another 27 distinct host transcripts (**Fig. 2-5A-B**). Thus, the RdRp, λ3, is not solely responsible for selecting host RNAs packaged in TC particles. Aside from λ3, several other reovirus proteins, including μNS, σ3, and σNS, interact with viral +RNA transcripts and potentially could contribute to overall RNA packaging specificity (Antczak and Joklik, 1992). Polymerase co-factor μ2 interfaces with viral inclusions and the host cytoskeleton through interactions with polymerized microtubules (Broering et al., 2002; Eichwald, Kim, and Nibert, 2017; Parker et al., 2002). Association with the host cytoskeleton dictates packaging efficiency and TC particle abundance for rsT1L and rsT3D reovirus (Shah et al., 2017). Reovirus replication efficiency in Madin-

Darby canine kidney cells can be modulated by the μ2- and λ3-encoding segments, with T3D exhibiting an apparent μ2-dependent packaging defect in these cells (Ooms et al., 2012; Ooms et al., 2010). Thus, roles of μ2 and other viral proteins in host transcript packaging merit further exploration.

Our NGS analyses indicated that an average of 50% of reads for rsT1L TC particles and 71% of reads for rsT3D^{I}T1L1 TC particles mapped to cellular RNA (**Table 2-2**). Of these, short, non-polyadenylated RNA species were enriched. Specifically, histone mRNAs, which are ~300-500 nucleotides in length and contain a conserved 3′ stem loop, represented the majority of cellular RNAs packaged by rsT1L TC particles and most of the shared genes packaged by both rsT1L and rsT3D^{I}T1L1 TC particles (Marzluff and Koreski, 2017). Since reovirus +RNAs are non-polyadenylated and contain predicted stem-loop structures in terminal UTRs, and genome segment termini are critical for packaging, packaging may be preferential for transcripts that conserve these features (Kobayashi et al., 2007; Demidenko et al., 2013; Roner and Steele, 2007; Zou and Brown, 1992; Chappell et al., 1994; Roner and Joklik, 2001). In addition to highly structured, non-polyadenylated cellular RNAs, polyadenylated host transcripts were packaged within TC particles, particularly in rsT3D^{I}T1L1 TC particles (**Table 2-3**). For rsT1L, there was no overlap in packaged transcripts and those that were upregulated in response to infection, and gene set over-representation analyses identified several distinct categories of RNAs enriched in rsT1L TC particles and rsT1L-infected L cells (**Fig. 2-4**). These findings suggest that reovirus packaging of host RNA is facilitated through conserved RNA features rather than transcript abundance.

Whether TC packaging of host RNA has significant functional consequences for reovirus replication is an open question. Reovirus packages viral +RNA and uses it as a template for minus-strand synthesis to make the dsRNA genome (McDonald, Tao, and Patton, 2009). Since TC particles package the viral RdRp and cellular RNA transcripts, these particles could conceivably generate dsRNA and synthesize nascent mRNA transcripts from cellular RNA (**Fig. 2-4 and Fig. 2-5**) (Dryden et al., 1998). Host RNA packaged within TC particles, however, was nearly always single-stranded, suggesting reovirus is incapable of using cellular RNAs as templates for replication (not shown). Furthermore, there were far fewer reads detected for most significantly enriched host RNAs than for viral +RNAs packaged by TC particles, even though total numbers of host transcript reads were high (**Table 2-2**). Rather than altering target cell biology, host RNA packaging may simply alter TC particle encapsidation of viral RNA or be permitted when a complete set of viral RNAs fails to be encapsidated.

RNA packaging by viruses belonging to the *Reoviridae* family is mediated by *cis*- and *trans*-segment interactions reliant upon specific nucleotide sequence and structural motifs. Here, I demonstrate that reovirus TC particles can package diverse cellular RNA transcripts, while virions fail to do so, supporting a highly selective genome packaging model for virions. Packaging of host transcripts within TC particles is not based solely on transcript abundance and may differ based on virus strain, suggesting some selectivity, but is not determined solely by the viral RdRp. I speculate that encapsidation of host transcripts is unlikely to significantly affect the biology of cells into which TC particles enter, as packaged cellular transcript abundance is low, and there is no apparent mechanism for host transcript exit or amplification. Rather, host transcript

packaging may interfere with viral +RNA packaging or simply be permitted when a full complement of viral +RNAs fails to be packaged. Future studies are required to reveal the mechanism and outcome of host transcript packaging by reovirus TC particles.

2.5. Summary

In conclusion, in this Chapter I show that infectious reovirus virions package the ten-segmented genome with incredible specificity. Reovirus is known to generate both “full” virions and “empty” top component particles throughout replication. Next-generation RNA sequencing of virions and top component particles revealed that while virions almost exclusively package the viral genome, top component contains numerous host RNA species. Although top component particles packaged a diverse suite of host RNAs, short, non-polyadenylated host mRNAs that form terminal secondary structures represented some of the most highly abundant transcripts. Reovirus genome segments are also non-polyadenylated and are predicted to form terminal stem loop structures, suggesting that these features may play an important role in packaging specificity. Thus, these data provide evidence for novel RNA features important for reovirus packaging and support an all-or-nothing model of reovirus packaging. Whether host RNA interferes with packaging of the viral genome, or if host RNA is only packaged in the absence of viral genome, remains an open question.

CHAPTER 3

REOVIRUS EFFICIENTLY REASSORTS GENOME SEGMENTS DURING COINFECTION AND SUPERINFECTION

This chapter was adapted from Thoner et al. 2022. Reovirus efficiently reassorts genome segments during coinfection and superinfection. *J Virol* 96:e00910-22.

3.1. Introduction

Genome segment reassortment is a major mechanism of genetic diversity acquisition among viruses with segmented genomes. Reassortment events can engender the generation of pandemic virus strains (Smith et al., 2009; Kawaoka, Krauss, and Webster, 1989), provide avenues for zoonotic transmission events (reviewed in Doro et al., 2015), and increase the prevalence of antiviral drug-resistant variants (Yang et al., 2011; Simonsen et al., 2007). Reassortment has been observed for viruses belonging to nearly every family with segmented genomes, including the *Arenaviridae* (Stenglein et al., 2015; Fernandes et al., 2018), *Bunyaviridae* (Nunes et al., 2005, reviewed in Briese, Calisher, and Higgs, 2013), *Orthomyxoviridae* (reviewed in Steel and Lowen, 2014), and *Reoviridae* (Lelli et al., 2015; Zhang et al., 2016; Qin et al., 2017; Matthijnssens and van Ranst, 2012; Nomikou et al., 2015) families. While reassortment occurs often in nature, limitations to gene segment exchange do exist. Specifically, it is well-established that reassortment events can disrupt critical interactions between viral RNA and proteins, leading to virus progeny that are less fit than parental viruses or are completely nonviable ((White, Steel, and Lowen, 2017; Huang et al., 2008; Lubeck, Palese, and

Schulman, 1979; Nibert, Margraf, and Coombs, 1996); reviewed in White and Lowen, 2018)). Limitations to reassortment as a result of parental incompatibilities are referred to as “segment mismatch.” While the influence of segment mismatch on reassortment is well-documented, other factors, which I refer to as “intrinsic influences,” may also contribute to the efficiency of reassortment even after a cell has been coinfected. Less is understood about intrinsic influences of reassortment, though some mechanisms, such as physical separation of viruses within coinfected cells, have been proposed (Lowen, 2018).

Reovirus is a member of the *Reoviridae* family and encapsidates a genome composed of ten double-stranded RNA segments named according to their respective sizes – large (L1, L2, L3), medium, (M1, M2, M3), and small (S1, S2, S3, S4). Reovirus reassortment has previously been described as a nonrandom process, such that the frequency of reassortment events is lower than expected, and specific gene constellations are preferred in coinfection progeny (Nibert, Margraf, and Coombs, 1996; Fields, 1971). Thus, reovirus reassortment appears to be constrained by segment mismatch.

Many RNA viruses compartmentalize replication processes within membranous and proteinaceous bodies in the cytoplasm, which may protect from antiviral responses and concentrate factors important for efficient viral replication. Reovirus replication occurs in cytoplasmic virus factories (VFs), which are assembled from interactions between non-structural proteins μNS and σNS and act as the primary site of viral positive-sense RNA (+RNA) synthesis, genome packaging, and new particle assembly (Becker, Peters, and Dermody, 2003; Miller et al., 2010). Recent studies indicate that reovirus +RNA

localizes to both the cytoplasm and VFs and that non-structural protein σNS is responsible for recruiting +RNA to VFs (Lee et al., 2021). Reovirus VFs are not static. First appearing as small, punctate bodies in the cytoplasm, VFs fuse and become larger as replication progresses (Ooms et al., 2010; Bussiere et al., 2017). However, it is unclear if +RNA traffics out of and between VFs and what effect trafficking may have on the capacity of transcripts from coinfecting viruses to colocalize and be copackaged into assembling virions. Thus, VFs may influence reassortment frequency either by sequestering viral RNA to prevent reassortment events or by facilitating the accumulation of viral RNA from coinfecting viruses to promote reassortment events. Recent work suggests that VF morphology is not an important determinant of reassortment frequency during simultaneous coinfection (Hockman et al., 2022). However, it is unknown whether newly synthesized viral RNA can enter mature VFs and, thus, how VFs affect reassortment during superinfection, when the timing of coinfection is asynchronous.

Superinfection exclusion, also known as viral interference, may also influence reassortment frequency when coinfection does not occur simultaneously. Superinfection exclusion occurs when infection with a first virus interferes with subsequent infection of the same cell or organism by a second virus. Multiple mechanisms of superinfection exclusion have been identified, including competition for host resources (Zou et al., 2009), degradation or downregulation of entry receptors (Huang et al., 2008; Palese et al., 1974; Michel et al., 2005), and antiviral host responses (Zhu, Sathish, Yuan, 2010; Isaacs and Lindenmann, 1957). Previous studies of reovirus reassortment have suggested that superinfection is not excluded, as reassortant progeny can be detected

even when there is a substantial time delay separating primary infection and superinfection (Keirstead and Coombs, 1998). However, type 3 reovirus is known to potently induce and to be susceptible to the antiviral effects of type 1 and type 3 interferons (Stuart, Holm, and Boehme, 2018; Jacobs and Ferguson, 1991; Baldridge et al., 2017). Whether reovirus limits superinfection, and what affect this may have on reassortment, is an open question.

In this Chapter, I sought to determine whether processes intrinsic to the reovirus replication cycle influence reassortment by examining reovirus reassortment in the absence of segment mismatch. I used a post-PCR genotyping method to quantify reassortment following coinfection and superinfection of cultured cells with type 3 reoviruses in wild-type and genetically-barcoded forms. I also determined viral RNA localization relative to VFs and quantified viral RNA abundance during coinfection and superinfection. Consistent with published data, I found that reassortment events are frequent during high multiplicity coinfection in the absence of segment mismatch (Hockman et al., 2022). However, reassortment frequency decreased as the time delay to superinfection was increased. During superinfection, the time to introduction of the superinfecting virus and the abundance of superinfecting virus +RNA displayed strong positive correlations with reassortment frequency. Furthermore, +RNA imaging during coinfection and superinfection revealed pools of cytoplasmic and VF-localized reovirus transcripts, and VFs did not appear to pose a significant barrier to reassortment events. Superinfection exclusion was not detected when primary infection and superinfection occurred within a single replication cycle. However, with greater time delay to superinfection, type 3 reovirus primary infection did reduce the abundance of

superinfecting reovirus transcripts. These findings suggest that infection multiplicity is a key determinant of reassortment during synchronous coinfection. Further, compartmentalization of replication is not a critical mediator of reassortment potential following superinfection; rather, the abundance of superinfecting virus transcripts appears to dictate reassortment frequency during superinfection. Lastly, superinfection exclusion is unlikely to influence reassortment during a single replication cycle but may influence reassortment potential in certain contexts.

3.2. Coauthor Contributions

Jacob Long engineered barcoded genome segments, rescued barcoded virus, and performed replication curves. Julia Diller and Madeline Meloy assisted with the collection of reassortment data by performing high-resolution melt analysis and performing coinfections for some samples. I coinfected and superinfected cells, developed +RNA imaging methodologies, quantified coinfectivity and imaged +RNA in coinfected and superinfected cells, determined reassortment frequency via high-resolution melt analysis, and quantified virus transcript abundance by RT-qPCR.

3.3. Results

3.3.1. A genetically barcoded reovirus displays identical replication kinetics and can be differentiated from wild-type reovirus during coinfection.

To quantify reassortment frequency in the absence of protein and RNA incompatibilities, I engineered a barcoded rsT3D^{I} reovirus (BC) that is isogenic to wild-type rsT3D^{I} (WT) except for 7 or 8 synonymous changes within a 21-24 nucleotide region of each viral

genome segment (**Table 3-1**). Barcodes are distal from terminal sequences required for packaging, assortment, transcription, and translation and are not anticipated to alter RNA folding or recognition in a way that will diminish viral fitness (**Fig. 3-1A**). To determine whether barcoding alters BC reovirus replication, I quantified virus titer from three plaque-purified clones of BC over a time course and found that these clones replicate with nearly identical kinetics to WT in murine L929 fibroblasts (L cells) (**Fig. 3-1B**). To differentiate WT and BC genomes in coinfected cells and quantify reassortment frequency, I used high-resolution melt analysis (HRM). HRM is a post-PCR genotyping method that enables the detection of genetic variants based on the melt temperature of PCR-amplified cDNA products and has been used to study reassortment of genetically barcoded influenza virus and reovirus (Marshall et al., 2013; Hockman et al., 2020). I extracted RNA from purified WT and BC reovirus stocks and conducted HRM for each genome segment using primers that amplify a region surrounding the genetic barcode. Melt temperatures for four genome segments were too similar to consistently differentiate the WT and BC sequences. However, difference plots of melt curves showed that six WT and BC genome segments could be easily differentiated after PCR amplification (**Fig. 3-1C**). Thus, I developed a system useful for quantifying reovirus reassortment, as the WT and BC viruses replicate with equivalent efficiency and six of their genome segments can be consistently distinguished by HRM.

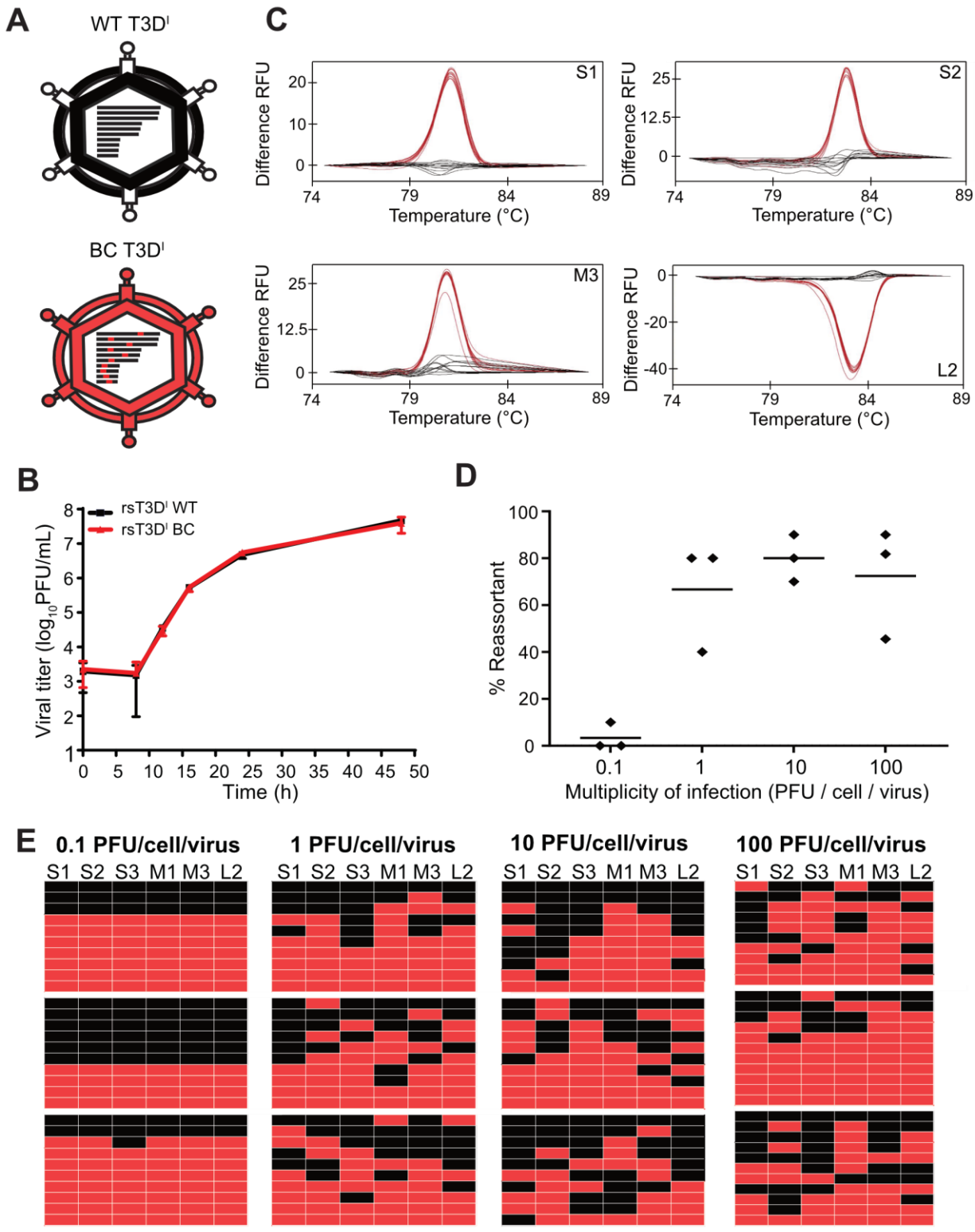

Figure 3-1. Reovirus reassortment is frequent during high multiplicity coinfection. (A) Schematic representation of reovirus virions, genome segments, and barcoding strategy. Black bars represent genome segments, with red representing barcodes, or

regions into which a series of silent, single-nucleotide substitutions were introduced. (B) L cells were adsorbed with WT or BC reovirus at a multiplicity of 0.1 PFU per cell and incubated for the indicated times prior to cell lysis. Virus titer in cell lysates was determined by plaque assay. n = 3 pairs of plaque-purified clones from each of two independent experiments. (C) Representative HRM difference plots indicating fluorescence relative to a WT control over a range of temperatures for indicated genome segments. n = 4 WT or BC clones, analyzed in triplicate. Black lines indicate WT genome segment. Red lines indicate BC genome segment. (D) L cells were coinfected with WT and BC reovirus at a MOI of 0.1, 1, 10, or 100 PFU per cell per virus before quantifying reassortment frequency using HRM. (E) Honeycomb plots indicate genotypes of individual coinfection progeny viruses analyzed from the experiment in (D). Each row represents an independently isolated clone. Each column represents the indicated genome segment. Black indicates WT genome segments, and red indicates BC genome segments. n = 3 independent experiments, with at least 10 progeny analyzed per experiment.

3.3.2. Reovirus reassortment occurs frequently during simultaneous coinfection.

To quantify the frequency of reovirus reassortment in the absence of segment mismatch, I simultaneously coinfected L cells with WT and BC reovirus at increasing multiplicities of infection (MOI). After 24 h, infectious progeny from these coinfections were isolated by plaque assay and amplified, their RNA was extracted, and the parental origin of the S1, S2, S3, M1, M3, and L2 segments was determined by HRM. At a MOI of 0.1 PFU per cell per virus, reassortment events were rare, with only 3% of progeny clones packaging a detectably reassorted genome (**Fig. 3-1D-E**). However, reassortment frequency increased with higher MOI; 67%, 80%, and 72% of clones were reassortants at MOIs of 1, 10, or 100 PFU per cell per virus, respectively (**Fig. 3-1D-E**). Thus, segment exchange occurred frequently beginning at a MOI of 1 PFU per cell per virus and increasing the MOI above this level did not substantially enhance reassortment frequency. Using HRM, I may not have detected every reassortant virus among our progeny, since four of the reovirus genome segments were not analyzed. However, I mathematically adjusted our expected results to account for analysis of only

six of the ten reovirus genome segments. When six segments are analyzed, there are 2^6, or 64, possible genome segment combinations. If reassortment was statistically random, 62 of every 64 virus progeny (~97%) would package a reassortant genotype, while only two would package the parental (WT or BC) genotype. Since reassortment frequency peaked at ~80%, in our assay it failed to reach a frequency suggestive of entirely random genome segment exchange. I was also curious whether certain genome segments are exchanged more frequently than others. Binomial and X^2 analyses indicate that there was no preference for certain segment size classes (L/M or S) to reassort more frequently (**Materials and Methods**). These findings suggest that following simultaneous coinfection, reovirus reassortment occurs frequently during a single cycle of replication, though there may be some limitations to this process that are unlikely to involve viral protein or RNA incompatibilities.

Table 3-1. Barcode sequences and locations.

Segment	Sequence	Length	Location (nucleotides)
L1	**T**GT**A**GG**A**AA**G**GA**G**CG**A**GC**C**AA**C**[a]	22	2424-2445
L2	**T**AC**T**AT**T**GA**T**CA**A**GC**G**GC**A**	19	1213-1231
L3	**T**GT**C**TT**T**GG**T**TC**A**GC**G**AA**CC**	20	2188-2207
M1	**C**AT**T**AA**A**TT**A**TT**C**TA**T**CA**A**	19	703-721
M2	**T**CC**C**AA**G**GG**A**AT**A**CT**C**TC**C**	19	1790-1808
M3	**A**GC**G**CC**C**GG**T**GT**C**GG**C**AA**C**	19	690-708
S1	**T**GT**T**AC**G**TC**A**AT**C**CA**G**GC**A**GA**C**	22	462-483
S2	**G**CT**T**GA**C**GG**G**TT**G**GT**T**GT**T**	19	318-336
S3	**T**TC**C**TA**C**AA**A**CG**C**GT**G**CC**C**AT**A**	22	492-513
S4	**A**GC**T**GT**G**TT**T**TC**T**GG**G**ATG**C**	18	839-858

[a]Bold sequences differ from those of wild-type rsT3D[I].

3.3.3. RNA abundance fails to explain reassortment frequency during coinfection.

The abundance of viral RNA from each coinfecting virus within a cell may influence reassortment frequency, as progeny virus particles are more likely to package abundant viral +RNA molecules. To quantify the abundance of WT and BC RNA transcripts during coinfection, I used RT-qPCR. Specifically, I designed primers targeting either the WT sequence or the barcoded region of the reovirus S4 segment that would allow for specific amplification of RNA from each virus. Experiments in which cells were uninfected, singly infected, or coinfected with both WT and BC indicated that the primers yielded low background amplification when the target virus was absent (C_T >28), but substantial amplification occurred when the target virus was present (C_T ~12-16) (**Fig. 3-2A-B**). These findings suggested that the WT- and BC-specific primers could accurately differentiate between the two viruses during coinfection to permit estimation of viral RNA abundance.

To determine effects of RNA abundance of the coinfecting viruses on reassortment frequency, I quantified WT and BC S4 transcripts after coinfection of L cells over a range of MOIs. I found that RNA abundance for both viruses increased exponentially until MOI = 10, at which point the amount of RNA from both viruses stabilized (**Fig. 3-2C**). Linear regression analyses indicate a modest positive correlation between RNA abundance and reassortment frequencies observed during coinfection at increasing multiplicity (WT R^2=0.6601; BC R^2=0.6005) (**Fig. 3-2D**). The ratio of BC:WT RNA showed a weak negative correlation to reassortment frequency ([BC]:[WT] R^2=0.5054), and the linear model does not appear to fit the data (**Fig. 3-2E**). These data suggest that the dramatic increase in RNA transcripts from both viruses provides ample

opportunity for reassortment. Further, while RNA abundance increases in concert with reassortment frequency, it incompletely explains the data, suggesting that other factors likely contribute to coinfection reassortment outcomes.

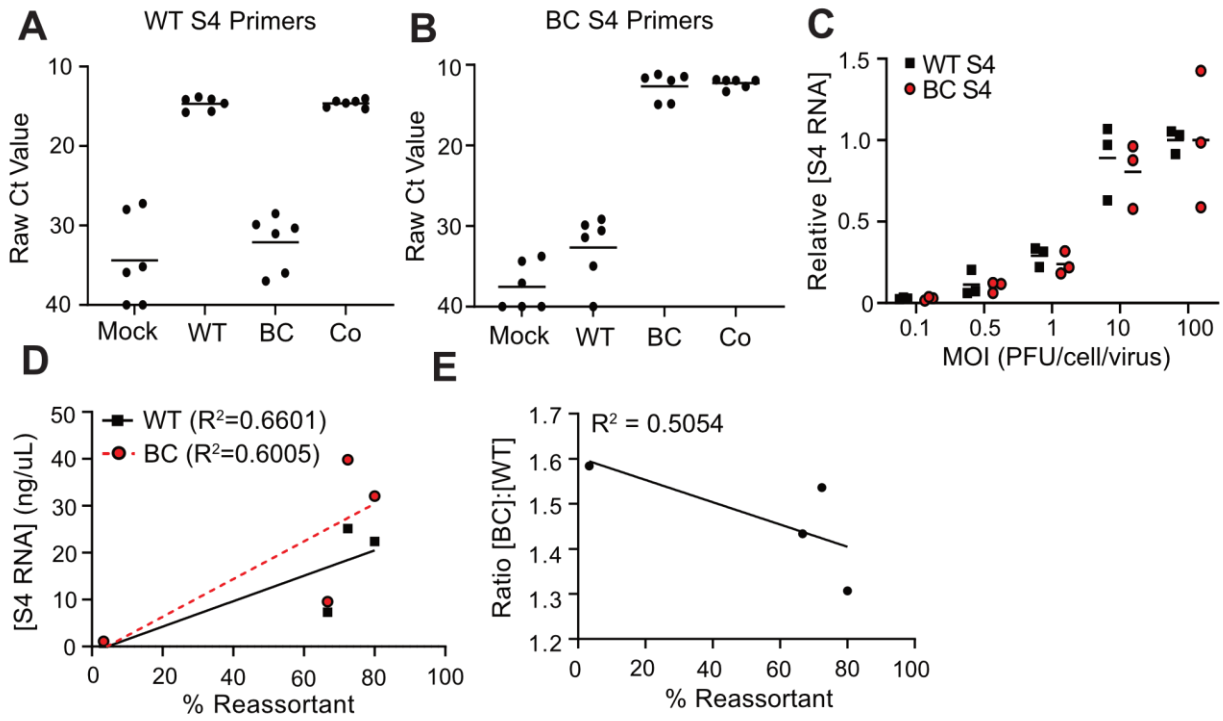

Figure 3-2. RNA abundance increases in concert with coinfection multiplicity. L cells were adsorbed with the indicated viruses at MOI = 10 PFU per cell per virus. RNA was extracted, cDNA was generated, and WT S4-specific primers (A) or BC S4-specific primers (B) were used to amplify cDNA. C_T values are shown for each infection condition. (C) L cells were coinfected at indicated multiplicities with WT and BC reovirus for 24 h before quantifying the concentration of WT and BC S4 RNA by RT-qPCR and normalizing based on MOI = 100 WT and BC RNA concentration. n = 3 pairs of independently plaque-purified clones (D-E) Simple linear regression analyses correlating the concentration of WT S4 RNA, BC S4 RNA (D), or the ratio of BC S4 RNA to WT S4 RNA (E) to reassortment frequency over a range of coinfection multiplicities.

3.3.4. Reovirus reassortment frequency decreases with time delay to superinfection.

In nature, viruses may infect a host or cell at different times, and primary infection may induce the organization of virus factories and host responses that can influence

secondary infection, with unknown effects on reassortment. To assess the effect of infection timing on reassortment, I coinfected cells with WT and BC reoviruses asynchronously at a MOI of 10 PFU per cell per virus with a range of times from 0-16 h separating primary and secondary infection (**Fig. 3-3A**). I then quantified reassortment frequency among infectious viral progeny at 24 h post primary infection using HRM. I found that as the time delay between primary and secondary infection was extended, reassortment frequency declined (**Fig. 3-3B-C**). During coinfection, roughly two-thirds of progeny were reassortants, mirroring what was observed previously (**Figs. 3-1E and 3-3B**). However, with a 4 h delay to superinfection, reassortment frequency decreased from 65% to 43%. Reassortment frequency continued to decrease with increasing time delays to superinfection, such that at the latest time point tested, when superinfection occurred 16 h post-primary infection, only a single reassortant clone was isolated from a total of 30, yielding a reassortment frequency of 3% (**Fig. 3-3B-C**). As during coinfection, small segments were equally likely to reassort as large and medium segments. I predict three potential explanations for the observed decrease in reassortment frequency with increasing time to superinfection. First, since the superinfecting virus had less time to replicate than the primary infecting virus, viral RNA abundance could drive the reduction in reassortment frequency. This idea is supported by the observation that as the time delay to superinfection increased, there was a corresponding decrease in the proportion of total segments that were derived from the superinfecting BC virus. Next, it is possible that the observed decrease in reassortment frequency is a result of physical sequestration of +RNA within viral factories. Finally, it is possible that primary infection induces responses in the infected cell that prevent

superinfection, such as the reduction of viral receptor expression or induction of interferon signaling.

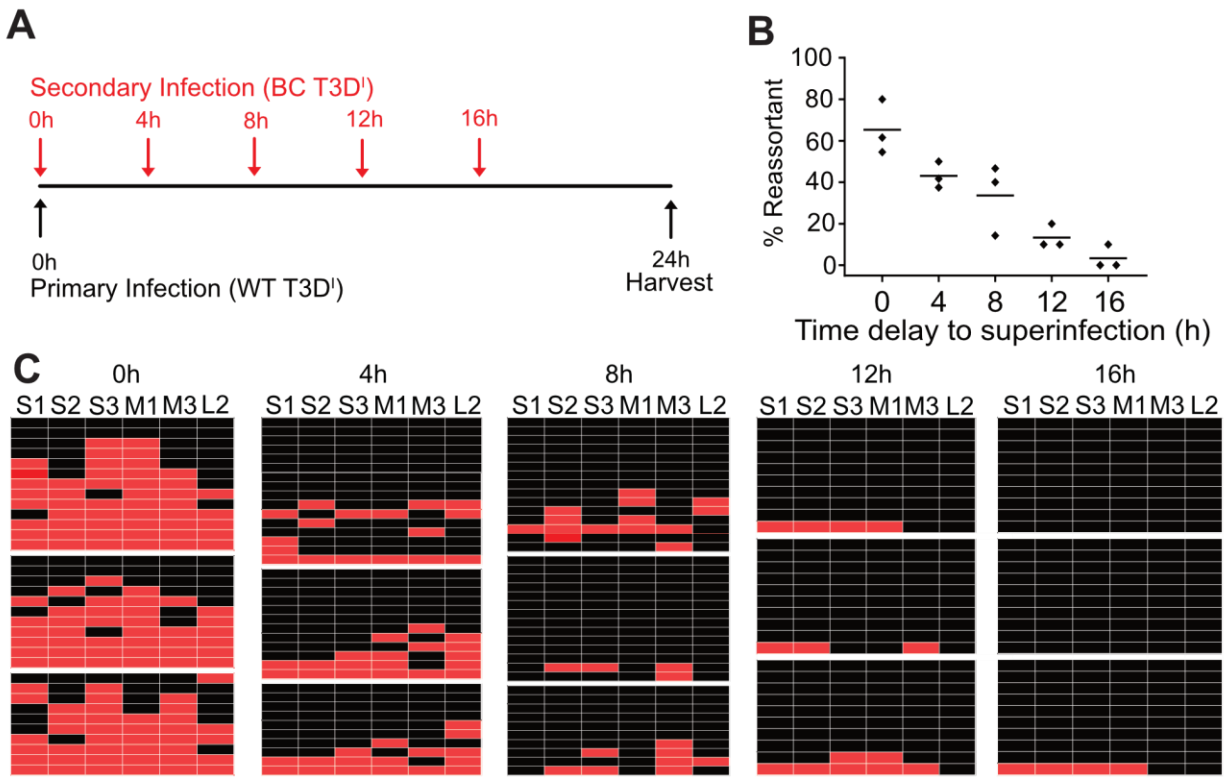

Figure 3-3. Reassortment frequency decreases with greater time delay to superinfection. (A) Schematic depicting the timing of coinfection and superinfection of L cells for superinfection time course. (B) L cells were adsorbed with WT prior to adsorption with BC at the indicated time post primary adsorption at MOI = 10 PFU per cell per virus. At 24 h post primary infection, reassortment frequency was quantified using HRM. (C) Honeycomb plots indicate genotypes of individual coinfection progeny viruses analyzed from the experiment in (B). Each row represents an independently isolated clone. Each column represents the indicated genome segment. Black indicates WT genome segments, and red indicates BC genome segments. n = 3 independent experiments with at least 10 progeny clones analyzed per experiment.

3.3.5. Viral RNA abundance correlates with reassortment frequency during superinfection.

To quantify the abundance of viral RNA from each parental virus during superinfection I adsorbed L cells with WT reovirus and superinfected with BC reovirus at 0 (coinfection

control), 4, 8, 12, or 16 h post primary infection. At 24 h post primary infection, I extracted total RNA and quantified S4 viral RNA abundance using RT-qPCR. I observed that while the abundance of RNA from the primary infecting WT virus remained stable or increased slightly over time, BC RNA abundance progressively declined, with the largest reduction in abundance coinciding with the longest time delays, consistent with reduced time for viral replication (**Fig. 3-4A**). Linear regression analysis revealed a weak negative correlation between the primary infecting virus RNA abundance and reassortment frequency (R^2=0.5055) (**Fig. 3-4B**); that is, despite a slight increase in WT transcripts, reassortment events became increasingly rare over time. Linear regression analyses also showed that the abundance of BC RNA and the ratio of BC:WT RNA positively correlate in a linear manner with reovirus reassortment frequency (BC +RNA R^2=0.9182; [BC]:[WT] R^2=0.8803) (**Fig. 3-4C-D**). Therefore, the observed decrease in reassortment frequency can be explained by the substantial reduction in superinfecting virus RNA transcripts over time. However, there may be other contributing influences.

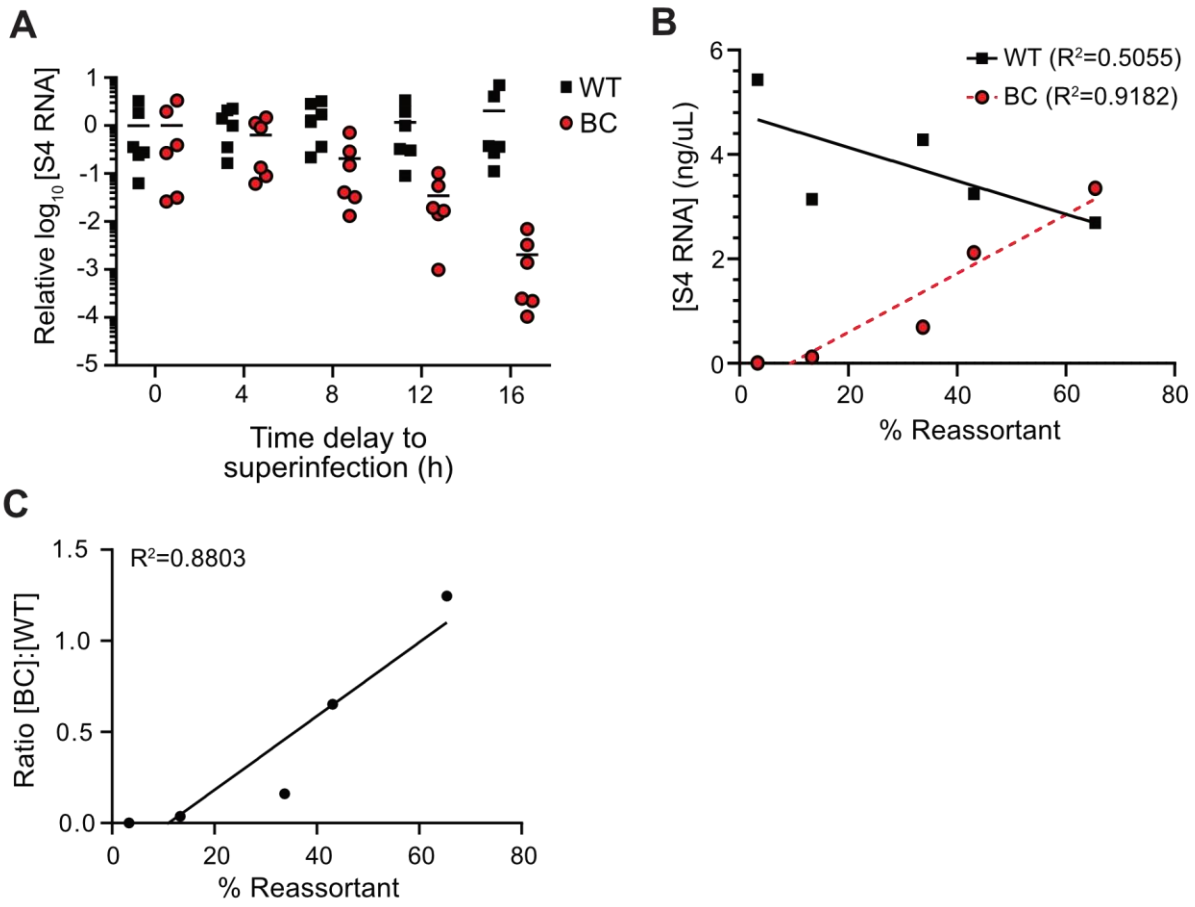

Figure 3-4. Superinfecting virus RNA abundance decreases with greater time to superinfection and correlates with reassortment frequency. (A) L cells were adsorbed with WT prior to adsorption with BC at the indicated time at MOI = 10 PFU per cell per virus. At 24 h p.i., WT and BC S4 RNA were quantified by RT-qPCR. (B) Simple linear regression analyses were used to correlate the concentration of WT S4 RNA or BC S4 RNA and (C) the ratio of BC:WT RNA to reassortment frequency at each superinfection time point. n = 3 pairs of plaque-purified clones from two independent experiments.

3.3.6. Branched DNA FISH enables specific detection of WT and BC +RNA transcripts during coinfection.

Coinfection of the host cell is required for two viruses to reassort genome segments. After observing that reovirus reassortment is non-random in the context of simultaneous coinfection, I sought to develop a tool with which I could quantify the percentage of cells

that were infected with both WT and BC reoviruses during coinfection at increasing MOI. To detect infectivity by each virus, I designed differentially fluoresceinated branched DNA fluorescence *in situ* hybridization (bDNA FISH) probes specific to the WT and BC sequences of the S3, S4, and L1 genome segments. To determine if the probes were specific for their targets, I conducted high multiplicity single infections and coinfections with WT and BC, or a mock infection, fixed and permeabilized cells, stained nuclei with DAPI, and incubated all samples in the presence of both WT and BC probes to permit hybridization. Using immunofluorescence microscopy, I detected WT- or BC-specific probe binding in a substantial proportion of total cells only when the appropriate target virus was present, with low background binding to the non-target virus (**Fig. 3-5A-C)**. Although several fluorophores are conjugated to each bDNA FISH probe, since only a single probe can bind to a given viral +RNA molecule, it is unlikely that this method of detection provides single-molecule sensitivity (van Buuren and Kirkegaard, 2018). To compare the sensitivity of bDNA FISH for detecting total infectivity with that of antibody staining, I infected L cells with WT at increasing multiplicity and quantified infectivity using immunofluorescence microscopy after staining with either WT-specific bDNA FISH probes or with polyclonal reovirus antiserum and fluorescently-conjugated secondary antibodies. While the bDNA FISH approach could detect up to 80% +RNA-positive cells, it was less sensitive than immunostaining at most MOIs (**Fig. 3-5D**). Therefore, while bDNA FISH staining provides the benefit of detecting each virus individually during coinfection, its sensitivity likely is limited.

To determine the effect of MOI on codetection of viral +RNA, I adsorbed L cells with WT and BC reoviruses at increasing multiplicities and quantified the percentage of

cells in which I could detect viral +RNA from a single virus or both viruses using bDNA FISH probes and immunofluorescence microscopy. The percent of cells in which I could detect +RNA from a single virus or from both viruses increased in concert with coinfection multiplicity, unlike the plateau observed for reassortment frequency at high MOIs (**Fig. 3-5E**). Even at the highest multiplicities assessed, 100% +RNA codetection was never achieved. While it is likely that the low sensitivity of the assay is in part responsible for this result, it may suggest that high levels of reassortment can occur under conditions of somewhat limited coinfection, or at least when limited amounts of both viral +RNAs are present. Considering that reassortment frequency began to plateau at a MOI of 1 PFU per cell per virus, while +RNA codetection continued to increase to a MOI of 100 PFU per cell per virus, factors other than +RNA codetection may impose barriers to entirely random reassortment.

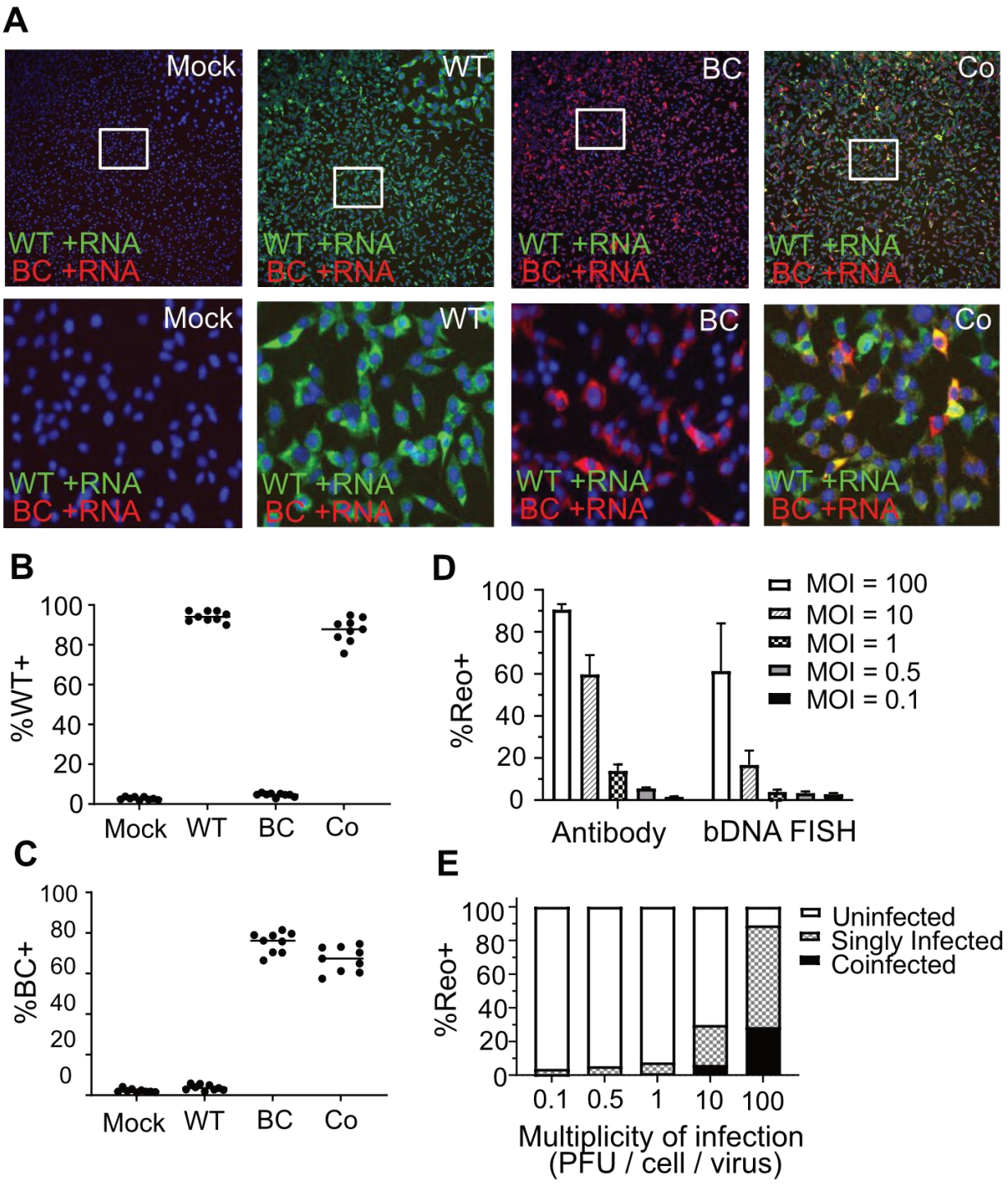

Figure 3-5. Branched DNA FISH enables specific detection of WT and BC +RNA during coinfection. L cells were adsorbed with medium (mock), WT only, BC only, or both WT and BC at a multiplicity of 10 PFU per cell per virus. Cells were fixed, stained for nuclei (blue), WT +RNA (green), and BC +RNA (red) using bDNA FISH probes, and visualized and quantified using an ImageXpress Micro high-content imaging system. Representative images are shown in (A). The percentage of total cells infected with WT

(B) or BC (C) for each infection condition are indicated. n = 9 fields of view from one representative experiment. (D) L cells were adsorbed with the indicated MOI of WT reovirus and fixed and processed for imaging with the ImageXpress either using traditional immunostaining or branched DNA FISH workflow. The average percentage of total infected cells from four fields of view is shown. n = 3 plaque-purified clones. (E) L cells were coinfected at the indicated MOI with WT and BC reovirus for 24 h then fixed and processed for imaging with the ImageXpress using bDNA FISH workflow. The average percentage of uninfected, singly infected, and coinfected cells from four fields of view per clone are shown. n = 3 plaque-purified clones.

3.3.7. VFs are unlikely to influence reovirus reassortment frequency during superinfection.

Reovirus establishes VFs within hours of entering host cells (Ooms et al., 2010). Viral transcription is initiated in the cytoplasm but primarily occurs within VFs as early as 6 h p.i. (Miller et al., 2010). In addition, VFs act as sites of reovirus genome packaging and new particle assembly (Miller et al., 2010). Therefore, it is possible that newly synthesized +RNA transcripts from coinfecting viruses may be isolated within distinct VFs, posing a physical barrier to reassortment. However, VFs also display liquid-like properties whereby these structures undergo fusion and fission events (Bussiere et al., 2017), which could effectively promote reassortment events between viruses that are isolated to distinct VFs. To determine whether VFs introduce a physical barrier to co-localization of coinfecting viral +RNA during superinfection, and thereby reassortment, I assessed +RNA localization from coinfecting WT and BC reoviruses using bDNA FISH and confocal microscopy. WT virus was used as the superinfecting virus because the fluorophores conjugated to WT-specific probes were of a shorter wavelength, making it possible to detect superinfecting virus +RNA at late time points of superinfection. Specifically, I adsorbed L cells with BC reovirus and then superinfected with WT either at 0 (coinfection), 8, or 16 h post primary infection. I determined WT and BC +RNA

localization by bDNA FISH at 24 h post primary infection using probes specific to the S3, S4, and L1 genome segments. At all time points of superinfection, +RNA from the superinfecting virus could be observed in the cytoplasm and within factories that were occupied by +RNA from the primary infecting virus (**Fig. 3-6A-C**). However, as the time delay to superinfection was increased, the percentage of factories within coinfected cells in which I detected +RNA from the superinfecting virus decreased (**Fig. 3-6D**). This decrease corresponded with a decrease in the percentage of VFs in which I detected +RNA from both the primary infecting and secondarily infecting viruses (**Fig. 3-6E**), and the ratio of VFs that were positive for WT +RNA relative to those that were positive for +RNA from both viruses remained constant at each time point (**Fig. 3-6F**). This finding suggests that the decrease in WT +RNA within VFs was responsible for the reduction in co-positive VFs. It was unclear, however, whether this reduction in the percentage of VFs containing +RNA from both viruses was due to superinfecting virus +RNA being excluded from existing VFs or was due to a reduction in superinfecting virus +RNA present within infected cells. To determine whether superinfecting virus +RNA was selectively excluded from VFs, I quantified the proportion of the total fluorescence intensity from superinfecting virus +RNA that was localized to VFs at each time point. I found that there were 22% and 27% reductions in sample means at 8 h and 16 h relative to 0 h, respectively, in the proportion of total WT superinfecting virus +RNA that localized to VFs (**Fig. 3-6G**). This represented a 7% reduction in superinfecting virus +RNA localized to VFs from 8h to 16h. However, there was an ~10-fold decrease in reassortment frequency from 8 h to 16 h (8 h = 34% reassortant; 16 h = 3% reassortant) (**Fig. 3-3B**). Therefore, if superinfecting virus +RNA is excluded from VFs, it is only a

small proportion of total +RNA and is unlikely to drive the observed reductions in reassortment frequency. The proportion of +RNA from the primary infecting virus localizing to VFs remained constant at each superinfection time point (**Fig. 3-6H**). Further analyses of +RNA within VFs revealed that superinfecting virus +RNA localized to progressively larger VFs as the time delay to superinfection increased (**Fig. 3-6I**). In contrast, +RNA from the primary infecting virus localized to VFs of roughly the same size at each superinfection time point (**Fig. 3-6J**). Additionally, the mean area of VFs containing +RNA from both viruses increased with greater time delay to superinfection (**Fig. 3-6K**). This finding provided additional evidence that large VFs do not exclude superinfecting virus +RNA, which suggests they do not preclude reassortment events. The mechanism through which superinfecting virus +RNA accesses mature VFs is open to further inquiry.

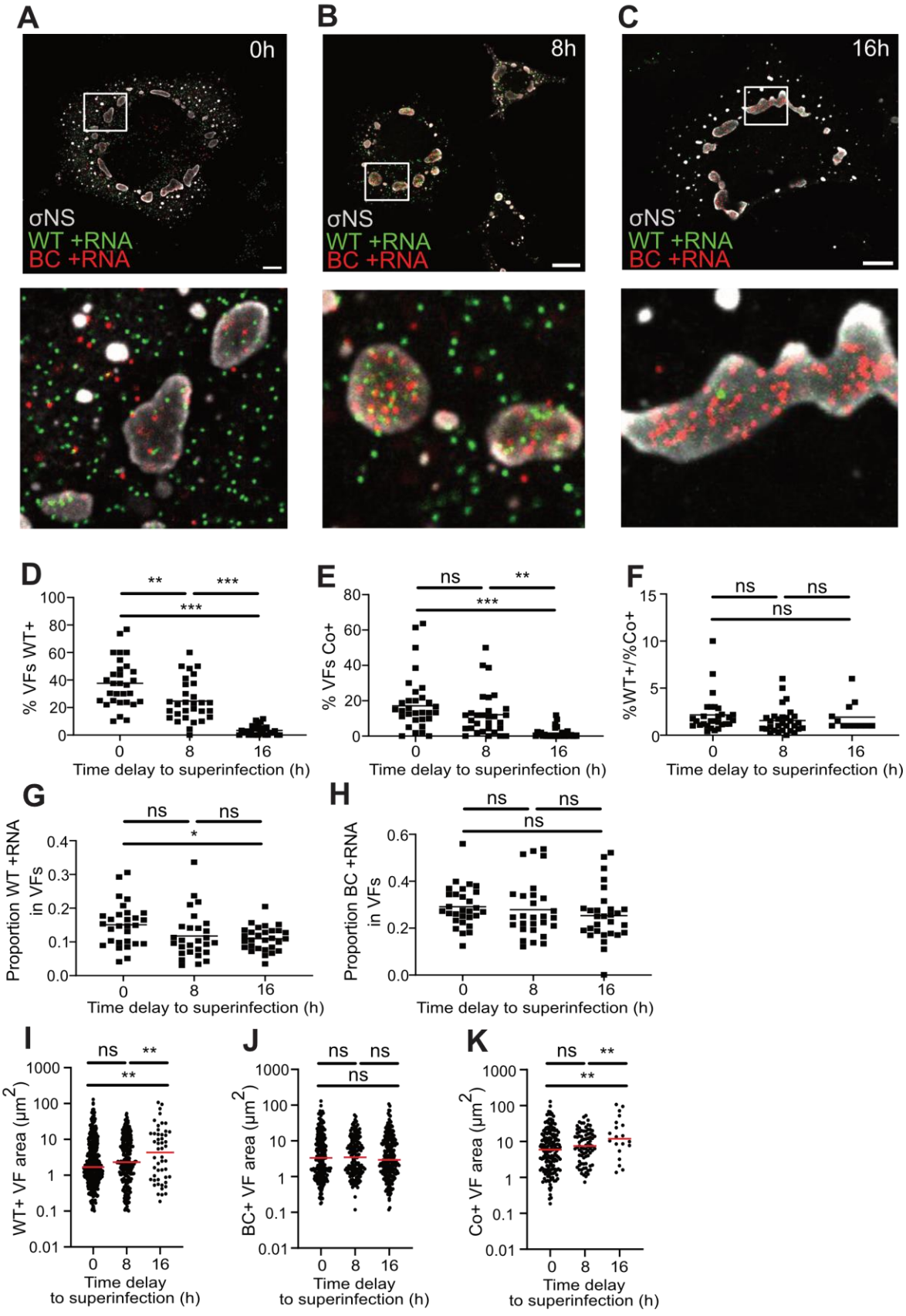
A
0h
σNS
WT +RNA
BC +RNA
B
8h
σNS
WT +RNA
BC +RNA
C
16h
σNS
WT +RNA
BC +RNA
D
% VFs WT+
Time delay to superinfection (h)
E
% VFs Co+
Time delay to superinfection (h)
F
%WT+/%Co+
Time delay to superinfection (h)
G
Proportion WT +RNA in VFs
Time delay to superinfection (h)
H
Proportion BC +RNA in VFs
Time delay to superinfection (h)
I
WT+ VF area (μm2)
Time delay to superinfection (h)
J
BC+ VF area (μm2)
Time delay to superinfection (h)
K
Co+ VF area (μm2)
Time delay to superinfection (h)

Figure 3-6. VFs do not exclude superinfecting virus +RNA. (A-C) L cells were coinfected with WT and BC reovirus simultaneously (A) or were infected at 0 h with BC and superinfected with WT 8 h (B) or 16 h (C) post primary infection. Cells were fixed and stained using bDNA FISH probes specific for S3, S4, and L1 +RNA of primary infecting BC (red) and superinfecting WT (green) and with antibodies against viral nonstructural protein σNS (gray) to define VFs. Cells were imaged using an LSM880 confocal microscope. Scale bar is 10 μm. (D-H) In 30 cells per condition, cells were segmented, and individual VFs were identified by thresholding based on σNS staining. WT and BC +RNA within all VFs and the cytoplasm were quantified using Fiji. The percentage of VFs that contain WT +RNA (D) or both WT and BC +RNA (E) is shown. The ratio of VFs that contain WT +RNA to those that contain both WT and BC +RNA is depicted in (F). The proportion of total fluorescence intensity from WT +RNA probes (G) and BC +RNA probes (H) that is localized to VFs at each superinfection time point is shown. (I-K) The average area of VFs positive for WT +RNA (I) BC +RNA (J), or both WT and BC +RNA (K) at the 0 h, 8 h, and 16 h superinfection time point is indicated. Significance determined by one-way ANOVA with Tukey's multiple comparisons test. n = 30 cells per time point. * = $p<0.05$, ** = $p<0.01$, *** = $p<0.001$.

3.3.8. T3D^{I} reovirus primary infection can limit superinfection.

T3D reovirus induces host expression of type I and type III interferons in response to infection and is also sensitive to the effects of interferon (Jacobs and Ferguson, 1991; Baldridge et al., 2017; Holm et al., 2007; Li and Sherry, 2010). Thus, I sought to determine whether type 3 reoviruses restrict reovirus superinfection. To first address this question, I adsorbed L cells with BC reovirus or medium alone (mock) at a MOI of 10 PFU per cell, coinfected or superinfected with WT reovirus at 0, 4, 8, or 16 h post primary infection, and quantified viral transcripts at 24 h p.i. Compared to the mock primary infection control, primary infection with BC reovirus had little to no effect on the abundance of viral transcripts generated by the superinfecting WT virus (**Fig. 3-7A**). However, maximal expression of interferon-β in response to reovirus infection does not occur until about 24 h p. i. (Stuart, Holm, and Boehme, 2018). Therefore, I conducted an additional experiment in which I delayed the time to superinfection to 24 h post primary infection and allowed the secondary virus to replicate for 24 h. There was an ~10-fold

decrease in superinfecting virus transcript abundance following primary infection at MOI = 10 PFU/cell, relative to mock-infected controls (**Fig. 3-7B**). To determine whether the increased time delay to superinfection, or the increased duration of superinfection, was responsible for the inhibition of secondary virus, I performed a time course in which I adsorbed L cells with BC reovirus or medium alone (mock) at a MOI of 10 PFU per cell, coinfected or superinfected with WT reovirus at 0, 4, 8, 16, or 24 h post primary infection, and quantified viral transcripts 24 h post secondary infection. By two-way ANOVA, overall there was a significant reduction in superinfecting virus transcript abundance following primary infection, relative to mock-infected controls (**Fig. 3-7C**). The magnitude of this reduction appeared more dramatic with increased time delay to superinfection and culminated in a difference comparable to that observed in Fig. 7B; however, the difference in transcript abundance at each time point failed to reach the level of statistical significance with multiple comparisons (**Fig. 3-7C**). Thus, over the time course during which I quantified reassortment frequency (**Fig. 3-3C**), superinfection exclusion is unlikely to have driven the observed reduction in reassortment frequency. However, given a sufficient time delay to superinfection, primary infection with type 3 reovirus can restrict superinfecting virus replication, either through antiviral host responses or some other mechanism.

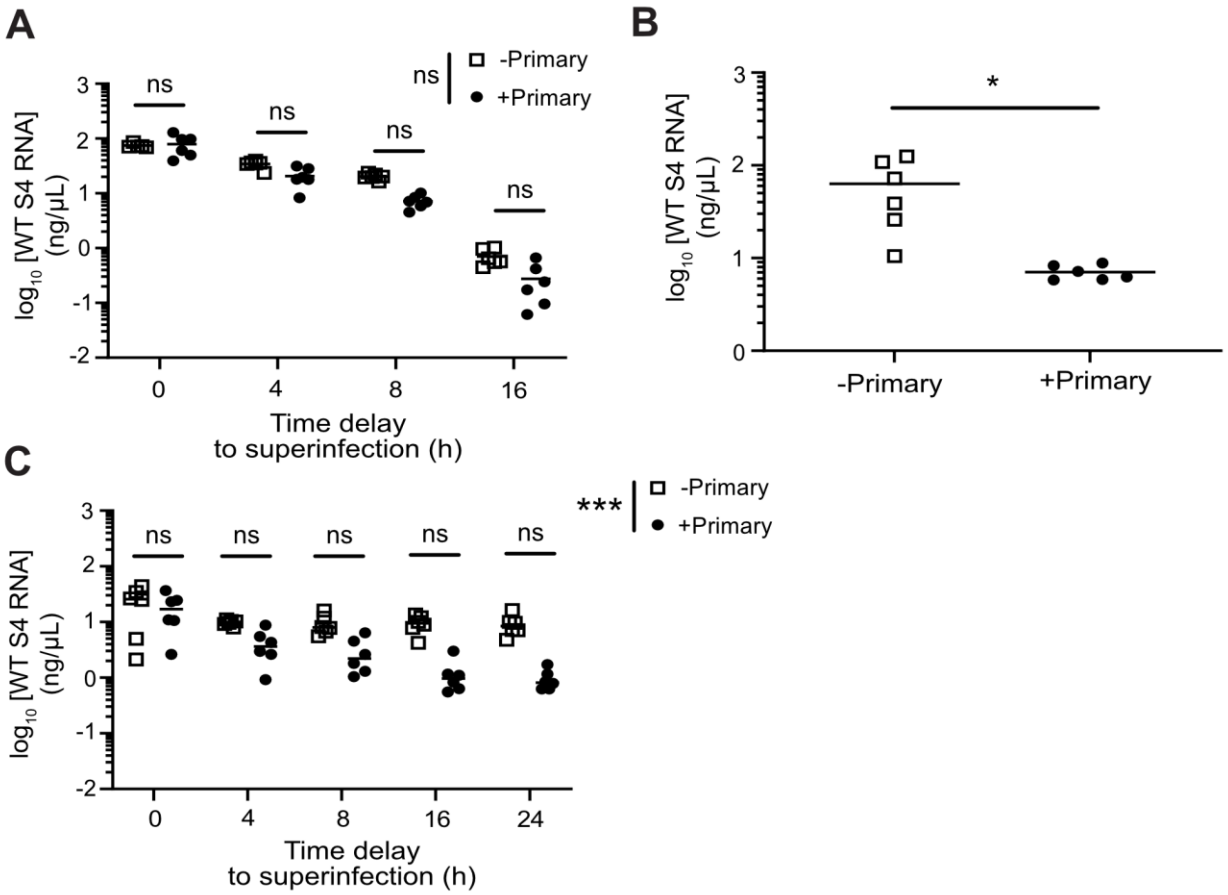

Figure 3-7. Superinfection is only inhibited by T3D^{I} reovirus with a 24 h superinfection. (A) L cells were adsorbed with medium (mock) or BC reovirus prior to adsorption with WT at the indicated time points. Superinfecting WT virus RNA concentration was quantified 24 h post primary infection by RT-qPCR. n = 3 plaque-purified clones from each of two independent experiments. (B) L cells were adsorbed with medium (mock) or BC and incubated for 24 h prior to adsorption with WT. Superinfecting WT virus RNA concentration was quantified 48 h post primary infection by RT-qPCR. n = 3 plaque-purified clones from each of two independent experiments. (C) L cells were adsorbed with medium (mock) or BC reovirus prior to adsorption with WT at the indicated time points. Superinfecting WT virus RNA concentration was quantified 24 h post secondary infection by RT-qPCR. n = 3 plaque-purified clones from each of two independent experiments. Statistical significance was determined by two-way ANOVA with Sidak's multiple comparisons test (A, C) or unpaired t-test (B) (* = $p<0.05$, *** = $p<0.001$).

3.4. Discussion

In this Chapter, I show that type 3 reoviruses reassort genome segments efficiently during coinfection and superinfection. +RNA transcripts from superinfecting reovirus gain access to dense, cytoplasmic virus factories, potentially facilitating generation of reassortant progeny. Additionally, superinfecting virus replication is not substantially limited by antiviral responses initiated by type 3 reovirus within a single cycle of replication, though superinfection exclusion was observed and could influence reassortment with greater time delays to superinfection and longer replication times for superinfecting virus.

I observed that reassortment between wild-type and genetically-barcoded type 3 reoviruses is frequent during high multiplicity coinfection (**Fig. 3-1D**), consistent with published findings (Hockman et al., 2022). RNA abundance failed to explain reassortment frequency during simultaneous coinfection (**Fig. 3-2D**), and the primary determinant of reassortment frequency during coinfection remains unclear. Coinfection of a cell is required for reassortment to occur. Thus, coinfection frequency is likely an important driver of reassortment frequency. However, quantitation of coinfection frequency with genetically-similar viruses remains technically difficult (Hockman et al., 2022). Our bDNA probes are insufficiently sensitive to accurately quantify coinfection for WT and BC viruses, which renders correlations between coinfection frequency and reassortment frequency dubious. I also observed that reassortment decreases in frequency with increasing time delay to superinfection. I proposed that this reduction in reassortment frequency could be explained by the fact that transcripts from the superinfecting virus are less abundant under the infection conditions or could be the

product of some other limiting intrinsic influence, including transcript compartmentalization in VFs or superinfection exclusion. Under the conditions tested, in which superinfection occurs within a single cycle of replication by the primary virus (<16 h), I found that the decrease in superinfecting virus transcripts strongly correlated with reassortment frequency (**Fig. 3-4B**), offering a potential explanation for why reassortment becomes less frequent with greater time delay to superinfection.

Nascent reovirus +RNA transcripts are generated after reovirus core particles are deposited into the cytoplasm (Nanoyama, Millward, and Graham, 1974; Watanabe, Millward, and Graham, 1968; Skehel and Joklik, 1969), and reovirus transcription is primarily localized to VFs as early as 6 h p.i. (Miller et al., 2010). Reovirus VFs form early in infection following transcription and translation of nonstructural proteins μNS and σNS, which associate with and recruit viral RNA and transcriptionally-active core particles (Ooms et al., 2010; Becker et al., 2001; Nibert et al., 2004; Broering et al., 2002). Thus, I initially anticipated that most viral +RNA would be localized to VFs and that +RNA from coinfecting viruses would quickly compartmentalize into distinct VFs, posing a barrier to reassortment. In contrast, I observed that reovirus +RNA localizes both to VFs and the cytoplasm and that +RNA from coinfecting and superinfecting viruses frequently co-occupied VFs (**Fig. 3-6A-C)**. Since initiating our study, others have also observed that reovirus +RNA localizes to both VFs and the cytoplasm (Lee et al., 2021). The mechanism through which +RNA from coinfecting viruses acquires access to the same VF remains unclear. However, reovirus core particles can be recruited to factory-like structures formed by μNS (Nibert et al., 2004), and the nonstructural protein σNS recruits viral RNA to VFs (Lee et al., 2021). Thus, μNS and σNS may

indiscriminately recruit cores and cytoplasmic pools of viral +RNA from distinct viruses to the same VF, providing opportunity for reassortment. It is also possible that VF fusion events facilitate co-occupation of VFs by +RNA from coinfecting viruses. Rotavirus viroplasms display properties of liquid condensates (Geiger et al., 2021), and reovirus VFs similarly undergo fusion and fission events which rely on stabilized microtubules (Bussiere et al., 2017). However, disruption of VFs with microtubule-depolymerizing drugs does not limit reassortment frequency in the context of simultaneous coinfection (Hockman et al., 2022), suggesting that VF fusion is not required for +RNA from coinfecting viruses to occupy the same VF. Importantly, I also found that superinfecting virus +RNA was not strictly localized to small VFs but was instead localized to VFs of a range of sizes (**Fig. 3-6I**). This observation suggests either that superinfecting virus does not establish distinct VFs, or that superinfecting virus establishes distinct VFs that quickly fuse with existing VFs. Further, the mean area of a VF occupied by +RNA from the superinfecting virus increased at later times of addition (**Fig. 3-6I**). The simplest explanation for this finding is that it is the result of omission bias; when there is less +RNA in the cell, it is more likely that +RNA will be detected in VFs that occupy a larger area. Given that the bDNA probes used were not sufficiently sensitive to detect all +RNA transcripts, probe sensitivity almost certainly has some effect. However, it is also possible that larger VFs, occupying a greater surface area, are more likely to be near incoming cores and recently transcribed +RNA, and as such are more likely to recruit superinfecting virus. Finally, rotavirus viroplasms lose their liquid-like properties later in infection, coinciding with phosphorylation of NSP5 (Geiger et al., 2021). If reovirus VFs behave similarly, this might suggest that established VFs are less likely to undergo

fusion events, and recruitment of superinfecting virus +RNA to large VFs likely is not due to fusion of small VFs with larger VFs.

Our findings suggest that superinfection exclusion is unlikely to influence reassortment frequency during the time course tested but may have an effect when secondary infection proceeds for longer. Previous explorations of *Reoviridae* virus superinfection exclusion have yielded mixed results. Prior work found that reassortment still occurs between coinfecting viruses with a time delay to superinfection up to 24 h, indicating that superinfection is not completely precluded by reovirus primary infection (Keirstead and Coombs, 1998). A similar observation has also been made for rotavirus (Ramig, 1990). In contrast, superinfection exclusion studies involving bluetongue virus indicate that primary infection restricts superinfection both *in vitro* and *in vivo* and that it does so as early as 4 h post-primary infection *in vitro*, at least upon secondary infection with extracellular vesicle-associated virus (Labadie and Roy, 2020; el Hussein et al., 1989; Ramig et al., 1989). The mechanism of reovirus superinfection exclusion is unclear. Known mechanisms of superinfection exclusion include antiviral host responses (Zhu et al., 2010; Isaacs and Lindenmann, 1957), inhibition of viral entry through various mechanisms (Huang et al., 2008; Michel et al., 2005; Vlasak et al., 1988; Maeda et al., 2022), and competition for host resources (Zou et al., 2009). Given that type 3 reoviruses are sensitive to type 1 interferon (Jacobs and Ferguson, 1991), antiviral responses seem a likely mechanism for superinfection exclusion. Mutations in μ2 which cause T1L reovirus to induce interferon responses similar to T3D (Zurney et al., 2009; Irvin et al., 2012) did not yield significant changes in reassortment frequency during simultaneous coinfection (Hockman et al., 2022). Thus, preexisting antiviral

responses may be required to limit viral replication to such an extent that reassortment is also inhibited.

Reovirus could also limit superinfection through other mechanisms. In the present study, exclusion was observed during high multiplicity superinfection and only when superinfecting viruses completed a full replication cycle. Given the abundance of new virus being generated under these conditions, it is possible that finite host resources are a limiting factor in the ability of superinfecting viruses to replicate. Furthermore, superinfection was inhibited to a greater extent as the time delay to superinfection increased. Apoptosis limits type 3 reovirus replication in the intestine (Brown et al., 2018). However, only a small percentage of cells undergo apoptosis and necroptosis by 24 h following type 3 reovirus infection (Tyler et al., 1996; Pruijssers et al., 2013; Berger and Danthi, 2013). Thus, cell death is unlikely to drive the observed exclusion.

Although not directly addressed in this study, other factors intrinsic to viral replication may also influence reassortment. For instance, +RNA that is synthesized later than 8 h p.i. is not used as a template for dsRNA, and dsRNA synthesis is nearly complete by 8 h p.i. (Acs et al., 1971), suggesting that assortment and reassortment may be limited to transcripts that are generated within the first 8 hours following coinfection or superinfection. Further, recent evidence suggests that core assembly, and by extension packaging of the reovirus genome, occurs in small factories at the cellular periphery, while outer capsid assembly and formation of infectious virions takes place in perinuclear factories (Kniert et al., 2022). Thus, reassortment may primarily occur in small, peripheral factories soon after coinfection and superinfection.

Furthermore, early studies that characterized packaged reovirus dsRNA found that virion-derived +RNA contains a 2'O-methyl cap at the 5'-terminus (Miura et al., 1974). While parent viruses generate capped +RNA similar to that which is packaged within virions (Furuichi, Muthukrishnan, and Shatkin, 1975), progeny viruses generate uncapped +RNA (Zarbl, Skup, and Millward, 1980). Recent findings suggest that rotavirus packages both capped and uncapped RNA (Moreno-Contreras et al., 2022); however, should reovirus preferentially package capped RNA, the likelihood of reassortment may decrease as replication progresses. I observed reassortment events occurring even when superinfection was delayed up to 16 h p.i. Thus, the requirements for reassortment must be met, to some degree, even late in infection. However, the nature of reovirus RNA being generated and the temporal dynamics of genome packaging may play an important role in determining reassortment potential.

What these findings mean for reassortment in nature is an open question. Reassortment events are considered disadvantageous to the virus in most instances, as reassortment can disrupt conserved RNA and protein interactions that are essential for virus replication (Li et al., 2008; Dudas et al., 2015), and reassortant influenza viruses have been shown to have fewer descendants than non-reassortants (Villa and Lässig, 2017). However, reassortant viruses are frequently identified in nature, and reassortment events are common in the evolutionary history of many viruses (Briese, Calisher, and Higgs, 2013; Nomikou et al., 2015; Villa and Lässig, 2017). In the current study, I analyzed reassortment in the absence of segment mismatch. These findings reveal distinct sets of influences from those at play when coinfecting virus sequences are highly divergent and may be more applicable to intrapopulation or intrasubtype

reassortment, which would involve highly genetically similar viruses. Influenza A virus reassortment has been shown to be under distance-dependent negative selection – that is, reassortment is more detrimental to progeny fitness when parent viruses are genetically dissimilar (Villa and Lässig, 2017). In the context of genetically-similar viruses, I detected few substantial restrictions to reassortment during coinfection and superinfection *in vitro*. Our work contributes to a growing literature suggesting that reassortment is tolerated and efficient for viruses that are highly similar (Hockman et al., 2022; Marshall et al., 2013). Whether reovirus has evolved to promote reassortment, or whether reassortment is simply tolerated as a by-product of the reovirus replication strategy, remains to be determined.

3.5. Summary

In conclusion, in this Chapter I have shown that reovirus reassortment proceeds relatively unimpeded during coinfection and superinfection *in vitro*. Despite evidence in the literature indicating that reovirus transcripts are primarily generated within virus factories, I show that viral +RNA is abundant in both the cytoplasm and virus factories late in infection, and +RNA from coinfecting and superinfecting viruses can be found within the same factories. Thus, factories are unlikely to impose a barrier to reassortment. In fact, within a single replication cycle, superinfecting virus transcript abundance is likely to be the primary determinant of reovirus reassortment frequency *in vitro*. The mechanism through which reovirus +RNA arrives in the cytoplasm and is recruited to existing factories is an open question. Furthermore, although viral transcript abundance is likely the primary driver of reassortment frequency when superinfection

occurs within a single replication cycle, superinfection can be inhibited by the primary infecting virus given sufficient time. Thus, superinfection exclusion may be an important determinant of reassortment frequency *in vivo*.

CHAPTER 4

ANTIVIRAL RESPONSES DIFFERENTIALLY MEDIATE SUPERINFECTION EXCLUSION *IN VITRO* AND *IN VIVO*

4.1. Introduction

Superinfection exclusion occurs when infection of a host by one virus limits or prevents subsequent infection (superinfection) by another virus. This interference can be labelled as i) homologous, when a virus prevents superinfection by the same virus, ii) heterotypic, when superinfection by different serotypes is prevented, or iii) heterologous, if superinfection by viruses in a distinct virus family is prevented (Singh et al., 1997; Dittmar, Castro, and Haines, 1982; Condit, 2001). From an evolutionary perspective, it has been proposed that superinfection exclusion may occur to prevent competition for limited host resources (Laureti et al., 2020; Folimonova, 2012) or to maintain genome stability by limiting opportunities for genomic recombination (Folimonova, 2012), though little experimental evidence exists to support these hypotheses. Viruses prevent superinfection at nearly all stages of infection and through various mechanisms, (Zhu et al., 2010; Isaacs and Lindenmann, 1957; Huang et al., 2008; Michel et al., 2005; Vlasak et al., 1988; Maeda et al., 2022; Zou et al., 2009). Indirect studies of reovirus reassortment have concluded that reovirus does not completely preclude superinfection (Keirstead and Coombs, 1998). Similar studies of rotavirus superinfection exclusion came to the same conclusion (Ramig, 1990); however, more recent evidence indicated that rotavirus does limit superinfection, just not completely (Maeda et al., 2022). Type 3 reoviruses induce and are sensitive to type I interferon (Stuart, Holm, and Boehme,

2018; Jacobs and Ferguson, 1991; Baldridge et al., 2018), and interferon responses are a known mechanism of superinfection exclusion (Isaacs and Lindenmann, 1957). Thus, interferon produced by the host in response to reovirus infection may limit superinfection.

Host cells initially recognize reovirus infection via the cytoplasmic dsRNA sensors retinoic acid-inducible gene I (RIG-I) and melanoma differentiation-associated protein 5 (MDA5), which respectively recognize long or short dsRNA genome segments (Stuart, Holm, and Boehme, 2018; Loo et al., 2008; Kato et al., 2008). These cytoplasmic sensors signal through mitochondrial antiviral signaling protein (MAVS) and transcription factor interferon regulatory factor 3 (IRF3) to induce the production of interferon-beta (interferon-β), and genetic knockout of MAVS from SV40-induced endothelial cells (SVEC) completely ablates the interferon response to reovirus infection. The magnitude of the host response to reovirus infection varies depending on the infecting strain. Specifically, T1L reovirus represses the induction of interferon-stimulated genes (ISGs) interferon regulatory factor 7 (IRF7) and signal transducer and activator of transcription 1 (STAT1), while T3D does not (Zurney et al., 2009), and significantly less interferon-β is produced in response to T1L infection than T3D (Stuart, Holm, and Boehme, 2018). Host responses to reovirus infection also vary depending on the infected cell type. For instance, in cardiac tissue, cardiac myocytes induce type I interferon production much more robustly in response to reovirus infection than do fibroblasts, while ISG expression is substantially higher in fibroblasts than myocytes (Li and Sherry, 2009). At mucosal sites of infection such as the lungs and gut, type III interferon responses are more critical for protection against reovirus infection (Peterson

et al., 2019; Baldridge et al., 2017), while type I interferon is important for restricting reovirus dissemination and infection of distal organs (Phillips et al., 2020; Johannson et al., 2007). Thus, both type I and type III interferon responses are critical for protection of the host against reovirus infection.

In Chapter 3, I showed that type 3 reoviruses induce homologous superinfection exclusion (**Fig. 3-7C**). In the present Chapter, I sought to determine the mechanism of reovirus superinfection exclusion *in vitro* and *in vivo* and assessed the influence of superinfection exclusion on reassortment. To do this, I quantified virus transcript levels following superinfection of interferon alpha/beta receptor (IFNAR)-deficient and MAVS-deficient cell lines. I also determined reassortment frequency following coinfection and superinfection of wild-type and type I and type III interferon receptor-deficient mouse pups. I observed that signaling through the type I interferon receptor was critical for reovirus to limit superinfection *in vitro* but had no influence on reassortment frequency *in vivo*. Furthermore, I found that while reassortment was common in coinfection progeny viruses, no reassortant viruses were present in superinfection progeny, regardless of genetic background. This may provide indirect evidence of superinfection exclusion *in vivo* and indicates that removal of type I and type III interferon responses in the gut are insufficient to restore coinfection and reassortment.

4.2. Coauthor Contributions

Alexa Roth inoculated mice with purified viruses and homogenized organs from infected mice. I generated purified WT and BC T3D^{I} reovirus stocks, performed high-resolution melt analysis on intestines from coinfected and superinfected mice, titrated

homogenized organs from coinfected and superinfected mice, and quantified virus transcript abundance from coinfected and superinfected cells by RT-qPCR.

4.3. Results

4.3.1. Type I interferon drives reovirus superinfection exclusion *in vitro*.

Type 3 reoviruses are known to potently induce type I interferon signaling in response to infection *in vitro.* In Chapter 3, I show that primary infection with a type 3 reovirus can limit replication of superinfecting viruses in L cells (**Fig. 3-7B-C**). To determine whether reovirus superinfection exclusion is mediated by type I interferon signaling, I primarily infected wild-type, IFNAR knockout (KO), and MAVS KO SVECs with a genetically-barcoded T3D^{I} reovirus (BC T3D^{I}) or T1L reovirus for 24 h before superinfecting with WT T3D^{I}. After a 24 h superinfection, I harvested cells and quantified superinfecting virus transcript abundance by RT-qPCR. As shown with L cells, in wild-type SVECs, the abundance of superinfecting virus transcripts was significantly decreased following primary infection with the BC T3D^{I} virus, compared to mock-infected controls (**Fig. 4-1**). Transcripts were also reduced following T1L primary infection, although not to the extent observed following T3D^{I} primary infection (**Fig. 4-1**). In IFNAR KO cells, superinfecting virus transcripts were significantly reduced by primary infection, but the magnitude of this decrease was smaller than that observed in wild-type cells. There was no significant difference between superinfecting virus transcript levels following T1L and T3D^{I} primary infection in IFNAR KO SVECs (**Fig. 4-1**). Together, these data suggest that amplification of the interferon response through IFNAR likely contributes to reovirus superinfection exclusion *in vitro*.

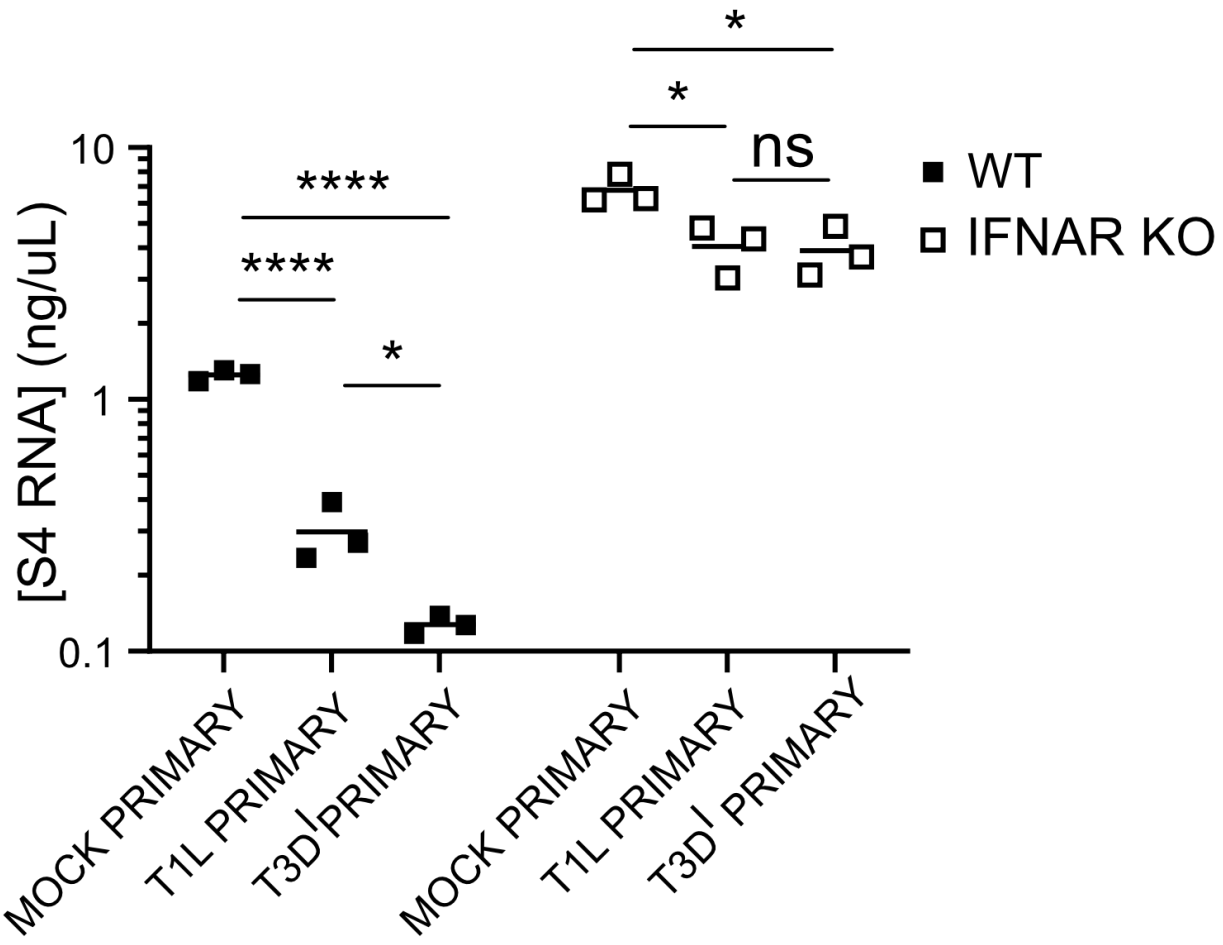

Figure 4-1. Signaling through IFNAR mediates reovirus superinfection exclusion. Wild-type or IFNAR KO SVECs were primarily infected with MOI = 10 PFU / cell with T1L, BC T3D^{I}, or media only (mock) for 24 h before adsorption with WT T3D^{I}. Superinfecting WT virus RNA concentration was quantified 48 h post primary infection by RT-qPCR. n = 3 plaque-purified clones from one independent experiment. Statistical significance determined by one-way ANOVA with Tukey's multiple comparisons test (* = $p < 0.05$; **** = $p < 0.0001$).

4.3.2. Type I and type III interferon signaling does suppress reovirus reassortment frequency during coinfection *in vivo*.

Type I interferon restricts reovirus replication at secondary sites of replication, including the heart and brain (Phillips et al., 2020). However, type III interferon is the primary host defense against reovirus infection in the intestine (Peterson et al., 2019; Baldridge et al.,

2017). To determine whether interferon signaling influences reovirus reassortment *in vivo*, I quantified reassortment frequency from intestinal homogenates of 3-day old wild-type, IFNAR KO, and interferon-lamda receptor (IFNLR) KO B6 mice following a 48 h coinfection with WT and BC T3D^{I} reoviruses. Reassortment proceeded efficiently in mice of all genetic backgrounds, with reassortant viruses making up between 20-40% of viral progeny from each group (**Fig. 4-2A-C**). Additionally, WT and BC viruses were similarly represented in coinfection progeny, suggesting that there were no major fitness differences for the two viruses *in vivo*. Thus, type I interferon is a driver of reovirus superinfection exclusion *in vitro*, but type I and type III interferon signaling do not influence reassortment frequency in the intestine during coinfection.

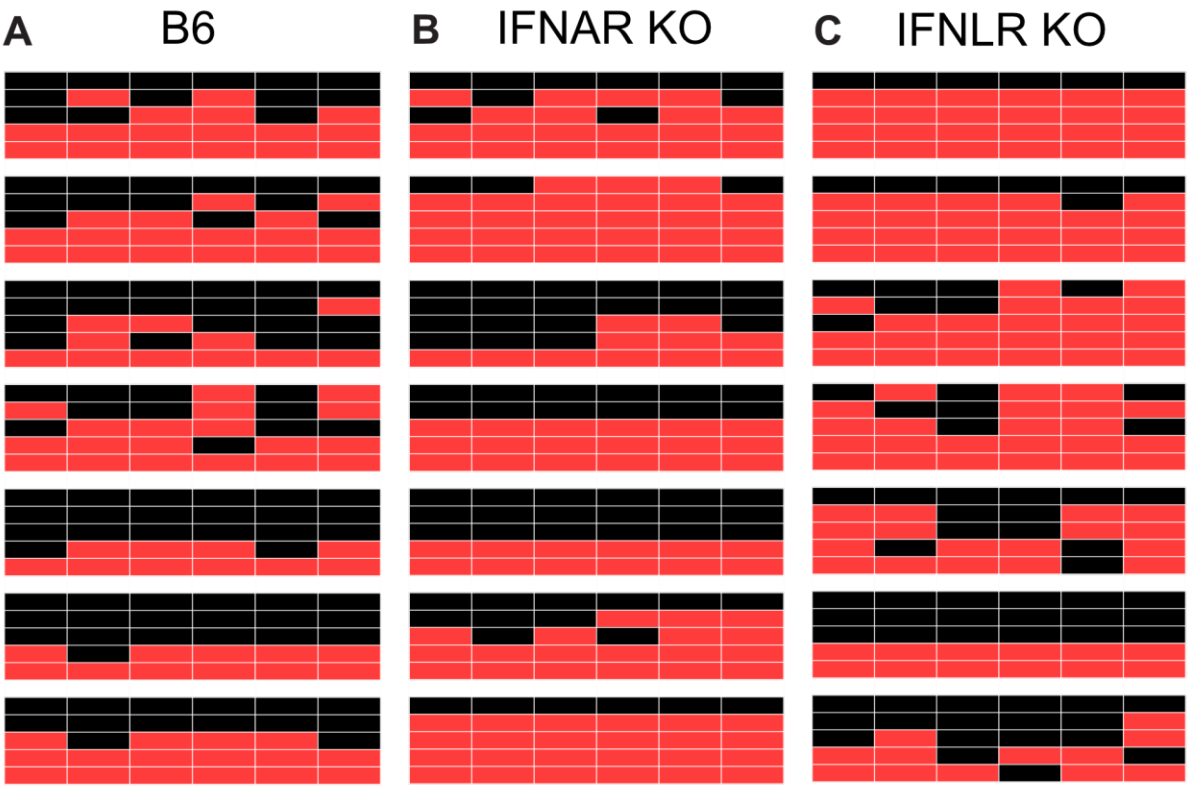

Figure 4-2. Reassortment occurs frequently during coinfection in mice, irrespective of genotype. 3-day old wild-type B6 (A), IFNAR KO (B), and IFNLR KO (C) mice were

perorally inoculated with 1 x 10^7 PFU WT and BC. At 48 h post-inoculation, mice were euthanized and reassortment frequency was quantified using HRM. Honeycomb plots indicate genotypes of individual coinfection progeny viruses. Each row represents an independently isolated clone. Each column represents the indicated genome segment. Black indicates WT genome segments, and red indicates BC genome segments. n = 7 mice with 5 progeny clones analyzed per experiment. Each block of 5 progeny clones is derived from the same mouse.

4.3.3. Reovirus reassortants were not detected during superinfection *in vivo*.

Administration of IFN-β prior to infection potently limits reovirus replication (Jacobs and Ferguson, 1991). As such, it is possible that preexisting interferon responses are required to limit reovirus superinfection and reassortment. Therefore, I sought to determine whether type I and type III interferon signaling might influence reassortment frequency during superinfection *in vivo*. To do this, 3-day old wild-type, IFNAR KO, and IFNLR KO mice were first infected with BC reovirus for 24 h before superinfection with the WT virus. 24 h after superinfection, mice were sacrificed, intestines were homogenized, and reassortment frequency was quantified from homogenized intestines by HRM. The BC primary infecting virus was much more highly represented in progeny viruses, constituting 94%, 100%, and 86% of all segments for progeny viruses from the wild-type, IFNAR KO, and IFNLR KO mice, respectively (**Fig. 4-3A-C**). Following this superinfection time course, no reassortant viruses were detected in any mice, irrespective of genetic background (**Fig. 4-3A-C**), in contrast to what was observed during simultaneous coinfection (**Fig. 4-2A-C**). Thus, despite the presence of both viruses in the superinfection progeny from wild-type and IFNLR KO mice, no reassortment was detected. Taken together, these findings suggest that signaling through type I and type III IFN receptors is not responsible for the lack of reassortment detected during superinfection *in vivo*.

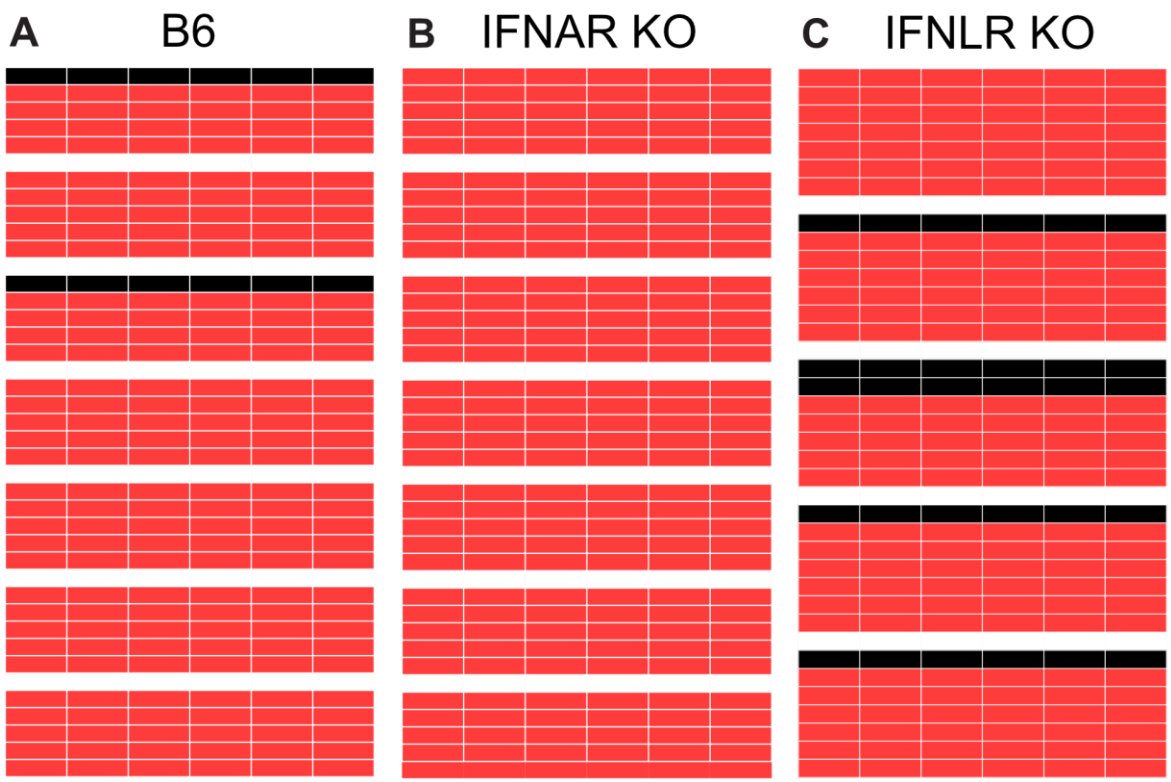

Figure 4-3. Reassortment does not occur following a 24 h superinfection time delay in mice, irrespective of genotype. 3-day old wild-type B6 (A), IFNAR KO (B), and IFNLR KO (C) mice were perorally inoculated with 1 x 10^7 PFU BC. 24 h post-inoculation, mice were superinfected with 1 x 10^7 PFU WT. At 48 h post-inoculation with the BC primary infecting virus, mice were euthanized and reassortment frequency was quantified using HRM. Honeycomb plots indicate genotypes of individual coinfection progeny viruses. Each row represents an independently isolated clone. Each column represents the indicated genome segment. Black indicates WT genome segments, and red indicates BC genome segments. n = 5-7 mice with 5-7 progeny clones analyzed per experiment, as indicated. Each block of 5 progeny clones is derived from the same mouse.

4.4. Discussion

Type I and type III interferon responses are important for protection of the host from viral infection. In Chapter 3 of this dissertation, I provided evidence that $T3D^I$ reovirus is capable of limiting superinfecting virus replication (**Fig. 3-7**). In this Chapter, I sought to better understand the mechanism of reovirus superinfection exclusion *in vitro* and *in*

vivo. Importantly, I observed that superinfection exclusion is almost completely rescued in IFNAR KO cells. Furthermore, while reovirus readily reassorted genome segments during coinfection *in vivo*, reassortment was never detected when a single replication cycle separated introduction of a first virus and inoculation with a second virus. During coinfection and superinfection, the ability of the mouse host to respond to type I or type III interferon failed to influence observed reassortment frequency, suggesting that interferon responses may not be a primary determinant of superinfection or reassortment phenotypes in this model.

In Chapter 3 of this dissertation, I showed that type 3 reoviruses limit superinfection in L cells (**Fig. 3-7B,C**). L cells are a murine fibroblast cell line that robustly induces the expression of IFN-beta in response to reovirus infection (Roebke et al., 2020). In this Chapter, I show that reovirus also limits superinfection in SVECs, an endothelial cell line that also responds strongly to reovirus infection. In SVECs lacking the type I interferon receptor, I observed a partial rescue of superinfecting virus transcript abundance following primary infection, suggesting that type I IFN signaling plays a role in driving superinfection exclusion *in vitro*. What impact superinfection exclusion has on reassortment *in vitro* remains an open question. However, primary infection with $T3D^{I}$ reovirus reduces superinfecting virus transcript abundance ~10-fold relative to mock-infected controls (**Fig. 4-1**). T1L primary infection also reduced superinfecting virus transcript levels, though to a lesser degree (~5-fold) than $T3D^{I}$. In Chapter 3, I showed that 10-fold reductions in input virus can yield a significantly lower infection and coinfection frequency (**Fig. 3-5D-E**). Thus, following primary infection with type 3 reoviruses, reassortment frequency is likely to be significantly diminished, especially

when superinfection proceeds for longer and superinfecting virus transcripts represent a progressively smaller portion of the total transcript pool (**Fig. 3-7C**). In this respect, primary infection with type 1 reovirus may allow for higher levels of reassortment during superinfection *in vitro*, relative to type 3 viruses.

Much remains to be determined regarding the extent and mechanism of reovirus-mediated superinfection exclusion *in vivo*. Despite an established importance of type I and type III interferon responses in regulating reovirus infectivity in the host, in this Chapter, I have shown that reovirus does not reassort genome segments during superinfection *in vivo*, even when mice are inoculated with virus titers sufficient to allow for reassortment during coinfection (**Fig. 4-3A-C**). This was true in wild-type mice and mice deficient in type I and type III interferon receptors, suggesting that the absence of reassortment during superinfection is not the result of signaling through type I and type III interferon receptors. While this is not direct evidence of *in vivo* superinfection exclusion *per se*, these findings do suggest that removal of these host antiviral responses does not allow for reassortment during superinfection. Furthermore, there was not a substantial increase in the abundance of superinfecting virus detected in superinfection progeny in type I and type III interferon receptor-deficient mice. In Chapter 3, I present data indicating that during superinfection *in vitro*, the abundance of superinfecting virus decreases in concert with reassortment frequency (**Fig. 3-4B,C**). Interestingly, *in vitro*, reassortment occurs even when superinfecting virus genome segments make up only a small fraction of total genome segments (**Fig. 3-3C**). In contrast, although the superinfecting virus is clearly present during superinfection in wild-type and IFNLR KO mice, no reassortment was detected (**Fig. 4-3A-C**). This

phenotype may indicate a lack of coinfection, suggesting that cells infected by the primary infecting virus are refractory to secondary infection. However, additional experiments are warranted to directly assess whether superinfection is potently inhibited by type 3 reoviruses *in vivo*, or if reassortment is not detected because viruses are not coinfecting cells after a time delay.

If future experiments determine that the lack of reassortment frequency observed during superinfection is due to superinfection exclusion, follow-up studies should determine the mechanism of superinfection exclusion *in vivo*. Why the mechanism of superinfection exclusion *in vivo* might differ from that observed *in vitro* is an open question. Given that superinfecting virus was present in superinfection progeny but no reassortment occurred, *in vivo* superinfection exclusion may be cell intrinsic – that is, only previously infected cells are refractory to subsequent infection, while neighboring cells remain permissive. Rotavirus is capable of limiting subsequent infection in a cell intrinsic manner by inhibiting endosomal pathways responsible for transcytosing rotavirus from the apical to basolateral membrane of intestinal epithelial cells (Maeda et al. 2022). However, there is debate about whether reovirus infects intestinal epithelial cells from the apical membrane, or if the virus exclusively infects intestinal epithelial cells basolaterally (Rubin, 1987; Excoffon et al., 2008). Bluetongue virus superinfection exclusion can only be overcome by free virus particles, not virus contained in extracellular vesicles, suggesting that exclusion is imparted at the stage of virus entry (Labadie and Roy, 2020). Apoptosis also limits reovirus replication (Pruijssers et al., 2013; Brown et al., 2018). While the percentage of cells undergoing apoptosis at 24 h is relatively small, cleaved caspase-3 expression is substantially induced by this time point

(Brown et al., 2018), suggesting that the process of cell death is already underway for many cells. Thus, cell death, as well as other host responses to infection, may be important mediators of reovirus superinfection exclusion.

4.5. Summary

In conclusion, in this Chapter, I have shown preliminary data suggesting that the mechanism of reovirus superinfection exclusion may differ *in vitro* and *in vivo*. Previous explorations on the topic of reovirus superinfection exclusion concluded that reovirus does not restrict superinfection, as reassortment still occurs when superinfecting virus is introduced within a single replication cycle. In Chapter 3, however, I provided evidence that primary infection with type 3 reoviruses does reduce superinfecting virus replication. In this Chapter, I present data supporting the idea that reovirus superinfection exclusion is mediated by type I interferon responses *in vitro*, but interferon responses did not suppress reassortment *in* vivo. Additionally, during coinfection *in vivo*, type 3 reoviruses readily reassort genome segments; however, when a single replication cycle separates primary and secondary infection in mice, no reassortment is detected. Genetic knockout of type I and type III interferon receptors did not rescue this phenotype, suggesting that other factors are preventing coinfection and reassortment *in vivo*. These data contribute to growing evidence that viruses of the *Reoviridae* family limit superinfection by closely related viruses through a variety of mechanisms.

CHAPTER 5

MATERIALS AND METHODS

5.1. Cell culture and antibodies.

L929 murine fibroblasts (L cells) were maintained in suspension in glass bottles containing a magnetic stir bar or as monolayers in flasks in Joklik's minimum essential medium (JMEM; US Biological) supplemented with 5% fetal bovine serum (FBS; Gibco). Baby hamster kidney cells expressing bacteriophage T7 RNA polymerase under the control of a cytomegalovirus promoter (BHK-T7; Komoto et al. 2014) were maintained in Dulbecco's minimum essential medium (DMEM; Corning) supplemented with 5% FBS (Gibco) and were treated with 1 mg/mL Geneticin (Gibco) every other passage. Wild-type, IFNAR KO, and MAVS KO SVEC cell lines were a gift from Dr. Karl Boehme and were maintained in DMEM supplemented with 10% FBS (Gibco). All media were supplemented with 2 mM L-glutamine, 100 U/mL penicillin, 100 µg/mL streptomycin (Corning), and 25 ng/mL amphotericin B.

Rabbit polyclonal reovirus antiserum and rabbit σNS-specific antiserum (Becker et al., 2001) were gifts from Dr. Terence Dermody.

5.2. Viruses.

A plasmid encoding T3D S1 in which a T249I mutation had been introduced into σ1 was engineered from the parental reverse genetics plasmid using 'round the horn PCR (https://openwetware.org/wiki/%27Round-the-horn_site-directed_mutagenesis) with

mutagenic primers (sequences available upon request) and Phusion High-Fidelity DNA Polymerase (New England Biolabs). Reovirus strain rsT3D^{I} is a variant of human reovirus laboratory strain rsT3D in which a T249I mutation has been introduced into the attachment protein, σ1, rendering it resistant to trypsin proteolysis (Kobayashi et al. 2007). Plasmids encoding rsT3D^{I} segments with silent barcode mutations (Table 1) were engineered from the parental rsT3D^{I} reverse genetics plasmids and pBac T7 rsT3D S1 T249I using 'round the horn PCR with mutagenic primers (sequences available upon request) and Phusion High-Fidelity DNA Polymerase. Recombinant strain (rs) T1L, rsT3D^{I} WT, rsT3D^{I} BC, and rsT3D^{I}T1L1 were generated by reverse genetics (Kobayashi et al., 2007; Kobayashi et al., 2010). rsT3D^{I}T1L1 is a T3D^{I} reovirus into which the λ3-encoding T3D L1 gene has been replaced with that of T1L. BHK-T7 cells at ~ 50% confluency in 6-well plates were transfected with 0.8 µg of each plasmid encoding the ten T1L genome segments, T3D^{I} wild-type or barcoded genome segments, or T3D^{I}T1L1 genome segments using TransIT LT-1 Reagent (Mirus Bio LLC). Transfected cells were cultured for 5 days or until the first signs of cytopathic effects before freezing at -80°C and thawing at room temperature twice to release virus into supernatant. Virus was then amplified in L cells for two passages. For viruses with swapped L1 and S1 segments between T1L and T3D^{I} viruses, RNA was extracted from virus stocks, and L1 and S1 identities were verified by Sanger sequencing. Virus titer was determined by standard plaque assay (Berard and Coombs, 2009). The presence of engineered barcoded mutations in the rsT3D^{I} BC virus was confirmed by Sanger sequencing following extraction of RNA from virus stocks with TRIzol (Invitrogen) and

cDNA amplification using a OneStep RT-PCR Kit (Qiagen) and segment-specific primers (sequences available upon request), according to manufacturer protocols.

5.3. Reovirus particle enrichment.

Reovirus virions and TC particles were enriched from infected L cells by Vertrel XF (DuPont) extraction and CsCl gradient centrifugation (Berard and Coombs, 2009). Briefly, L cells (2×10^8) in suspension were adsorbed with media (mock-infected) or rsT1L or rsT3D^{I}T1L1 reovirus at a multiplicity of ~10 plaque-forming units (PFU) per cell and incubated at 37°C for 48 h. Virus-infected or mock-infected cells were pelleted by centrifugation at 3,000 rpm for 10 min prior to resuspension in homogenization buffer (25 mM NaCl, 10 mM Tris-HCl, pH 7.4, 10 mM β-mercaptoethanol) and stored at -80°C. Cell pellets were thawed, incubated with 0.14% deoxycholate for 30 min on ice, then sonicated in the presence of Vertrel XF to release virus particles from cells. Virions and TC particles, or mock preparations thereof, were separated by ultracentrifugation at 25,000 × *g* for 16 h in a 1.2-1.4 g/cm^3 cesium chloride density gradient. Mock-virion and mock-TC preparations were collected by aligning a gradient containing virions and TC particles next to a gradient made using mock-infected L cells, marking the expected position of virions and TC particles on the mock gradient, aspirating liquid above the expected position, and transferring 250 µL of the gradient from the expected position of virions and TC particles into clean Eppendorf tubes. Mock preparations, complete virions, and TC particles were collected and dialyzed in virion storage buffer (150 mM NaCl, 15 mM $MgCl_2$, 10 mM Tris-HCl, pH 7.4). When indicated, dialyzed particle preparations were rebanded by an additional round of ultracentrifugation at 25,000 × *g*

for 16 h in a 1.2-1.4 g/cm^3 cesium chloride density gradient prior to another round of dialysis.

5.4. Virus particle normalization.

For experiments in which virions and TC particles were normalized by protein content, 10 µL of three independent stocks of virions and TC particles were resolved by SDS-10% PAGE and stained with colloidal Coomassie. Relative intensity of multiple reovirus protein bands was quantified with the Odyssey Infrared Imaging System (LI-COR) or ChemiDoc MP (BIO-RAD). Virions and TC particles were subsequently resolved by SDS-10% PAGE, adjusting volumes to normalize relative intensity units, and stained with colloidal Coomassie. Then, relative intensity was quantified again to validate that protein content was successfully normalized for virion and TC samples. Volumes of virions and TC particles that provided equal relative intensity units were used to compare the infectivity and RNA content of equal particle numbers of virions and TC particles.

5.5. Bioanalyzer analysis.

Equivalent protein amounts (0.8-3 × 10^{12} particles) of rsT1L or rsT3D^{l}T1L1 virions or TC particles were diluted in benzonase buffer (50 mM Tris-HCl, 2 mM $MgCl_2$, pH 8.0) and either mock-treated or treated with 1 U/µL of benzonase (Millipore) at room temperature or at 37°C for 1 h to remove extra-particle nucleic acids. Based on protein normalization, virions were diluted approximately three- to four-fold relative to TC

particles. Benzonase was inactivated with 0.5 M EDTA (pH 8.0), and RNA was extracted from virions and TC particles by TRIzol (Invitrogen) extraction per manufacturer's protocol. Concentration and quality of RNA were determined using a 2100 Bioanalyzer (Agilent) and visualized as a gel display of electropherograms. Displays are automatically adjusted for fluorescence level so that RNA peaks are visible.

5.6. Library preparation and next-generation RNA-sequencing.

Libraries were prepared for Illumina sequencing using RNA extracted from two or three independent preparations of purified, benzonase-treated rsT1L or rsT3D^{I}T1L1 reovirus virions or TC particles, RNA extracted from benzonase-treated preparations of virion and TC preparations from mock-infected L cells (mock-virion and mock-TC controls), and from preparations of total RNA extracted from mock-infected or rsT1L-infected L cells in two independent experiments. To obtain total RNA preparations, L cell monolayers were adsorbed with media (mock-infected) or rsT1L reovirus at a multiplicity of 10 PFU/cell for 48 h. RNA was extracted from cells using TRIzol (Invitrogen) or from equivalent protein amounts of enriched reovirus particles (1-6 × 10^{12}) using TRIzol LS Reagent (Invitrogen), according to the manufacturer's protocol. Contaminating DNA was degraded by treating extracted RNA with RNase-free DNase I (New England Biolabs) for 10 min at 37°C. RNA was re-extracted using TRIzol LS Reagent, and the concentration and quality of RNA was quantified using a 2100 Bioanalyzer (Agilent). RNA library preparation for Illumina sequencing was conducted using 5 ng of RNA and the NEBNext Ultra II RNA Library Prep Kit for Illumina (New England Biolabs),

according to the manufacturer's instructions. Briefly, ribosomal RNA was depleted from L cell samples via RNase H and DNase I digestion, and RNA was subsequently purified using RNAClean XP beads (Beckman Coulter). RNA was fragmented prior to first-strand and second-strand synthesis and RNAClean XP purification. PCR enrichment of adaptor ligated DNA was conducted using NEBNext Multiplex Oligos for Illumina (New England Biolabs) to produce Illumina-ready libraries. Illumina-ready libraries were sequenced by 150 base pair paired-end sequencing on the NovaSeq 6000 Sequencing System (Illumina).

5.7. Next-generation sequencing analysis.

Raw read quality was assessed using FastQC (v0.11.5) (Andrews, 2010). STAR (v2.7.3a) (Dobin et al., 2014) was used to align reads to the *Mus musculus* genome (mm10; http://hgdownload.soe.ucsc.edu/goldenPath/mm10/chromosomes/) or to T1L and T3D reovirus segment sequences. GenBank Accession numbers for individual reference reovirus genome segments are M24734.1, AF378003.1, AF129820.1, AF461682.1, AF490617.1, AF174382.1, EF494445.1, L19774.1, M18389.1, M13139.1, EF494436.1, EF494437.1, EF494438.1, EF494439.1, EF494440.1, EF494441.1, EF494442.1, EF494443.1, and EF494444.1. Transcript quantification was done using featureCounts (Liao et al., 2014) using the paired-end mode to count both reads that mapped uniquely. Then, the enriched transcripts were called using edgeR (v2.26.5) (Robinson et al., 2010) with a Benjamini-Hochberg adjusted p value < 0.01. Only transcripts with counts per million (CPM) > 1 in at least two samples were included in the initial analysis. Enriched transcripts were further screened for at least an eight-fold

change over matched mock preparations and an average log_2CPM > 0.5 across samples of the particle type of interest. Comparisons of RNA content between samples or layers were conducted using edgeR (version 3.30.3). Pearson correlation coefficients were calculated using the log_2 fold change as input to cor() function in R base package stats. ClusterProfiler (v3.12.0) (Yu et al., 2012) was used for the gene set over-representation analysis with GO terms (msigdbr_7.1.1) (Liberzon et al., 2015). To illustrate Illumina reads mapping to the plus-strand and minus-strand of each viral genome segment, bam files were transformed into bedGraph files using bedtools (scaled to one million with bedtools use command 'bedtools genomecov -bg -pc -scale 0.000001') (Quinlan and Hall, 2010). The bedGraph files were loaded into IGV to view the read distribution on target genes in a strand specific manner (Robinson et al., 2011). Figures were made using using GraphPad Prism 8.4.3.

5.8. Quantitative reverse transcription PCR (RT-qPCR).

To quantify the abundance of viral and host transcripts within virions and TC particles, RNA was isolated from the equivalent of 10^{11} particles of rsT1L virion and TC particle preparations using Trizol LS, per manufacturer's protocol. Virion and TC RNA were primed with random hexamers (Invitrogen), and cDNA was generated by reverse transcription using SuperScript III reverse transcriptase (ThermoFisher) per manufacturer's protocol. Quantitative PCR amplification was performed using PowerUp SYBR Green Master Mix (ThermoFisher) and primers specific to the reovirus T1L S4 gene (F: 5'-CGCTTTTGAAGGTCGTGTATCA -3'; R: 5'-CTGGCTGTGCTGAGATTGTTTT -3') or murine *HIST1H1E* (F: 5'-

GGTACGATGTGGAGAAGAACAA-3'; R: 5'-CGCCTTCTTGTTGAGTTTGAAG -3'), *HIST1H2AI* (F: 5'-TCCGCAAAGGCAACTACTC -3'; R: 5'- TGATGCGCGTCTTCTTGT-3'), or *HIST2H3C2* (F: 5'- GATCGCGCAGGACTTCAA-3'; R: 5'-GGTTGGTGTCCTCGAACAG -3').

To quantify virus transcripts from coinfected and superinfected cells, L cell monolayers were disrupted by scraping and were pelleted at 200 x g for 5 min before RNA was isolated from 2 x 10^5 cells using the RNeasy Plus Mini RNA extraction kit (Qiagen) per manufacturer's protocol. RNA concentration was quantified by Nanodrop. Equal amounts of total RNA (400 ng) were primed with random hexamers (Invitrogen), and cDNA was generated using SuperScript III reverse transcriptase (ThermoFisher) using manufacturer's protocol. For viral RNA standards, RNA was extracted from WT and BC $T3D^I$ viruses purified by cesium-chloride gradient ultracentrifugation, normalized based on concentration, serially diluted to achieve target standard curve concentrations, and reverse transcribed. cDNA was amplified and quantified using PowerUP SYBR Green Master Mix (ThermoFisher) and primers specific to the wild-type or barcoded region of the reovirus S4 gene (WT F: 5'-GGCCGTATTCTCAGGAATGTT-3'; BC F: 5'-AGCTGTGTTTTCTGGGATGC-3'; WT/BC R: 5'-AATCTTCTCGACACCCCAAG-3'). To calculate the concentration of RNA, the concentration of total RNA from standard curve stocks was quantified by Nanodrop. Genome segments are anticipated to be present in equimolar concentrations in purified particle preparations (43). The concentration of S4 was calculated as a proportion of total viral genome length. C_T values of serially diluted standards were determined, and the concentrations of all other samples were interpolated relative to standards of known concentration.

5.9. Fluorescent focus assay.

L cells (2×10^4 per well) were seeded into 96-well, black-walled plates and adsorbed with serial ten-fold dilutions of protein-normalized virion and TC preparations or volumes of serially diluted mock preparations at 37°C for 1 h. After removing inocula, cells were washed and incubated in fresh medium at 37°C for 24 h. After fixing with cold methanol, reovirus proteins in virus factories in the cell cytoplasm were detected using polyclonal reovirus antiserum in PBS containing 0.5% Triton X-100 at 37°C, followed by washing and incubation with Alexa Fluor 488-labeled secondary IgG (Invitrogen) and DAPI (4′,6′-diamidino-2-phenylindole) to detect nuclei. Four fields of view per well were imaged with an ImageXpress Micro XL automated microscope (Molecular Devices). Then, total and percent infected cells were quantified with MetaXpress high-content image acquisition and analysis software (Molecular Devices).

To quantify coinfectivity using branched DNA FISH probes specific to WT and BC T3D^I viruses, L cells (2×10^4 cells per well) in 96-well black-walled plates were adsorbed with 0.1, 0.5, 1, 10, or 100 PFU WT and BC reovirus for 1 hour at room temperature. Cells were washed with complete JMEM, and infection was allowed to proceed for 24 h. Infected cells were fixed and stained using branched DNA FISH probes specific to the wild-type or barcoded region of the T3D reovirus L1, S3, and S4 +RNA, per manufacturer's protocol. Cells were then stained with DAPI in PBS for 10 minutes at room temperature before washing with PBS and imaging on the ImageXpress high-content imaging system (Molecular Devices). Coinfectivity was determined using a custom module in MetaXpress software by thresholding images and quantifying and

averaging the percentage of cells from four fields of view positive for AlexaFluor488 (WT T3D^{I}) and AlexaFluor647 (BC T3D^{I}).

5.10. Negative-stain electron microscopy.

Freshly glow-discharged Formvar/carbon grids (EMS) were incubated with 2µL of purified reovirus virions or TC particles for one minute, washed twice by brief contact with a 50 µL water droplet, and stained for 10 seconds in 2% uranyl acetate. Imaging was performed on a Tecnai T12 operating at 100 kV using a drift-corrected AMT CMOS camera. Images were analyzed with FIJI (Schindelin et al., 2012).

5.11. Multi-step replication.

L cells (8×10^5 cells per well) in 12-well plates were adsorbed with stocks generated from three independent clones each of WT and BC diluted in phosphate-buffered saline (PBS) to a MOI of 0.1 plaque-forming units (PFU) per cell for 1 h at room temperature. Inocula were aspirated, cells were washed, and 1 ml of JMEM supplemented to contain 5% FBS per well was added. Cells were incubated for 0, 8, 12, 16, 20, 24, or 48 h prior to two cycles of freezing at -80°C and thawing at room temperature, to lyse cells. Virus titer in cell lysates was determined by plaque assay. Two independent experiments were conducted. Data at each time point were compared by unpaired student's *t* test.

5.12. Coinfection experiments.

L cells (4×10^5 cells per well) in 12-well plates were adsorbed with WT, BC, or both viruses. Virus was diluted in complete JMEM to a MOI of 0.1, 0.5, 1, 10, or 100 PFU per cell per virus for 1 h at room temperature. Cells were washed, and 1 ml per well of complete JMEM was added. Leftover inocula were stored at 4°C for back-titration. Cells were incubated for 24 h prior to two cycles of freezing at -80°C and thawing at room temperature to lyse cells. Individual viral progeny were isolated by plaque purification (41). Plaques were vortexed in 0.25 ml complete JMEM and amplified by adsorption on L cell monolayers in 12-well plates. Total RNA was extracted from monolayers at 48-72 h post infection (p.i.) using TRIzol (Invitrogen), according to the manufacturer protocol. Viral +RNA was quantified by RT-qPCR, and parental segment origins were determined by high-resolution melt (HRM) analysis, as described below.

5.13. Superinfection experiments.

L cells (4×10^5 cells per well) in 12-well plates were adsorbed with WT diluted in complete JMEM to a MOI of 10 PFU per cell for 1 h at room temperature. Cells were washed with 1 mL complete JMEM, and at 0, 4, 8, 12, 16, or 24 h p.i., the cells were superinfected with BC diluted in complete JMEM to a MOI of 10 PFU per cell. Cells were washed, and 1 ml per well of complete JMEM was added. Leftover inocula were stored at 4°C for back-titration. At 24 h post primary infection, two cycles of freezing at -80°C and thawing at room temperature were conducted to lyse cells. Individual viral progeny were isolated by plaque purification (Berard and Coombs, 2009). Plaques were vortexed in 0.25 ml complete JMEM and amplified by adsorption on L cell monolayers in

12-well plates. Total RNA was extracted from monolayers at 48-72 h p.i. using TRIzol (Invitrogen), following manufacturer's protocol. Viral +RNA was quantified by RT-qPCR, and parental segment origins were determined by HRM analysis, as described below.

5.14. Mouse coinfection and superinfection experiments.

3-day old mouse pups were inoculated perorally with 1 x 10^7 PFU per mouse with WT and BC rsT3D^l reoviruses diluted in PBS without calcium and magnesium with a 1:100 dilution of 0.2µm PES filter-sterilized green food coloring to a volume of 50 µl. For coinfection experiments, both viruses were introduced at the same time and coinfection proceeded for 48 h. For superinfection experiments, BC virus was introduced first for 24 h before inoculation with the secondary WT virus for an additional 24 h. At the infection end point, mice were euthanized and small intestines were harvested. Intestines were homogenized by freezing samples at -80°C, thawing at room temperature, and bead-disrupting using the TissueLyser (Qiagen). Intestinal homogenates were again frozen at -80°C until they were thawed at room temperature for plaque assay and high-resolution melt analysis.

5.15. Viral genotyping by high resolution melt analysis.

RNA extracted from a single amplified plaque was randomly primed, and cDNA was generated using SuperScript III reverse transcriptase (Invitrogen). cDNA was amplified using MeltDoctor HRM Master Mix (Applied Biosystems) and primers surrounding either the wild-type or barcoded region of the reovirus S1 (F 5'-CATTGACCACCGAGCTATC-

3’; R 5’-CCCATGGTCATACGGTTATT-3’), S2 (F 5’-ATTCCGTTCCGTCCTAAC-3’; R 5’-CAGTCGTACACTCGATCTG-3’), S3 (F 5’-CACTTGCCAGATTGTTTACC-3’; R 5’-CAGCGTCATACAGTCCAA-3’), M1 (F 5’-GTGTTCCTCACTCTCGATTT-3’; R 5’-GCAGACGCTTTCTGTTTATC-3’), M3 (F 5’-TCTGACGCTAAAGGGATAATG-3’; R 5’-GCAGTCTCCAAGGTGAAATA-3’), or L2 (F 5’-AGACTCGGCATGAGAATATC-3’; R 5’-TAACGGGAGTTGCGTAAG -3’) genome segments. Melt curves were generated following cDNA amplification and WT and BC genotyping was performed with High Resolution Melt Software ver. 3.0.1 (Applied Biosystems). All clones were run in duplicate or triplicate to validate the called genotype. Most clones were consistently called as either wild-type or barcode for a given segment. Clones that consistently melted at a temperature in between the expected melt temperatures for the wild-type and barcode genotypes, yielding an ambiguous parental genotype, were removed from the analysis. Such clones represented a small fraction (2.8%) of total isolated plaques. Studies of genetically-marked polioviruses revealed that virion aggregates led to 5-7% of total plaques being formed by more than a single virion (42). Thus, clones with an ambiguous parental origin may represent plaques that were formed by aggregated WT and BC virions. Plaques amplified from cells infected with only WT or BC were included in each run, in triplicate, as genotype references.

5.16. Branched DNA FISH staining and image analysis of +RNA and VFs.

L cells were seeded onto coverslips in a 24-well plate and infected with MOI = 10 PFU per cell per virus of WT and BC at indicated time points. Infected cells were fixed and stained to detect S3, S4, and L1 +RNAs from WT and BC, and viral nonstructural

protein σNS to identify VFs, using the ViewRNA Cell Plus assay kit (ThermoFisher) according to manufacturer's recommendations. Coverslips were mounted using Prolong Gold antifade reagent with DAPI (Invitrogen). Confocal imaging was performed with a Zeiss LSM880 confocal microscope equipped with 40× 1.30 C Plan-Apochromat Oil objective lens. Image analysis was conducted with FIJI (v.1.53c). VFs were identified by performing a gaussian blur and subtracting background to remove low intensity signal in the cytoplasm associated with σNS, thresholding on the σNS channel, and analyzing particles. Regions of interest corresponding to VFs were compiled for each analyzed cell. VFs identified in this manner were visually confirmed to represent true staining before determining whether VFs contained WT and BC +RNA. To quantify the proportion of +RNA within and outside of VFs, raw integrated density associated with WT and BC +RNA within an individual cell, and within all VFs within that cell, was measured. To determine whether VFs contained +RNA from WT and BC, background was subtracted, and images were thresholded on the WT +RNA (AlexaFluor488) and BC +RNA (AlexaFluor647) channels. The regions of interest identifying VFs from each cell were overlayed onto the thresholded +RNA channels and the mean fluorescence intensity of +RNA signal within VFs was quantified. VFs that contained +RNA corresponding to the AlexaFluor488 channel, AlexaFluor647 channel, or both channels were called as WT+, BC+, or WT+BC+, respectively. Data were collected for a total of 30 cells and ~1200-1500 VFs at each time point.

5.17. Statistical analysis.

For experiments in Chapter 2, Statistical analyses were conducted using GraphPad Prism 8.4.3, www.graphpad.com. For FFA titers (Fig. 1E) and RTqPCR (Figs. 2B and 4C), results were found to be statistically different by one-way or two-way ANOVA. Then, titers of TC at each concentration were compared to those of virions or C_T values were compared using Sidak's multiple comparison test. Plaque titers of rsT1L virions and TC (Fig. 1F-G) were compared by unpaired *t* test. The percent of packaged viral reads for each reovirus segment for each particle type was compared to the percent of total T1L reference genome length using a one-sample *t* test (Fig. 3).

For experiments in Chapter 3, binomial analyses were used to determine whether reassortment occurred randomly. Given that reassortment was assessed for six genome segments, and there were two possible genotypes for each segment, either WT or BC, there were 2^6, or 64, possible combinations of segments. Two (3%) of these 64 combinations would represent the WT and BC parental genotypes, while the other 62 (97%) would represent reassortant genotypes. If genome segments were randomly exchanged, the number of reassortant progeny should not significantly deviate from the expected percentage of reassortant progeny.

To determine whether larger or small genome segments undergo reassortment more frequently, genome segments from each clone were divided into triplets based on size – small segments (S1, S2, and S3) and medium/large segments (M1, M3, and L2). The percentage of segments of WT origin for medium/large and small segments, and the percentage of medium/large and small segment triplets that were reassortant, were totaled for all coinfection and superinfection progeny. Chi squared analyses were then

used to determine if the observed number of medium/large segments that were i) of WT origin, or ii) were reassortant, differed from that observed for small segments. Comparison of small and medium/large segments revealed no statistically significant differences in the proportion of segments that were WT during coinfection at any MOI (MOI = 0.1 PFU/cell/virus, $p = 0.937$; MOI = 1 PFU/cell/virus, $p = 0.813$; MOI = 10 PFU/cell/virus, $p = 0.644$; MOI = 100 PFU/cell/virus, $p = 0.318$) or during superinfection at any time point (0 h superinfection= 0.735; 4 h superinfection= 0.537; 8 h superinfection= 0.248; 12 h superinfection= 0.572; 16 h superinfection= 0.538). Additionally, no differences were observed for the percentage of clones that were reassortant between medium/large and small segments during coinfection (MOI = 0.1 PFU/cell/virus, $p = 0.343$; MOI = 1 PFU/cell/virus, $p = 1.0000$; MOI = 10 PFU/cell/virus, $p = 0.813$; MOI = 100 PFU/cell/virus, $p = 0.634$) or superinfection (0 h superinfection= 0.623; 4 h superinfection= 0.114; 8 h superinfection= 0.095; 12 h superinfection= 0.442; 16 h superinfection= 0.343).

Simple linear regression analyses were conducted to compare transcript abundance to reassortment frequency during coinfection and superinfection. To determine if primary infection restricted superinfecting virus transcript abundance at a 24 h superinfection time point, statistical significance was determined by unpaired t-test. One-way ANOVA with Tukey's multiple comparisons test was conducted to determine whether significant differences existed between time points for the proportion and ratio of VFs containing +RNA from WT and BC viruses. For experiments comparing transcript abundance in mock primary infection and BC primary infection over a time course, statistical

significance was determined by two-way ANOVA with Sidak's multiple comparison test. All statistical analyses were conducted using GraphPad Prism version 9.3.1.

In Chapter 4, to determine whether superinfecting virus transcript abundance was changed following T1L or T3D primary infection relative to mock primary infection in wild-type or IFNAR KO SVECs, one-way ANOVA analysis with Tukey's multiple comparisons test was performed. Statistical analyses were conducted using GraphPad Prism version 9.3.1.

5.18. Data Availability.

Data generated from Illumina RNA-seq can be accessed at NCBI Gene Expression Omnibus (GEO) under accession number GSE164270. Illumina RNA-seq data for rsT1L virions can also be accessed at NCBI Sequence Read Archive (SRA) under the BioProject accession PRJNA669717.

CHAPTER 6

SUMMARY AND FUTURE DIRECTIONS

6.1. Introduction

Efficient packaging of the viral genome is critical to the formation of infectious virus particles. Packaging of segmented viral genomes is generally thought to occur through one of two mechanisms, a core-filling model, where genome segments are introduced into a pre-existing capsid, and a concerted model, where viral RNA associates to form a packageable supramolecular complex prior to encapsidation (McDonald et al., 2016). Most recent evidence suggests that viruses of the *Reoviridae* family, including rotavirus, bluetongue virus, and mammalian orthoreovirus (reovirus) follow the concerted model to package their segmented, double-stranded RNA (dsRNA) genome. Recent *in vitro* studies of bluetongue virus and rotavirus packaging have significantly advanced our understanding of genome packaging requirements for these viruses; however, prior to my dissertation research, little was known about the specificity of packaging and the capacity of these viruses to package non-viral RNA.

When viruses with segmented genomes coinfect a host, they can exchange genome segments to generate genetically novel strains through a process called reassortment. Reassortment events directly contributed to the generation of the influenza A viruses that caused the pandemics of 1957, 1968, and 2009 (Kawaoka, Krauss, and Webster, 1989; Fang et al., 1981; Garten et al., 2009), leading to millions of deaths globally (Mostafa et al., 2018), and have driven zoonotic transmission and led to the development of antiviral resistance (Lin et al., 2000; Simonsen et al., 2007). As such,

understanding how reassortment is regulated is critically important to predicting the occurrence of future outbreaks. Incompatibility between coinfecting viruses can restrict reassortment; however, little is known about other processes that influence reassortment. Many viruses, including those with segmented genomes, compartmentalize replication in the host cytoplasm, and how this is executed in the context of coinfection, and the influence of intracellular compartmentalization on reassortment, had yet to be explored when I began my thesis work. Furthermore, host responses to infection, as well as interference from other viruses, can limit viral infection. Little was understood about the contribution of these virus-host and virus-virus interactions to reovirus reassortment at the beginning of my studies.

6.2. Reovirus packaging is precise and only allows for introduction of novel RNA species in the absence of genome.

Most evidence suggests that viruses of the *Reoviridae* family package their segmented, dsRNA genomes using a concerted packaging model. Specifically, bluetongue virus packaging is mediated by *cis*- and *trans*-segment interactions that are initiated by the smallest genome segments (Sung and Roy, 2014; Fajardo, Sung, and Roy, 2015; Fajardo et al., 2017). The 5'- and 3'- untranslated regions of *Reoviridae* family virus genome segments are highly conserved, and these regions, as well as some internal sites, are critical for successful packaging of the genome (Kobayashi et al., 2007; Demidenko et al., 2013; Roner and Steele, 2007; Zou and Brown, 1992; Chappell et al., 1994; Roner and Joklik, 2001; AlShaikhahmed et al., 2018). Furthermore, during infection, reovirus generates genome-containing virions as well as "genomeless" top

component particles, suggesting that assembling particles either package all ten genome segments or none (Smith, Zweerink, and Joklik, 1969; Lai, Wérenne, and Joklik, 1973). However, influenza A virus, which also packages its genome in a concerted manner, can package multiple copies of a single genome segment, and rotavirus has been shown to package duplications within genome segments (Enami et al., 1991). Furthermore, about 25% of the RNA within reovirus virions are short, abortive transcripts (Shatkin and Sipe, 1968). Thus, it was known that there is excess volume within reovirus particles, especially genomeless top component particles.

In Chapter 2, I provide further evidence that reovirus virions strictly package the viral genome. Specifically, next-generation RNA sequencing analyses indicated that virions exclusively package viral genome segments, and read counts mapping to each segment are proportional to the size of a given segment (**Fig. 2-3 and Table 2-2**). In contrast, top component particles package many host RNAs, and show a preference for packaging histone transcripts (**Fig. 2-4 and Table 2-3**). Packaging of host transcripts by top component was unlikely to be driven by increased expression of host transcripts, as there was no overlap in genes that were upregulated in top component compared to those that were upregulated in infected cell monolayers, relative to their respective mock fractions. In addition to providing support for an all-or-nothing packaging scheme, these studies were the first to determine that any virus of the *Reoviridae* family packages host RNA. These findings provide support for the importance of specific structural features in driving packaging of viral and host transcripts within assembling reovirus particles and raise questions regarding the importance of reovirus top component particles to reovirus replication.

A major open question related to host RNA packaging by top component is what influence packaging of host RNA has on viral genome packaging. Like viral +RNA, histone transcripts are non-polyadenylated (Marzluff, Wagner, and Duronio, 2008), form terminal stem loop structures (Dominski and Marzluff, 2007), and are relatively short in length (Marzluff and Koreski, 2017). Given that many of the host RNAs packaged by top component share structural features with reovirus +RNA transcripts, it is possible that packaging of these host RNAs interferes with reovirus genomic packaging. To directly test the influence of host RNA packaging on the ability of reovirus to package its viral genome, host RNAs that are packaged into top component particles could be transiently overexpressed by transfection just prior to reovirus infection. Transmission electron microscopy on infected cells could then be used to determine whether the proportion of particles that contain the genome are decreased when specific host RNAs are overexpressed. A complementary experiment could use short-interfering RNAs targeting the host RNA of interest to reduce its expression and determine if the decreased expression of packaged host RNAs increases the proportion of genome-containing virions in infected cells. It is also possible that host RNAs do not compete with viral RNA for packaging and that packaging of host RNAs occurs only in the absence of efficient viral genome packaging. Type 1 reovirus packages its genome much more efficiently than do type 3 viruses, and this difference corresponds to the propensity for these viruses to associate with the host cytoskeleton (Shah et al., 2017). Type 1 reovirus VFs track along microtubules through association with the polymerase cofactor, μ2, and differences in a single amino acid at residue 208 in μ2 determines whether forms filamentous VFs or globular VFs (Parker et al., 2002). This may suggest

the presence of a viral factor, such as μ2, is responsible for determining whether genome is incorporated into assembling reovirus particles. To directly test the contribution of μ2 association with microtubules on genome packaging efficiency and the incorporation of host RNA into top component, T1L and T3D viruses with swapped M1 segments (the segment encoding μ2), or with M1 segments engineered to have the 208 amino acid residue from the opposite strain, could be generated by reverse genetics. Electron microscopy as well as purification of virions and top component after infection would reveal whether T3D generates less top component, and by extension packages its genome more efficiently, when T3D expresses μ2 from a T1L virus. Subsequent next-generation RNA sequencing from top component particles from T1L, T3D, T1L-M1T3D and T3D-M1T1L viruses would further determine whether the identity of host RNA packaged into top component is driven by μ2.

How viral and host RNAs are selected for packaging is also of interest. I found that top component particles generated by T1L reovirus package various histone transcripts, while top component from a T3D virus with a T1L polymerase primarily packages transcripts involved in the host response to infection (**Fig. 2-5**). The prevalence of transcripts involved in host defense may suggest that, in addition to structural features, increased concentration of some transcripts may be important in driving packaging of some transcripts. Beyond determining how host RNA is selected for packaging into assembling virus particles, it will also be important to understand how host RNAs gain access to sites of genome assembly. Reovirus replicates and packages its genome within VFs that are surrounded by viral nonstructural proteins (Miller et al., 2010; Shah et al., 2017; Broering et al., 2005; Becker, Peters, and Dermody, 2003; Tenorio et al.,

2019). It has recently been appreciated that nonstructural protein σNS is responsible for recruiting viral +RNA into VFs (Lee et al., 2021); however, it has yet to be shown whether σNS, or any other viral protein, associates with host RNA. If only select host RNAs gain access to VFs, whether through interaction with viral proteins or some other mechanism, this selection process may be an important determining factor in what host RNAs can be packaged into assembling reovirus particles. Fluorescent *in situ* hybridization (FISH) probes designed to target host RNAs that are packaged by top component could reveal whether these host RNAs gain access to VFs. Lee et al. generated constructs with mutations in predicted RNA-binding regions of σNS and demonstrated that viral RNA does not localize to VFs when σNS does not bind viral RNA (Lee et al., 2021). These same constructs could be transfected into cell lines stably-expressing siRNA towards S3, the gene encoding σNS, to determine whether the ability of host RNAs to access VFs is also dependent on the RNA binding properties of σNS. FISH probes targeting host RNAs that are packaged by top component, and those that are not packaged by top component, would determine whether some amount of specificity in packaging is determined by the ability of host RNAs to gain access to VFs.

Finally, the importance of host RNA packaging for reovirus replication has yet to be determined. Given that packaged host transcripts were largely single-stranded and were not increased in abundance in infected cells (**Fig. 2-4**), it seems unlikely that the reovirus RNA-dependent RNA polymerase is capable of using these transcripts as templates for transcription. Reovirus extrudes transcribing RNA from turrets formed by λ2 on core particles lacking an outer capsid (Reinisch, Nibert, and Harrison, 2000). As such, recognition and transcription of RNA by the polymerase is likely critical for top

component particles to release packaged host transcripts. Therefore, packaging of host RNA into top component particles is unlikely to affect host cells that take up top component particles. Furthermore, electron micrographs have shown that nearly all particles generated during T1L reovirus infection are genome-containing virions, while about half of particles made during T3D infection are genomeless (Shah et al., 2017). Electron micrographs from studies of reovirus egress pathways also indicate that despite top component particles being abundant in VFs, only mature virions gain access to sorting organelles and membranous carriers, which are responsible for transporting virus to the plasma membrane (Fernández de Castro et al., 2020). To determine if top component egresses from host cells, supernatant from infected cells could be overlayed on a cesium chloride density gradient and ultracentrifuged to separate virions from top component. If top component egresses, a top component band should be easily differentiated from virions on the density gradient. If reovirus top component does egress from the host cell, it may reduce the likelihood of successful infection by decreasing the total proportion of genome-containing particles entering host cells. In this case, the ability of reovirus to efficiently package the genome, and potential competition for packaging by host RNAs, could determine the abundance of infectious progeny that is formed within host cells.

6.3. Reassortment is an efficient process for many viruses with segmented genomes.

Reassortment among viruses of the *Reoviridae* family occurs frequently during natural infection (Qin et al., 2017; Zhang et al., 2016; Naglič et al., 2018; Wang et al., 2015;

Mikuletič et al., 2019; Dóró et al., 2015; Nomikou et al., 2015). However, for viruses to reassort their genomes, they must be compatible enough that their genome segments can be co-packaged and that their proteins cooperate to form functional progeny (McDonald et al., 2016; Phipps et al., 2015; Nibert, Margraf, and Coombs, 1996). Incompatibilities among parent viruses was a well-established limitation to reassortment when I initiated my studies (Lubeck, Palese, and Schulman, 1979; Wenske et al., 1985); however, little was known about what other limitations exist. Studies of influenza A virus reassortment showed that in the absence of segment mismatch, coinfection via distinct routes of inoculation leads to spatial compartmentalization within the respiratory tract of an infected host, almost completely preventing reassortment (Richard et al., 2018). Reovirus and other members of the *Reoviridae* family compartmentalize replication within cytoplasmic VFs (Tenorio et al., 2019). Thus, spatial compartmentalization was a recently appreciated influence of reassortment potential, but the influence of intracellular compartmentalization had yet to be determined.

My studies were the first to define reovirus reassortment frequency in the absence of segment mismatch. Quantitation of influenza A virus reassortment in the absence of segment mismatch showed that reassortment occurs frequently during simultaneous coinfection and with a time delay to superinfection up to 8 hours (Marshall et al., 2013). However, reassortment frequency is reduced dramatically with greater time delay to superinfection (Marshall et al., 2013). While I found that reovirus reassorts genome segments frequently when viruses coinfect at the same time, reassortment frequency gradually decreases with greater time to superinfection, and this correlates well with the abundance of superinfecting virus +RNA (**Fig. 3-4A,B**). Furthermore, +RNA was not

strictly compartmentalized within VFs, suggesting that intracellular compartmentalization is not a significant determinant of reassortment frequency (**Fig. 3-6A-C**). These studies advanced the existing understanding of reassortment, as they revealed that intracellular compartmentalization, at least for reovirus, is not a major determinant of reassortment frequency, and that replication dynamics for a given virus within an infected host influence the likelihood of reassortment. Coinfection is required for reassortment, but the likelihood of reassortment, and the genetic makeup of reassortant progeny, are influenced by the intracellular abundance of coinfecting viruses. This is likely to be especially important during coinfection with viruses that differ in replicative fitness in a given host, as viruses that replicate to lower titers are less likely to be represented in reassortant progeny, if the virus manages to reassort its genes at all.

When I began my studies, the working hypothesis for regulation of reovirus transcription and RNA localization suggested that initial rounds of transcription occurred in the cytoplasm early in infection but that the bulk of viral transcription occurred within VFs (Shatkin and Lafiandra, 1972; Antczak and Joklik, 1992; Miller et al., 2010). In Chapter 3, I show that +RNA is localized to both the cytoplasm and VFs throughout infection (**Fig. 3-6A-C**). Furthermore, I observed that a time delay between introduction of a primary infecting virus and introduction of a second virus did not alter this pattern of +RNA localization; regardless of when the second virus was introduced, +RNA from both coinfecting viruses was localized to both the cytoplasm and VFs (**Fig. 3-6A-C,G-H**). These findings are supported by fluorescent *in situ* hybridization studies which indicate that the majority of reovirus mRNA is not localized to VFs (Lee et al., 2021). Because reovirus +RNA synthesis is primarily localized to VFs following the initial

rounds of transcription in the cytoplasm (Miller et al., 2010), this provides evidence for a model of reovirus transcription whereby reovirus +RNA is synthesized within VFs but can then traffic to the cytoplasm, and potentially other VFs. Live-cell imaging of reovirus +RNA could definitively determine whether +RNA freely traffics into and out of VFs. Recent developments in RNA imaging technologies allow for live-cell, single-molecule detection of coding and non-coding RNAs tagged with RNA aptamers, such as Mango II, without altering subcellular localization of the modified RNAs (Cawte, Unrau, and Rueda, 2020). The reovirus S4 genome segment is amenable to introduction of exogenous sequence as long as the 5' and 3' terminal sequences are conserved (Kobayashi et al., 2007). Introduction of Mango II aptamers into the S4 segment, along with transfection of plasmids encoding σNS and a tetracysteine-tagged μNS would reveal whether S4 RNA traffics into factory-like structures. Transfection of this S4-Mango II construct and tetracysteine-tagged μNS into infected cells that constitutively express σ3, the protein encoded by S4, would allow for the assessment of RNA trafficking into and out of VFs in the context of infection. The contribution of various viral proteins, such σNS, on the ability of viral RNA to traffic back to the cytoplasm could also be determined using this system. This RNA imaging system would also help to determine if viral RNA only gains access to large VFs by fusion events, or whether RNA from superinfecting viruses is directly recruited from the cytoplasm. Why reovirus RNA might traffic back into the cytoplasm would be an important topic of future investigation.

Viruses with segmented genomes replicate within host cells by different strategies; however, all of these viruses must coordinate replication such that the viral genome is co-localized with the appropriate viral proteins to be encapsidated. In this dissertation, I

show that reovirus +RNA is not precluded from accessing existing VFs. While this only represents one of many viruses with segmented genomes, this finding may still have broader implications. For instance, many viruses of the *Reoviridae* family replicate within proteinaceous VFs that are similar to those established by reovirus (Tenorio et al., 2019). As such, the ability of +RNA from coinfecting viruses to readily access VFs from both viruses may translate to other viruses of the *Reoviridae* family and may help explain why reassortment is common in the evolutionary history of many of these viruses. More broadly, this may highlight the importance of viruses to be able recruit RNA to sites of replication for reassortment to occur. Thus, future investigations into RNA localization from coinfecting viruses with segmented genomes that utilize distinct replication strategies from reovirus could reveal whether all viruses with segmented genomes allow RNA from coinfecting viruses to co-localize with replication compartments.

6.4. Superinfection exclusion may pose a barrier to reovirus reassortment.

Before I initiated my studies, superinfection exclusion was a well-defined phenomenon for many viruses (Zou et al., 2009; Karpf et al., 1997; Laliberte and Moss, 2014; Huang et al., 2008; Wildum et al., 2006). In fact, multiple reports had provided evidence for superinfection exclusion in bluetongue virus, a *Reoviridae* family member (Ramig et al., 1989; Labadie and Roy, 2020). However, previous assessments of superinfection exclusion for reovirus and rotavirus suggested that these viruses do not prevent superinfection, as reassortment can be observed following superinfection (Ramig 1990; Keirstead and Coombs, 1998). In Chapter 3, I provide additional support that reovirus is

capable of reassorting genome segments during superinfection, and I show that this occurs even in the absence of segment mismatch (**Fig. 3-3C**). However, I also show that superinfection is suppressed following primary infection with a type 3, and to a lesser extent type 1, reovirus (**Fig. 3-7B-C; Fig. 4-1**). These studies were the first to exhibit that reovirus suppresses superinfection by closely related viruses and may have important implications for reovirus reassortment.

In Chapter 4, I begin to assess the mechanism of reovirus-mediated superinfection exclusion. Given that reovirus induces the expression of type 1 interferon, this seemed an obvious candidate for potentially driving superinfection exclusion. My *in vitro* studies indicated that suppression of secondary virus replication is minimal in type I IFN receptor knockout cells, suggesting that type I IFN is a major driver of reovirus mediated superinfection exclusion in cell culture. However, in mouse models, type I IFN and type III IFN signaling had no influence on reassortment, regardless of whether coinfection was simultaneous or asynchronous (**Fig. 4-2; Fig. 4-3**). In fact, reassortant viruses were not detected following a 24-hour time delay to superinfection in mice, even in the absence of segment mismatch. Similar observations have been made for influenza A virus (Marshall et al., 2013). The observation that reassortants were not detected during superinfection *in vivo* is not necessarily indicative of superinfection exclusion. Rather, it likely stresses the requirement of coinfection for reassortment to occur, and future studies should directly address whether the absence of reassortment is due to superinfection exclusion or is a byproduct of how reovirus spreads within a host. This could be determined by quantifying the number of cells infected by a superinfecting virus following a mock primary infection or primary infection with a type 3 reovirus.

Branched DNA FISH probes specific to coinfecting viruses, which were developed as part of this dissertation, paired with flow cytometry would be useful tools in future studies of *in vivo* coinfection frequency and superinfection exclusion. Specifically, the number of cells that are infected by a superinfecting virus following mock primary infection or 24-hour primary infection of wild-type, type 1 IFN knockout, and type 3 IFN knockout mice with $T3D^{I}$ reovirus could be quantified with branched DNA FISH probes specific to the superinfecting virus by flow cytometry. If superinfection is reduced in wild-type mice and knockout of IFN receptors does not recover the reduction of superinfection, this would indicate that superinfection exclusion is not mediated by IFN in mice. To further assess the mechanism of superinfection exclusion, antibodies that specifically bind the reovirus receptor JAM-A, or staining for caspase expression, would reveal whether cells in the infected host show reduced expression of the entry receptor, or are undergoing cell death, in response to infection. This may suggest that one of these factors contributes to reovirus superinfection exclusion.

Reassortment frequency can differ depending on the host species (Postnikova et al., 2021; Lin et al., 2017). For instance, influenza A virus frequently reassorts genome segments in avian hosts, but rarely reassorts in humans (Leonard et al., 2017). Although the precise frequency of reovirus infection and coinfection has not been determined, over half of children have been exposed to type 3 reovirus by the age of 5 (Tai et al., 2005). The finding that reassortment is frequent during coinfection of mice, but was not detected during superinfection, could have important implications for natural infection. If this finding translates to other host species, it may suggest that hosts not only need to be coinfected, but must be coinfected within a narrow time frame, to allow

for robust reassortment. This observation may be indicative of an additional layer of regulation that is required for reassortment to occur during natural infection and may highlight the importance of frequent coinfection as a requirement for reassortment. Furthermore, within a given host, viruses undergo frequent genetic bottlenecks in infected cells (Zwart and Elena, 2015). Viruses with RNA genomes often have error prone polymerases that lead to the rapid accumulation of mutations, such that viral populations can be thought of as “mutant clouds” made up of a large number of variant genomes (Domingo and Perales, 2019). I have demonstrated that reassortment is most frequent when reoviruses enter cells at the same time and are equally abundant within a coinfected cell. Taken together, this may suggest that within an infected host, reassortment occurs frequently among highly-similar variants. Whether this is true, and whether reassortment among minor variants confers an advantage to viruses with segmented genomes would be an interesting course of future investigation.

6.5. Concluding Remarks

Viruses with segmented genomes must synchronize many complex processes to successfully package the correct number and species of RNA to form infectious particles. To exchange genome segments, these viruses must coinfect the same host, the same cell within that host, and be able to form viable progeny. My dissertation work provided valuable knowledge to our understanding of how viruses package and reassort segmented genomes. For instance, I showed for the first time that viruses of the *Reoviridae* family package host RNA and that these host RNAs share structural features with viral +RNA. This moves forward our fundamental understanding of

packaging of segmented viral genomes by stressing the importance of structural features of RNA in this process and suggests that competition with host RNA for packaging may be important in determining packaging efficiency. Furthermore, I defined reovirus reassortment frequency in the absence of segment mismatch and show that the abundance of virus within cells, but not the compartmentalized replication strategy, dictates reassortment frequency. Finally, I show that the timing of coinfection is important in determining how frequently coinfecting viruses exchange genome segments.

Reassortment events can enable viruses to make host jumps into humans and can generate viruses with enhanced transmission that cause significant morbidity and mortality. Collectively, the work presented in this dissertation advances the understanding of how coinfecting viruses coordinate replication processes to reassort their genomes during coinfection and temporal regulation of this process. On a broader scale, this may help others to better understand why reassortment occurs with varying frequency in different hosts and may assist with predicting the likelihood of reassortment among naturally circulating strains.

REFERENCES

Acs G., Klett H., Schonberg M., Christman J., Levin D.H., Silverstein S.C. (1971) Mechanism of reovirus double-stranded ribonucleic acid synthesis in vivo and in vitro. J Virol, 8, 684-689.

Aguilera E.R., Erickson A.K., Jesudhasan P.R., Robinson C.M., Pfeiffer J.K. (2017) Plaques formed by mutagenized viral populations have elevated coinfection frequencies. mBio, 8, e02020-16.

AlShaikhahmed, K. Leonov, G. Sung, P. Y. Bingham, R. J. Twarock, R. Roy, P. (2018) Dynamic network approach for the modelling of genomic sub-complexes in multi-segmented viruses. Nucleic Acids Res, 46, 12087-12098.

Andrews, S. (2010) FastQC: A Quality Control Tool for High Throughput Sequence Data [Online].

Antczak J.B., Chmelo R., Pickup D.J., Joklik W.K. (1982) Sequences at Both Termini of the 10 Genes of Reovirus Serotype 3 (Strain Dearing). Virology, 121, 307-319.

Antczak, J. B. Joklik, W. K. (1992) Reovirus genome segment assortment into progeny genomes studied by the use of monoclonal antibodies directed against reovirus proteins. Virology, 187, 760-76.

Baldridge M.T., Lee S., Brown J.J., McAllister N., Urbanek K., Nice T.J., Dermody T.S., Virgin H.W. (2017) Expression of Ifnlr1 on intestinal epithelial cells is critical to the antiviral effects of interferon lambda against norovirus and reovirus. J Virol, 91, e02079-16.

Ballard, A. McCrae, M. A. Desselberger, U. (1992) Nucleotide sequences of normal and rearranged RNA segments 10 of human rotaviruses. J Gen Virol, 73, 633-638.

Bányai K., Martella V., Molnár P., Mihály I., van Ranst M., Matthijnssens J. (2009) Genetic heterogeneity in human G6P[14] rotavirus strains detected in Hungary suggests independent zoonotic origin. J Infect, 59, 213-224.

Becker M.M., Goral M.I., Hazelton P.R., Baer G.S., Rodgers S.E., Brown E.G., Coombs K.M., Dermody T.S. (2001) Reovirus σNS protein is required for nucleation of viral assembly complexes and formation of viral inclusions. J Virol, 75, 1459–1475.

Becker M.M., Peters T.R., Dermody T.S. (2003) Reovirus σNS and μNS Proteins Form Cytoplasmic Inclusion Structures in the Absence of Viral Infection. J Virol, 77, 5948–5963.

Bellamy A.R., Xhapiro L., August J.T., Joklik W.K. (1967) Studies on reovirus RNA I. Characterization of reovirus genome RNA. J Mol Biol, 29, 1-17.

Berard A., Coombs K.M. (2009) Mammalian reoviruses: Propagation, quantification, and storage. Curr Protoc Microbiol 15C.1.1-15C.1.18.

Berger A.K., Danthi P. (2013) Reovirus activates a caspase-independent cell death pathway. mBio, 4, e00178-13.

Bishop, J. M. Levinson, W. E. Sullivan, D. Fanshier, L. Quintrell, N. Jackson, J. (1970) The low molecular weight RNAs of Rous sarcoma virus. II. The 7 S RNA. Virology**,** 42, 927-937.

Bodkin D.K., Fields B.N. (1989) Growth and Survival of Reovirus in Intestinal Tissue: Role of the L2 and S1 Genes. J Virol, 63, 1188-1193.

Borodavka, A. Ault, J. Stockley, P. G. Tuma, R. (2015) Evidence that avian reovirus σNS is an RNA chaperone: implications for genome segment assortment. Nucleic Acids Res, 43, 7044-57.

Borodavka, A. Desselberger, U. Patton, J. T. (2018) Genome packaging in multi-segmented dsRNA viruses: distinct mechanisms with similar outcomes. Curr Opin Virol, 33, 106-112.

Borodavka, A. Dykeman, E. C. Schrimpf, W. Lamb, D. C. (2017) Protein-mediated RNA folding governs sequence-specific interactions between rotavirus genome segments. eLife, 6.

Bouziat, R. Hinterleitner, R. Brown, J. J. Stencel-Baerenwald, J. E. Ikizler, M. Mayassi, T. Meisel, M. Kim, S. M. Discepolo, V. Pruijssers, A. J. Ernest, J. D. Iskarpatyoti, J. A. Costes, L. M. Lawrence, I. Palanski, B. A. Varma, M. Zurenski, M. A. Khomandiak, S. McAllister, N. Aravamudhan, P. Boehme, K. W. Hu, F. Samsom, J. N. Reinecker, H. C. Kupfer, S. S. Guandalini, S. Semrad, C. E. Abadie, V. Khosla, C. Barreiro, L. B. Xavier, R. J. Ng, A. Dermody, T. S. Jabri, B. (2017) Reovirus infection triggers inflammatory responses to dietary antigens and development of celiac disease. Science, 356, 44-50.

Bravo, J. P. K. Borodavka, A. Barth, A. Calabrese, A. N. Mojzes, P. Cockburn, J. J. B. Lamb, D. C. Tuma, R. (2018) Stability of local secondary structure determines selectivity of viral RNA chaperones. Nucleic Acids Res, 46, 7924-7937.

Brentano L., Noah D.L., Brown E.G., Sherry B. (1998) The Reovirus Protein μ2, Encoded by the M1 Gene, Is an RNA-Binding Protein. J Virol, 72, 8354–8357.

Briese T., Calisher C.H., Higgs S. (2013) Viruses of the family *Bunyaviridae*: are all available isolates reassortants? Virology, 446, 207–216

Broering T.J., Arnold M.M., Miller C.L., Hurt J.A., Joyce P.L., Nibert M.L. (2005) Carboxyl-Proximal Regions of Reovirus Nonstructural Protein μNS Necessary and Sufficient for Forming Factory-Like Inclusions. J Virol, 79, 6194–6206.

Broering T.J., Parker J.S.L., Joyce P.L., Kim J., Nibert M.L. (2002) Mammalian reovirus nonstructural protein μNS forms large inclusions and colocalizes with reovirus microtubule-associated protein μ2 in transfected cells. J Virol, 76, 8285–8297.

Brown J.J., Short S.P., Stencel-Baerenwald J., Urbanek K., Pruijssers A.J., McAllister N., Ikizler M., Taylor G., Aravamudhan P., Khomandiak S., Jabri B., Williams C.S., Dermody T.S. (2018) Reovirus-induced apoptosis in the intestine limits establishment of enteric infection. J Virol, 92, e02062-17.

Burivong P., Pattanakitsakul S-N., Thongrungkiat S., Malasit P., Flegel T.W. (2004) Markedly reduced severity of Dengue virus infection in mosquito cell cultures persistently infected with *Aedes albopictus* densovirus (AalDNV). Virology, 329, 261–269.

Burkhardt C., Sung P.Y., Celma C.C., Roy P. (2014) Structural constraints in the packaging of bluetongue virus genomic segments. J Gen Virol, 95, 2240–2250.

Bussiere L.D., Choudhury P., Bellaire B., Miller C.L. (2017) Characterization of a replicating mammalian orthoreovirus with tetracysteine-tagged μNS for live-cell visualization of viral factories. J Virol, 91, e01371-17.

Cabral-Romero C., Padilla-Noriega L. (2006) Association of rotavirus viroplasms with microtubules through NSP2 and NSP5. Mem Inst Oswaldo Cruz, 101, 603-611.

Cawte A.D., Unrau P.J., Rueda D.S. (2020) Live cell imaging of single RNA molecules with fluorogenic Mango II arrays. Nat Commun, 11, 1283.

Chandran K., Parker J.S.L., Ehrlich M., Kirchhausen T., Nibert M.L. (2003) The δ Region of Outer-Capsid Protein μ1 Undergoes Conformational Change and Release from Reovirus Particles during Cell Entry. J Virol, 77, 13361–13375.

Chapell, J. D. Goral, M. I. Rodgers, S. E. dePamphilis, C. W. Dermody, T. S. (1994) Sequence diversity within the reovirus S2 gene: reovirus genes reassort in nature, and their termini are predicted to form a panhandle motif. J Virol, 68, 750-756.

Chappell J.D., Barton E.S., Smith T.H., Baer G.S., Duong D.T., Nibert M.L., Dermody T.S. (1998) Cleavage Susceptibility of Reovirus Attachment Protein 1 during Proteolytic Disassembly of Virions Is Determined by a Sequence Polymorphism in the σ1 Neck. J Virol, 72, 8205-8215.

Chappell J.D., Goral M.I., Rodgers S.E., Dermody T.S., Depamphilis C.W. (1994) Sequence diversity within the reovirus S2 gene: Reovirus genes reassort in nature, and their termini are predicted to form a panhandle motif. J Virol, 68, 750–756.

Cleveland D.R., Zarbl H., Millward S. (1986) Reovirus Guanylyltransferase Is L2 Gene Product Lambda 2. J Virol, 60, 307-311.

Coombs K.M. (1998) Stoichiometry of Reovirus Structural Proteins in Virus, ISVP, and Core Particles. Virology, 243, 218–228.

Crawford S.E., Ramani S., Tate J.E., Parashar U.D., Svensson L., Hagbom M., Franco M.A., Greenberg H.B., O'Ryan M., Kang G., Desselberger U., Estes M.K. (2017) Rotavirus infection. Nat Rev Dis Primers 3.

de Castro I.F., Volonté L., Risco C. (2013) Virus factories: Biogenesis and structural design. Cell Microbiol, 15, 24-34.

Demidenko, A. A. Blattman, J. N. Blattman, N. N. Greenberg, P. D. Nibert, M. L. (2013) Engineering recombinant reoviruses with tandem repeats and a tetravirus 2A-like element for exogenous polypeptide expression. Proc Nat Acad Sci, 110, e1867-76.

Dermody, T. S. Parker, J. S. Sherry, B., Orthoreoviruses. In *Fields Virology*, Sixth ed. Knipe, D. M. Howley, P. M., Eds. Lippincott Williams & Wilkins: Philadelphia, 2013 Vol. 2, pp 1304-1346.

Desmet E.A., Anguish L.J., Parker J.S.L. (2014) Virus-mediated compartmentalization of the host translational machinery. mBio, 5, e01463-14.

Dionne K.R., Galvin J.M., Schittone S.A., Clarke P., Tyler K.L. (2011) Type I interferon signaling limits reoviral tropism within the brain and prevents lethal systemic infection. J Neurovirol, 17, 314–326.

Dittmar D., Castro A., Haines H. (1982) Demonstration of interference between dengue virus types in cultured mosquito cells using monoclonal antibody probes. J Gen Virol, 59, 273–282.

Dobin, A. Davis, C. A. Schlesinger, F. Drenkow, J. Zaleski, C. Jha, S. Batut, P. Chaisson, M. Gingeras, T. R. (2013) STAR: ultrafast universal RNA-seq aligner. Bioinformatics 29, 15-21.

Domingo E., Perales C. (2019) Viral quasispecies. PLoS Genet, 15, e1008271.

Dominski Z., Marzluff W.F. (2007) Formation of the 3′ end of histone mRNA: Getting closer to the end. Gene, 396, 373–390.

Donato C.M., Ch'Ng L.S., Boniface K.F., Crawford N.W., Buttery J.P., Lyon M., Bishop R.F., Kirkwood C.D. (2012) Identification of strains of rotateq rotavirus vaccine in infants with gastroenteritis following routine vaccination. J Infect Dis, 206, 377–383.

Doro R., Farkas S.L., Martella V., Banyai K. (2015) Zoonotic transmission of rotavirus: surveillance and control. Expert Rev Anti Infect Ther, 13, 1337–1350.

Dryden K.A., Wang G., Yeager M., Nibert M.L., Coombs K.M., Furlong D.B., Fields B.N., Baker T.S. (1993) Early Steps in Reovirus Infection Are Associated with Dramatic Changes in Supramolecular Structure and Protein Conformation: Analysis of Virions and Subviral Particles by Cryoelectron Microscopy and Image Reconstruction. J Cell Biol, 122, 1023-1041.

Dryden, K. A. Farsetta, D. L. Wang, G. Keegan, J. M. Fields, B. N. Baker, T. S. Nibert, M. L. (1998) Internal/structures containing transcriptase-related proteins in top component particles of mammalian orthoreovirus. Virology**,** 245, 33-46.

Dudas G., Bedford T., Lycett S., Rambaut A. (2015) Reassortment between influenza B lineages and the emergence of a coadapted PB1-PB2-HA gene complex. Mol Biol Evol, 32, 162–172.

Ebert D.H., Deussing J., Peters C., Dermody T.S. (2002) Cathepsin L and cathepsin B mediate reovirus disassembly in murine fibroblast cells. J Biol Chem, 277, 24609–24617.

Eckwahl, M. J. Sim, S. Smith, D. Telesnitsky, A. Wolin, S. L. (2015) A retrovirus packages nascent host noncoding RNAs from a novel surveillance pathway. Genes Dev, 29, (6), 646-57.

Eichwald C., Ackermann M., Nibert M.L. (2018) The dynamics of both filamentous and globular mammalian reovirus viral factories rely on the microtubule network. Virology, 518, 77–86.

Eichwald C., Arnoldi F., Laimbacher A.S., Schraner E.M., Fraefel C., Wild P., Burrone O.R., Ackermann M. (2012) Rotavirus Viroplasm Fusion and Perinuclear Localization Are Dynamic Processes Requiring Stabilized Microtubules. PLoS One, 7, e47947.

Eichwald C., Rodriguez J.F., Burrone O.R. (2004) Characterization of rotavirus NSP2/NSP5 interactions and the dynamics of viroplasm formation. J Gen Virol, 85, 625–634.

Eichwald, C. Kim, J. Nibert, M. L. (2017) Dissection of mammalian orthoreovirus µ2 reveals a self-associative domain required for binding to microtubules but not to factory matrix protein µNS. PLoS One, 12, e0184356.

el Hussein A., Ramig R.F., Holbrook F.R., Beaty B.J. (1989) Asynchronous mixed infection of *Culicoides variipennis* with bluetongue virus serotypes 10 and 17. J Gen Virol, 70, 3355–3362.

Enami M., Sharma G., Benham C., Palese P. (1991) An Influenza Virus Containing Nine Different RNA Segments. Virology, 185, 291-298.

Epstein R.L., Powers M.L., Weiner H.L. (1981) Interaction of reovirus with cell surface. J Immunol, 127, 1800-1803.

Ernst H., Shatkin A.J. (1985) Reovirus hemagglutinin mRNA codes for two polypeptides in overlapping reading frames (bicistronic mRNA/Sl gene structure/translation initiation). Proc Nati Acad Sci, 82, 48-52.

Excoffon K.J.D.A., Guglielmi K.M., Wetzel J.D., Gansemer N.D., Campbell J.A., Dermody T.S., Zabner J. (2008) Reovirus preferentially infects the basolateral surface and is released from the apical surface of polarized human respiratory epithelial cells. J Infect Dis, 197, 1189-1197.

Fajardo T., Sung P.Y., Roy P. (2015) Disruption of Specific RNA-RNA Interactions in a Double-Stranded RNA Virus Inhibits Genome Packaging and Virus Infectivity. PLoS Pathog, 11, e1005321.

Fajardo, T. Sung, P. Y. Celma, C. C. Roy, P. (2017) Rotavirus Genomic RNA Complex Forms via Specific RNA-RNA Interactions: Disruption of RNA Complex Inhibits Virus Infectivity. Viruses 9, 167.

Fang R., Jou W.M., Huylebroeck D., Devos R., Fiers W. (1981) Complete Structure of A/duck/Ukraine/63 Influenza Hemagglutinin Gene: Animal Virus As Progenitor of Human H3 Hong Kong 1968 Influenza Hemagglutinin. Cell, 25, 315-323.

Farsetta D.L., Chandran K., Nibert M.L. (2000) Transcriptional activities of reovirus RNA polymerase in recoated cores. J Biol Chem, 275, 39693–39701.

Fernandes J., Guterres A., de Oliveira R.C., Chamberlain J., Lewandowski K., Teixeira B.R., Coelho T.A., Crisóstomo C.F., Bonvicino C.R., D'Andrea P.S., Hewson R., de

Lemos E.R.S. (2018) Xapuri virus, a novel mammarenavirus: natural reassortment and increased diversity between New World viruses. Emerg Microbes Infect, 7, 120.

Fernández de Castro, I. Zamora, P. F. Ooms, L. Fernández, J. J. Lai, C. M. Mainou, B. A. Dermody, T. S. Risco, C. (2014) Reovirus forms neo-organelles for progeny particle assembly within reorganized cell membranes. mBio, 5, e00931-13.

Fields B.N. (1971) Temperature-sensitive mutants of reovirus type 3 features of genetic recombination. Virology, 46, 142-148.

Folimonova S.Y. (2012) Superinfection Exclusion Is an Active Virus-Controlled Function That Requires a Specific Viral Protein. J Virol, 86, 5554–5561.

Furuichi Y., Muthukrishnan S., Shatkin A.J. (1975) 5'-terminal m7G(5')ppp(5')Gmp in vivo: identification in reovirus genome RNA. Proc Nat Acad Sci, 72, 742-745.

Garten R.J., Davis C.T., Russell C.A., Shu B., Lindstrom S., Balish A., Sessions W.M., Xu X., Skepner E., Deyde V., Okomo-Adhiambo M., Gubareva L., Barnes J., Smith C.B., Emery S.L., Hillman M.J., Rivailler P., Smagala J., de Graaf M., Burke D.F., Fouchier R.A.M., Pappas C., Alpuche-Aranda C.M., López-Gatell H., Olivera H., López I., Myers C.A., Faix D., Blair P.J., Yu C., Keene K.M., Dotson P.D., Boxrud D., Sambol A.R., Abid S.H., St. George K., Bannerman T., Moore A.L., Stringer D.J., Blevins P., Demmler-Harrison G.J., Ginsberg M., Kriner P., Waterman S., Smole S., Guevara H.F., Belongia E.A., Clark P.A., Beatrice S.T., Donis R., Katz J., Finelli L., Bridges C.B., Shaw M., Jernigan D.B., Uyeki T.M., Smith D.J., Klimov A.I., Cox N.J. (2009) Antigenic and genetic characteristics of swine-origin 2009 A(H1N1) influenza viruses circulating in humans. Science, 325, 197–201.

Gauliard N., Billecocq A., Flick R., Bouloy M. (2006) Rift Valley fever virus noncoding regions of L, M and S segments regulate RNA synthesis. Virology, 351, 170–179.

Geiger F., Acker J., Papa G., Wang X., Arter W.E., Saar K.L., Erkamp N.A., Qi R., Bravo J.P., Strauss S., Krainer G., Burrone O.R., Jungmann R., Knowles T.P., Engelke H., Borodavka A. (2021) Liquid–liquid phase separation underpins the formation of replication factories in rotaviruses. EMBO J, 40, e107711.

George A., Kost S.I., Witzleben C.L., Cebra J.J., Rubin, D.H. (1990) Reovirus-induced liver disease in severe combined immunodeficient (SCID) mice. A Model for the Study of Viral Infection, Pathogenesis, and Clearance. J Exp Med, 171, 929-934.

Gerber M., Isel C., Moules V., Marquet R. (2014) Selective packaging of the influenza A genome and consequences for genetic reassortment. Trends Microbiol, 22, 446-455.

Gethmann J., Probst C., Conraths F.J. (2020) Economic Impact of a Bluetongue Serotype 8 Epidemic in Germany. Front Vet Sci 7.

Gombold J.L., Ramig R.F. (1986) Analysis of Reassortment of Genome Segments in Mice Mixedly Infected with Rotaviruses SA11 and RRV. J Virol, 57, 110-116.

Gombold J.L., Ramig R.F. (1989) Passive Immunity Modulates Genetic Reassortment between Rotaviruses in Mixedly Infected Mice. J Virol, 63, 4525-4532.

Gonzalez-Hernandez M.B., Liu T., Payne H.C., Stencel-Baerenwald J.E., Ikizler M., Yagita H., Dermody T.S., Williams I.R., Wobus C.E. (2014) Efficient Norovirus and Reovirus Replication in the Mouse Intestine Requires Microfold (M) Cells. J Virol, 88, 6934–6943.

Gottlieb P., Strassman J., Frucht A., Qiao X., Mindich L. (1991) In Vitro Packaging of the Bacteriophage ¢6 ssRNA Genomic Precursors. Virology, 181, 589-594.

Gottlieb P., Strassman J., Qiao X., Frucht A., Mindich L. (1990) In Vitro Replication, Packaging, and Transcription of the Segmented Double-Stranded RNA Genome of Bacteriophage Φ6: Studies with Procapsids Assembled from Plasmid-Encoded Proteins. J Bacteriol, 172, 5774-5782.

Heinrich M.J., Purcell C.A., Pruijssers A.J., Zhao Y., Spurlock C.F., Sriram S., Ogden K.M., Dermody T.S., Scholz M.B., Crooke P.S., Karijolich J., Aune T.M. 2019. Endogenous double-stranded Alu RNA elements stimulate IFN-responses in relapsing remitting multiple sclerosis. J Autoimmun, 100, 40–51.

Hockman M.R., Jacobs N.T., Mainou B.A., Koelle K., Lowen A.C. (2022) Mammalian Orthoreovirus Reassortment Proceeds with Little Constraint on Segment Mixing. J Virol, 96, e01832-21.

Hockman M.R., Phipps K.L., Holmes K.E., Lowen A.C. (2020) A method for the unbiased quantification of reassortment in segmented viruses. J Virol Methods, 280, 113878.

Holm G.H., Zurney J., Tumilasci V., Leveille S., Danthi P., Hiscott J., Sherry B., Dermody T.S. (2007) Retinoic acid-inducible gene-I and interferon-β promoter stimulator-1 augment proapoptotic responses following mammalian reovirus infection via interferon regulatory factor-3. J Biol Chem, 282, 21953–21961.

Hoyt C.C., Richardson-Burns S.M., Goody R.J., Robinson B.A., DeBiasi R.L., Tyler K.L. (2005) Nonstructural Protein σ1s Is a Determinant of Reovirus Virulence and Influences the Kinetics and Severity of Apoptosis Induction in the Heart and Central Nervous System. J Virol, 79, 2743–2753.

Huang I., Li W., Sui J., Marasco W., Choe H., Farzan M. (2008) Influenza A virus neuraminidase limits viral superinfection. J Virol, 82, 4834–4843.

Huang Y., Dai H., Ke R. (2019) Principles of Effective and Robust Innate Immune Response to Viral Infections: A Multiplex Network Analysis. Front Immunol, 10, 1736.

Huang, Y. Mak, J. Cao, Q. Li, Z. Wainberg, M. A. Kleiman, L. (1994) Incorporation of excess wild-type and mutant tRNA(3Lys) into human immunodeficiency virus type 1. J Virol, 68, 7676-7683.

Hundley, F. Biryahwaho, B. Gow, M. Desselberger, U. (1985) Genome rearrangements of bovine rotavirus after serial passage at high multiplicity of infection. Virology, 143, 88-103.

Irvin S.C., Zurney J., Ooms L.S., Chappell J.D., Dermody T.S., Sherry B. (2012) A single-amino-acid polymorphism in reovirus protein μ2 determines repression of interferon signaling and modulates myocarditis. J Virol, 86, 2302-2311.

Isaacs A., Lindenmann J. (1957) Virus interference. I. The interferon. Proc R Soc Lond B Biol Sci, 147, 258–267.

Ito T., Nelson J., Couceiro S.S., Kelm S., Baum L.G., Krauss S., Castrucci M.R., Donatelli I., Kida H., Paulson J.C., Webster R.G., Kawaoka Y. (1998) Molecular Basis for the Generation in Pigs of Influenza A Viruses with Pandemic Potential. J Virol, 72, 7367-7373.

Jacobs B.L., Ferguson R.E. (1991) The Lang Strain of reovirus serotype 1 and the Dearing strain of reovirus serotype 3 differ in their sensitivities to beta interferon. J Virol, 65, 5102-5104.

Johansson C., Wetzel J.D., He J.P., Mikacenic C., Dermody T.S., Kelsall B.L. (2007) Type I interferons produced by hematopoietic cells protect mice against lethal infection by mammalian reovirus. J Exp Med, 204, 1349–1358.

Johnson E.M., Doyle J.D., Wetzel J.D., McClung R.P., Katunuma N., Chappell J.D., Washington M.K., Dermody T.S. (2009) Genetic and Pharmacologic Alteration of Cathepsin Expression Influences Reovirus Pathogenesis. J Virol, 83, 9630–9640.

Joklik W., Roner M. (1995) What reassorts when reovirus gene segments reassort? J Biol Chem, 270, 4181–4184.

Joklik W.K. (1981) Structure and Function of the Reovirus Genome. Microbiol Rev, 45, 483-501.

Karapanagiotou E.M., Roulstone V., Twigger K., Ball M., Tanay M.A., Nutting C., Newbold K., Gore M.E., Larkin J., Syrigos K.N., Coffey M., Thompson B., Mettinger K., Vile R.G., Pandha H.S., Hall G.D., Melcher A.A., Chester J., Harrington K.J. (2012) Phase I/II trial of carboplatin and paclitaxel chemotherapy in combination with intravenous oncolytic reovirus in patients with advanced malignancies. Clin Cancer Res, 18, 2080–2089.

Karpf A.R., Lenches E., Strauss E.G., Strauss J.H., Brown D.T. (1997). Superinfection Exclusion of Alphaviruses in Three Mosquito Cell Lines Persistently Infected with Sindbis Virus. J Virol, 71, 7119–7123.

Kato H., Takeuchi O., Mikamo-Satoh E., Hirai R., Kawai T., Matsushita K., Hiiragi A., Dermody T.S., Fujita T., Akira S. (2008) Length-dependent recognition of double-stranded ribonucleic acids by retinoic acid-inducible gene-I and melanoma differentiation-associated gene 5. J Exp Med, 205, 1601–1610.

Kawaoka Y., Krauss S., Webster R.G. (1989) Avian-to-Human Transmission of the PB1 Gene of Influenza A Viruses in the 1957 and 1968 Pandemics. J Virol, 63, 4603-4608.

Kedl R., Schmechel S., Schiff L. (1995) Comparative Sequence Analysis of the Reovirus S4 Genes from 13 Serotype 1 and Serotype 3 Field Isolates. J Virol, 69, 552–559.

Keirstead N.D., Coombs K.M. (1998) Absence of superinfection exclusion during asynchronous reovirus infections of mouse, monkey, and human cell lines. Virus Res, 4, 225-235.

Kell A.M., Gale M. (2015) RIG-I in RNA virus recognition. Virology, 479-480, 110-121.

Kim H., Webster R.G., Webby R.J. (2018) Influenza Virus: Dealing with a Drifting and Shifting Pathogen. Viral Immunol, 31, 174–183.

Kniert J., dos Santos T., Eaton H.E., Cho W.J., Plummer G., Shmulevitz M. (2022) Reovirus uses temporospatial compartmentalization to orchestrate core versus outercapsid assembly. bioRxiv, doi: 10.1101/2022.06.06.494974.

Kobayashi T., Antar A.A.R., Boehme K.W., Danthi P., Eby E.A., Guglielmi K.M., Holm G.H., Johnson E.M., Maginnis M.S., Naik S., Skelton W.B., Wetzel J.D., Wilson G.J., Chappell J.D., Dermody T.S. (2007) A plasmid-based reverse genetics system for animal double-stranded RNA viruses. Cell Host Microbe, 1, 147-157.

Kobayashi, T. Ooms, L. S. Ikizler, M. Chappell, J. D. Dermody, T. S. (2010) An improved reverse genetics system for mammalian orthoreoviruses. Virology, 398, 194-200.

Kojima, K. Taniguchi, K. Kawagishi-Kobayashi, M. Matsuno, S. Urasawa, S. (2000) Rearrangement generated in double genes, NSP1 and NSP3, of viable progenies from a human rotavirus strain. Virus Res, 67, 163-71.

Komoto S., Kawagishi T., Kobayashi T., Ikizler M., Iskarpatyoti J., Dermody T.S., Taniguchi K. (2014) A plasmid-based reverse genetics system for mammalian orthoreoviruses driven by a plasmid-encoded T7 RNA polymerase. J Virol Methods, 196, 36–39.

Komoto, S. Fukuda, S. Ide, T. Ito, N. Sugiyama, M. Yoshikawa, T. Murata, T. Taniguchi, K. (2018) Generation of Recombinant Rotaviruses Expressing Fluorescent Proteins by Using an Optimized Reverse Genetics System. J Virol, 92, e00588-18.

Kopek B.G., Perkins G., Miller D.J., Ellisman M.H., Ahlquist P. (2007) Three-dimensional analysis of a viral RNA replication complex reveals a virus-induced mini-organelle. PLoS Biol, 5, 2022–2034.

Kumar N., Sharma S., Barua S., Tripathi B.N., Rouse B.T. (2018) Virological and Immunological Outcomes of Coinfections. Clin Microbiol Rev, 31, e00111-17.

Labadie T., Roy P. (2020) A non-enveloped arbovirus released in lysosome-derived extracellular vesicles induces super-infection exclusion. PLoS Pathog, 16, e1009015.

Lai, M. H. Wérenne, J. J. Joklik, W. K. (1973) The preparation of reovirus top component and its effect on host DNA and protein synthesis. Virology 54, 237-244.

Laliberte J.P., Moss B. (2014) A Novel Mode of Poxvirus Superinfection Exclusion That Prevents Fusion of the Lipid Bilayers of Viral and Cellular Membranes. J Virol, 88, 9751–9768.

Laureti M., Paradkar P.N., Fazakerley J.K., Rodriguez-Andres J. (2020) Superinfection exclusion in mosquitoes and its potential as an arbovirus control strategy. Viruses, 12, 1259.

Lazear H.M., Nice T.J., Diamond M.S. (2015) Interferon-λ: Immune Functions at Barrier Surfaces and Beyond. Immunity, 43, 15-28.

Lee C.H., Raghunathan K., Taylor G.M., French A.J., Tenorio R., de Castro I.F., Risco C., Parker J.S.L., Dermody T.S. (2021) Reovirus nonstructural protein σNS recruits viral RNA to replication organelles. mBio, 12, e01408-21.

Lelli D., Moreno A., Steyer A., Naglič T., Chiapponi C., Prosperi A., Faccin F., Sozzi E., Lavazza A. (2015) Detection and characterization of a novel reassortant mammalian orthoreovirus in bats in Europe. Viruses, 7, 5844–5854.

Li C., Hatta M., Watanabe S., Neumann G., Kawaoka Y. (2008) Compatibility among polymerase subunit proteins is a restricting factor in reassortment between equine H7N7 and human H3N2 influenza viruses. J Virol, 82, 11880–11888.

Li L., Sherry B. (2010) IFN-α expression and antiviral effects are subtype and cell type specific in the cardiac response to viral infection. Virology, 396, 59–68.

Liao, Y. Smyth, G. K. Shi, W. (2014) featureCounts: an efficient general purpose program for assigning sequence reads to genomic features. Bioinformatics, 30, 923-30.

Liberzon, A. Birger, C. Thorvaldsdóttir, H. Ghandi, M. Mesirov, J. P. Tamayo, P. (2015) The Molecular Signatures Database (MSigDB) hallmark gene set collection. Cell Syst, 1, 417-425.

Liemann S., Chandran K., Baker T.S., Nibert M.L., Harrison S.C. (2002) Structure of the Reovirus Membrane-Penetration Protein, μ1, in a Complex with Its Protector Protein, σ3. Cell, 108, 283–295.

Lin J., Feng N., Sen A., Balan M., Tseng H.C., McElrath C., Smirnov S., Peng J., Yasukawa L.L., Durbin R.K., Durbin J.E., Greenberg H.B., Kotenko S. (2016) Distinct Roles of Type I and Type III Interferons in Intestinal Immunity to Homologous and Heterologous Rotavirus Infections. PLoS Pathog, 12, e1005600.

Lin X., Ginsburg G.S., Gilbert A.S., Halpin R.A., Das S.R., Lambkin-Williams R., Sobel Leonard A., Woods C.W., Illingworth C.J.R., McClain M.T., Smith G.J.D., Wentworth D.E., Koelle K., Ransier A., Stockwell T.B. (2017) The effective rate of influenza reassortment is limited during human infection. PLoS Pathog, 13, e1006203.

Linial, M. L. Miller, A. D. (1990) Retroviral RNA packaging: sequence requirements and implications. Curr Top Microbiol Immunol**,** 157, 125-152.

Loo Y-M., Fornek J., Crochet N., Bajwa G., Perwitasari O., Martinez-Sobrido L., Akira S., Gill M.A., Garcia-Sastre A., Katze M.G., Gale M. (2008) Distinct RIG-I and MDA5 Signaling by RNA Viruses in Innate Immunity. J Virol, 82, 335–345.

Lourenco S., Roy P. (2011) In vitro reconstitution of bluetongue virus infectious cores. Proc Natl Acad Sci, 108, 13746–13751.

Lowen A.C. (2018) It's in the mix: Reassortment of segmented viral genomes. PLoS Pathog, 14, e1007200.

Lu X., McDonald S.M., Tortorici M.A., Tao Y.J., Vasquez-Del Carpio R., Nibert M.L., Patton J.T., Harrison S.C. (2008) Mechanism for Coordinated RNA Packaging and Genome Replication by Rotavirus Polymerase VP1. Structure, 16, 1678–1688.

Lubeck M.D., Palese P., Schulman J.L. (1979) Nonrandom association of parental genes in influenza A virus recombinants. Virology, 95, 269-274.

Maeda K., Zachos N.C., Orzalli M.H., Schmieder S.S., Chang D., Gwilt K.B., Doucet M., Baetz N.W., Lee S., Crawford S.E., Estes M.K., Kagan J.C., Turner J.R., Lencer W.I. (2022) Depletion of the apical endosome in response to viruses and bacterial toxins provides cell-autonomous host defense at mucosal surfaces. Cell Host Microbe, 30, 216-231.

Mahlakõiv T., Hernandez P., Gronke K., Diefenbach A., Staeheli P. (2015) Leukocyte-Derived IFN-α/β and Epithelial IFN-λ Constitute a Compartmentalized Mucosal Defense System that Restricts Enteric Virus Infections. PLoS Pathog, 11, e1004782.

Marshall N., Priyamvada L., Ende Z., Steel J., Lowen A.C. (2013) Influenza virus reassortment occurs with high frequency in the absence of segment mismatch. PLoS Pathog, 9, e1003421.

Marzluff W.F., Koreski K.P. (2017) Birth and Death of Histone mRNAs. Trends Genet, 33, 745-759.

Marzluff W.F., Wagner E.J., Duronio R.J. (2008) Metabolism and regulation of canonical histone mRNAs: Life without a poly(A) tail. Nat Rev Genet, 9, 843-854.

Marzluff, W. F. Koreski, K. P. (2017) Birth and Death of Histone mRNAs. Trends Genet 33, 745-759.

Matthijnssens J., Heylen E., Zeller M., Rahman M., Lemey P., van Ranst M. (2010) Phylodynamic analyses of rotavirus genotypes G9 and G12 underscore their potential for swift global spread. Mol Biol Evol, 27, 2431–2436.

Matthijnssens J., van Ranst M. (2012) Genotype constellation and evolution of group A rotaviruses infecting humans. Curr Opin Virol, 2, 426–433.

Mccutcheon A.M., Broering T.J., Nibert M.L. (1999) Mammalian Reovirus M3 Gene Sequences and Conservation of Coiled-Coil Motifs near the Carboxyl Terminus of the μNS Protein. Virology, 264,16-24.

McDonald, S. M. Patton, J. T. (2011) Assortment and packaging of the segmented rotavirus genome. Trends Microbiol, 19, 136-44.

McDonald, S. M. Tao, Y. J. Patton, J. T. (2009) The ins and outs of four-tunneled Reoviridae RNA-dependent RNA polymerases. Curr Opin Struct Biol, 19, 775-82.

McDonald S.M., Nelson, M.I., Turner, P.E., Patton, J.T. (2016) Reassortment in segmented RNA viruses: mechanisms and outcomes. Nat Rev Microbiol, 14, 448-460.

Michel N., Allespach I., Venzke S., Fackler O.T., Keppler O.T. (2005) The Nef protein of human immunodeficiency virus establishes superinfection immunity by a dual strategy to downregulate cell-surface CCR5 and CD4. Curr Biol, 15, 714–723.

Midgley S.E., Bányai K., Buesa J., Halaihel N., Hjulsager C.K., Jakab F., Kaplon J., Larsen L.E., Monini M., Poljšak-Prijatelj M., Pothier P., Ruggeri F.M., Steyer A., Koopmans M., Böttiger B. (2012) Diversity and zoonotic potential of rotaviruses in swine and cattle across Europe. Vet Microbiol, 156, 238–245.

Mikuletič T., Steyer A., Kotar T., Zorec T.M., Poljak M. (2019) A novel reassortant mammalian orthoreovirus with a divergent S1 genome segment identified in a traveler with diarrhea. Infect Genet Evol, 73, 378–383.

Miller C.L., Arnold M.M., Broering T.J., Hastings C.E., Nibert M.L. (2010) Localization of mammalian orthoreovirus proteins to cytoplasmic factory-like structures via nonoverlapping regions of μNS. J Virol, 84, 867–882.

Miura K-I., Watanabe K., Sugiura M., Shatkin A.J. (1974) The 5'-terminal nucleotide sequences of the double-stranded RNA of human reovirus. Proc Nat Acad Sci, 71, 3979-3983.

Moreno-Contreras J., Sánchez-Tacuba L., Arias C.F., López S. (2022) Mature rotavirus particles contain equivalent amounts of 7me GpppGcap and noncapped viral positive-sense RNAs. bioRxiv, doi: 10.1101/2022.06.03.494783.

Morgan E.M., Zweerink H.J. (1975) Characterization of transcriptase and replicase particles isolated from reovirus-infected cells. Virology, 68,455-466.

Morin M., Warner A., Fields B. (1996) Reovirus Infection in Rat Lungs as a Model To Study the Pathogenesis of Viral Pneumonia. J Virol, 70, 541–548.

Naglič T., Rihtarič D., Hostnik P., Toplak N., Koren S., Kuhar U., Jamnikar-Ciglenečki U., Kutnjak D., Steyer A. (2018) Identification of novel reassortant mammalian orthoreoviruses from bats in Slovenia. BMC Vet Res, 14, 264.

Nanoyama M., Millward S., Graham A.F. (1974) Control of transcription of the reovirus genome. Nucleic Acids Res, 1, 373-386.

Neumann G., Noda T., Kawaoka Y. (2009) Emergence and pandemic potential of swine-origin H1N1 influenza virus. Nature, 459, 931-939.

Nibert M.L., Kim J., Broering T.J., Dinoso J.B., Miller C.L., Piggott C.D.S., Parker J.S.L. (2004) Reovirus nonstructural protein μNS recruits viral core surface proteins and entering core particles to factory-like inclusions. J Virol, 78, 1882–1892.

Nibert M.L., Kim J., Broering T.J., Dinoso J.B., Miller C.L., Piggott C.D.S., Parker J.S.L. (2004) Reovirus Nonstructural Protein μNS Recruits Viral Core Surface Proteins and Entering Core Particles to Factory-Like Inclusions. J Virol, 78, 1882–1892.

Nibert M.L., Margraf R.L., Coombs K.M. (1996) Nonrandom segregation of parental alleles in reovirus reassortants. J Virol, 70, 7295–7300.

Nikolic J., le Bars R., Lama Z., Scrima N., Lagaudrière-Gesbert C., Gaudin Y., Blondel D. (2017) Negri bodies are viral factories with properties of liquid organelles. Nat Commun, 8.

Nomikou K., Hughes J., Wash R., Kellam P., Breard E., Zientara S., Palmarini M., Biek R., Mertens P. (2015) Widespread reassortment shapes the evolution and epidemiology of bluetongue virus following european invasion. PLoS Pathog, 11, e1005056.

Nomikou K., Hughes J., Wash R., Kellam P., Breard E., Zientara S., Palmarini M., Biek R., Mertens P. (2015) Widespread Reassortment Shapes the Evolution and Epidemiology of Bluetongue Virus following European Invasion. PLoS Pathog, 11.

Novoa R.R., Calderita G., Cabezas P., Elliott R.M., Risco C. (2005) Key Golgi Factors for Structural and Functional Maturation of Bunyamwera Virus. J Virol, 79, 10852–10863.

Nunes M.R.T., Travassos da Rosa A.P.A., Weaver S.C., Tesh R.B., Vasconcelos P.F.C. (2005) Molecular epidemiology of group C viruses (*Bunyaviridae*, Orthobunyavirus) isolated in the Americas. J Virol, 79, 10561–10570.

Ogden K.M., Johne R., Patton J.T. (2012) Rotavirus RNA polymerases resolve into two phylogenetically distinct classes that differ in their mechanism of template recognition. Virology, 431, 50–57.

Ooms L.S., Kobayashi T., Dermody T.S., Chappell J.D. (2010) A post-entry step in the mammalian orthoreovirus replication cycle is a determinant of cell tropism. J Biol Chem, 285, 41604–41613.

Ooms, L. S. Jerome, W. G. Dermody, T. S. Chappell, J. D. (2012) Reovirus replication protein μ2 influences cell tropism by promoting particle assembly within viral inclusions. J Virol, 86, 10979-10987.

Palese P., Tobita K., Ueda M., Compans R.W. (1974) Characterization of temperature sensitive influenza virus mutants defective in neuraminidase. Virology, 61, 397-410.

Parashar U. (2003) Global Illness and Deaths Caused by Rotavirus Disease in Children. Emerg Infect Dis, 9, 565-572.

Parker, J. S. Broering, T. J. Kim, J. Higgins, D. E. Nibert, M. L. (2002) Reovirus core protein mu2 determines the filamentous morphology of viral inclusion bodies by interacting with and stabilizing microtubules. J Virol, 76, 4483-96.

Peterson S.T., Kennedy E.A., Brigleb P.H., Taylor G.M., Urbanek K., Bricker T.L., Lee S., Shin H., Dermody T.S., Boon A.C.M., Baldridge M.T. (2019) Disruption of Type III Interferon (IFN) Genes Ifnl2 and Ifnl3 Recapitulates Loss of the Type III IFN Receptor in the Mucosal Antiviral Response. J Virol, 93, e01073-19.

Philip, A. A. Perry, J. L. Eaton, H. E. Shmulevitz, M. Hyser, J. M. Patton, J. T. (2019) Generation of Recombinant Rotavirus Expressing NSP3-UnaG Fusion Protein by a Simplified Reverse Genetics System. J Virol, 93, e01616-19.

Phillips M.B., Dina Zita M., Howells M.A., Weinkopff T., Boehme K.W. (2021) Lymphatic type-1 interferon responses are critical for control of systemic reovirus dissemination. J Virol, 95, e02167-20.

Phipps K.L., Marshall N., Tao H., Danzy S., Onuoha N., Steel J., Lowen A.C. (2017) Seasonal H3N2 and 2009 Pandemic H1N1 Influenza A Viruses Reassort Efficiently but Produce Attenuated Progeny. J Virol, 91, e00830-17.

Postnikova Y., Treshchalina A., Boravleva E., Gambaryan A., Ishmukhametov A., Matrosovich M., Fouchier R.A.M., Sadykova G., Prilipov A., Lomakina N. (2021) Diversity and reassortment rate of influenza a viruses in wild ducks and gulls. Viruses, 13, 1010.

Pruijssers A.J., Hengel H., Abel T.W., Dermody T.S. (2013) Apoptosis Induction Influences Reovirus Replication and Virulence in Newborn Mice. J Virol, 87, 12980–12989.

Qin P., Li H., Wang J.W., Wang B., Xie R.H., Xu H., Zhao L.Y., Li L., Pan Y., Song Y., Huang Y.W. (2017) Genetic and pathogenic characterization of a novel reassortant mammalian orthoreovirus 3 (MRV3) from a diarrheic piglet and seroepidemiological survey of MRV3 in diarrheic pigs from east China. Vet Microbiol, 208, 126–136.

Quinlan, A. R. Hall, I. M. (2010) BEDTools: a flexible suite of utilities for comparing genomic features. Bioinformatics, 26, 841-842.

R. C. Condit. Principles of virology. Fields Virology 4th Edition. D.M.Knipe and P. M. Howley, Eds. 48–49, Lippincott Williams& Wilkins, Philadelphia, Pa, USA, 4th edition, 2001.

Ramig R.F. (1990) Superinfecting rotaviruses are not excluded from genetic interactions during asynchronous mixed infections in vitro. Virology, 176, 308-310.

Ramig R.F., Garrison C., Chen D., Bell-Robinson D. (1989) Analysis of reassortment and superinfection during mixed infection of vero cells with bluetongue virus serotypes 10 and 17. J Gen Virol, 70, 3355-3362.

Reinisch K.M., Nibert M.L., Harrison S.C. (2000) Structure of the reovirus core at 3.6 Å resolution. Nature, 404, 960-967.

Richard M., Herfst S., Tao H., Jacobs N.T., Lowen A.C., Schultz-Cherry S., Jude S. (2018) Influenza A Virus Reassortment Is Limited by Anatomical Compartmentalization following Coinfection via Distinct Routes. J Virol, 92, e02063-17.

Robinson, J. T. Thorvaldsdóttir, H. Winckler, W. Guttman, M. Lander, E. S. Getz, G. Mesirov, J. P. (2011) Integrative genomics viewer. Nat Biotechnol, 29, 24-26.

Robinson, M. D. McCarthy, D. J. Smyth, G. K. (2010) edgeR: a Bioconductor package for differential expression analysis of digital gene expression data.Bioinformatics, 26, 139-40.

Roebke K.E., Guo Y., Parker J.S.L., Danthi P. (2020) Reovirus σ3 Protein Limits Interferon Expression and Cell Death Induction. J Virol, 94, e01485-20.

Roner M.R., Sutphin L.A., Joklik, W.K. (1990) Reovirus RNA is infectious. Virology, 179, 845-852.

Roner, M. R. Bassett, K. Roehr, J. (2004) Identification of the 5' sequences required for incorporation of an engineered ssRNA into the Reovirus genome. Virology, 329, 348-60.

Roner, M. R. Joklik, W. K. (2001) Reovirus reverse genetics: Incorporation of the CAT gene into the reovirus genome. Proc Nat Acad Sci, 98, 8036-8041.

Roner, M. R. Roehr, J. (2006) The 3' sequences required for incorporation of an engineered ssRNA into the Reovirus genome. Virol J, 3, 1.

Roner, M. R. Steele, B. G. (2007) Features of the mammalian orthoreovirus 3 Dearing l1 single-stranded RNA that direct packaging and serotype restriction. J Gen Virol, 88, 3401-3412.

Roner, M. R. Steele, B. G. (2007) Localizing the reovirus packaging signals using an engineered m1 and s2 ssRNA. Virology, 358, 89-97.

Rosen, L. 1960. Serologic grouping of reoviruses by hemagglutination inhibition. Am J Hyg, 71, 242-249.

Routh, A. Domitrovic, T. Johnson, J. E. (2012) Host RNAs, including transposons, are encapsidated by a eukaryotic single-stranded RNA virus. Proc Nat Acad Sci, 109, 1907-1912.

Roy, P. (2017) Bluetongue virus structure and assembly. Curr Opin Virol, 24, 115-123.

Rubin, D.H., Kornstein M.J., Anderson A. (1985) Reovirus Serotype 1 Intestinal Infection: a Novel Replicative Cycle with Ileal Disease. J Virol, 53, 391-398.

Sabin, A.C. (1959) Reoviruses: A new group of respiratory and enteric viruses formerly classified as ECHO type 10 is described. Science, 130, 1387-1389.

Santos N., Lima R.C.C., Nozawa C.M., Linhares R.E., Gouvea V. (1999) Detection of Porcine Rotavirus Type G9 and of a Mixture of Types G1 and G5 Associated with Wa-Like VP4 Specificity: Evidence for Natural Human-Porcine Genetic Reassortment. J Clin Microbiol, 37, 2734-2736

Schindelin, J. Arganda-Carreras, I. Frise, E. Kaynig, V. Longair, M. Pietzsch, T. Preibisch, S. Rueden, C. Saalfeld, S. Schmid, B. Tinevez, J. Y. White, D. J. Hartenstein, V. Eliceiri, K. Tomancak, P. Cardona, A. (2012) Fiji: an open-source platform for biological-image analysis. Nat Methods 9, 676-82.

Scholtissek C. (1996) Molecular Evolution of Influenza Viruses. Virus Genes, 11, 209-215.

Shah, P. N. M. Stanifer, M. L. Höhn, K. Engel, U. Haselmann, U. Bartenschlager, R. Kräusslich, H. G. Krijnse-Locker, J. Boulant, S. (2017) Genome packaging of reovirus is mediated by the scaffolding property of the microtubule network. Cell Microbiol, 19, e12765.

Shatkin A.J., Roche A.J.L. (1972) Transcription by Infectious Subviral Particles of Reovirus. J Virol, 10, 698-706.

Shatkin A.J., Sipe J.D., Loh P. (1968) Separation of Ten Reovirus Genome Segments by Polyacrylamide Gel Electrophoresis. J Virol, 2, 986-991.

Sherry B., Torres J., Blum M.A. (1998) Reovirus Induction of and Sensitivity to Beta Interferon in Cardiac Myocyte Cultures Correlate with Induction of Myocarditis and Are Determined by Viral Core Proteins. J Virol, 72, 1314–1323.

Shrestha, N. Weber, P. H. Burke, S. V. Wysocki, W. P. Duvall, M. R. Bujarski, J. J. (2018) Next generation sequencing reveals packaging of host RNAs by brome mosaic virus. Virus Res, 252, 82-90.

Simonsen L., Viboud C., Grenfell B.T., Dushoff J., Jennings L., Smit M., Macken C., Hata M., Gog J., Miller M.A., Holmes E.C. (2007) The genesis and spread of reassortment human influenza A/H3N2 viruses conferring adamantane resistance. Mol Biol Evol, 24, 1811–1820.

Singh R., Suomalainen M., Varadarajan S., Garoff H, Helenius A. (1997) Multiple mechanisms for the inhibition of entry anduncoating of superinfecting Semliki Forest virus. Virology, 231, 59–71.

Skehel J.J., Joklik W.K. (1969) Studies on the *in vitro* transcription of reovirus RNA catalyzed by reovirus cores. Virology, 39, 822-831.

Smith G.J.D., Vijaykrishna D., Bahl J., Lycett S.J., Worobey M., Pybus O.G., Ma S.K., Cheung C.L., Raghwani J., Bhatt S., Peiris J.S.M., Guan Y., Rambaut A. (2009) Origins and evolutionary genomics of the 2009 swine-origin H1N1 influenza A epidemic. Nature, 459,1122–1125.

Smith, R. E. Zweerink, H. J. Joklik, W. K. (1969) Polypeptide components of virions, top component and cores of reovirus type 3. Virology, 39, 791-810.

Steel J., Lowen A.C. (2014) Influenza A virus reassortment. Curr Top Microbiol Immunol, 385, 377–401.

Stenglein M.D., Jacobson E.R., Chang L.W., Sanders C., Hawkins M.G., Guzman D.S.M., Drazenovich T., Dunker F., Kamaka E.K., Fisher D., Reavill D.R., Meola L.F., Levens G., DeRisi J.L. (2015) Widespread recombination, reassortment, and transmission of unbalanced compound viral genotypes in natural arenavirus infections. PLoS Pathog, 11, e1004900.

Stuart J.D., Holm G.H., Boehme K.W. (2018) Differential delivery of genomic dsRNA causes reovirus strain-specific differences in IRF3 activation. J Virol, 92, e01947-17.

Sung P.Y., Roy P. (2014) Sequential packaging of RNA genomic segments during the assembly of bluetongue virus. Nucleic Acids Res, 42, 13824–13838.

Sutton, G. Sun, D. Fu, X. Kotecha, A. Hecksel, C. W. Clare, D. K. Zhang, P. Stuart, D. I. Boyce, M. (2020) Assembly intermediates of orthoreovirus captured in the cell. Nat Commun 11, 4445.

Tai J.H., Williams J., Edwards K.M., Wright P.F., Crowe J.E., Dermody T.S. (2005) Prevalence of Reovirus-Specific Antibodies in Young Children in Nashville, Tennessee. J Infect Dis, 191, 1221–1224.

Tao H., Steel J., Lowen A.C. (2014) Intrahost Dynamics of Influenza Virus Reassortment. J Virol, 88, 7485–7492.

Tao Y., Farsetta D.L., Nibert M.L., Harrison S.C. (2002) RNA Synthesis in a Cage-Structural Studies of Reovirus Polymerase λ3. Cell, 111, 733–745.

Taraporewala, Z. F. Patton, J. T. (2004) Nonstructural proteins involved in genome packaging and replication of rotaviruses and other members of the Reoviridae. Virus Res 101, 57-66.

Taterka J., Cebra J.J., Rubin D.H. (1995) Characterization of Cytotoxic Cells from Reovirus-Infected SCID Mice: Activated Cells Express Natural Killer-and Lymphokine-Activated Killer-Like Activity but Fail To Clear Infection. J Virol, 69, 3910–3914.

Telesnitsky, A. Wolin, S. L. (2016) The Host RNAs in Retroviral Particles. Viruses, 8.

Teodoroff T.A., Tsunemitsu H., Okamoto K., Katsuda K., Kohmoto M., Kawashima K., Nakagomi T., Nakagomi O. (2005) Predominance of porcine rotavirus G9 in Japanese piglets with diarrhea: Close relationship of their VP7 genes with those of recent human G9 strains. J Clin Microbiol, 43, 1377–1384.

Twigger K., Vidal L., White C.L., de Bono J.S., Bhide S., Coffey M., Thompson B., Vile R.G., Heinemann L., Pandha H.S., Errington F., Melcher A.A., Harrington K.J. (2008) Enhanced in vitro and in vivo cytotoxicity of combined reovirus and radiotherapy. Clin Cancer Res, 14, 912–923.

Tyler K.L. 1991. Pathogenesis of reovirus infections of the central nervous system. Semin Neurosci, 3, 117-124.

Tyler K.L., Squier M.K.T., Brown A.L., Pike B., Willis D., Oberhaus S.M., Dermody T.S., Cohen J.J.(1996) Linkage between reovirus-induced apoptosis and inhibition of cellular DNA synthesis: Role of the S1 and M2 Genes. J Virol, 70, 7984–7991.

Urquidi V., Bishop D.H.L. (1992) Non-random reassortment between the tripartite RNA genomes of La Crosse and snowshoe hare viruses. J Gen Virol, 73, 2255-2226.

van Buuren N., Kirkegaard K. (2018) Detection and differentiation of multiple viral RNAs using branched DNA FISH coupled to confocal microscopy and flow cytometry. Bio Protoc, 8, doi:10.21769/BioProtoc.3058.

Vignuzzi, M. López, C. B. (2019) Defective viral genomes are key drivers of the virus-host interaction. Nat Microbiol, 4, 1075-1087.

Villa M., Lässig M. (2017) Fitness cost of reassortment in human influenza. PLoS Pathog, 13, e1006685.

Vlasak R., Luytjes W., Leider J., Spaan W., Palese P. (1988) The E3 protein of bovine coronavirus is a receptor-destroying enzyme with acetylesterase activity. J Virol, 62, 4686-4690.

Wang L., Fu S., Cao L., Lei W., Cao Y., Song J., Tang Q., Zhang H., Feng Y., Yang W., Liang G. (2015) Isolation and Identification of a Natural Reassortant Mammalian Orthoreovirus from Least Horseshoe Bat in China. PLoS One, 10, e0118598.

Watanabe Y., Millward S., Graham A.F. (1968) Regulation of transcription of the reovirus genome. J Mol Biol, 36, 107-123.

Weiner H.L., Drayna D., Averill D.R., Fields B.N. (1977) Molecular basis of reovirus virulence: Role of the SI gene. Proc Natl Acad Sci, 74, 5744-5748.

Wenske E.A., Chanock S.J., Krata L., Fields B.N. (1985) Genetic Reassortment of Mammalian Reoviruses in Mice. J Virol, 56, 613-616.

Weyer C.T., Grewar J.D., Burger P., Rossouw E., Lourens C., Joone C., le Grange M., Coetzee P., Venter E., Martin D.P., Maclachlan N.J., Guthrie A.J. (2016) African horse sickness caused by genome reassortment and reversion to virulence of live, attenuated vaccine viruses, South Africa, 2004–2014. Emerg Infect Dis, 22, 2087–2096.

White M.C., Lowen A.C. (2018) Implications of segment mismatch for influenza A virus evolution. J Gen Virol, 99, 3–16.

White M.C., Steel J., Lowen A.C. (2017) Heterologous packaging signals on segment 4, but not segment 6 or segment 8, limit influenza A virus reassortment. J Virol, 91, e00195-17.

Wichgers Schreur P.J., Kormelink R., Kortekaas J. (2018) Genome packaging of the Bunyavirales. Curr Opin Virol, 33, 151–155.

Wichgers Schreur P.J., Kortekaas J. (2016) Single-Molecule FISH Reveals Non-selective Packaging of Rift Valley Fever Virus Genome Segments. PLoS Pathog, 12, e1005800.

Wildum S., Schindler M., Münch J., Kirchhoff F. (2006) Contribution of Vpu, Env, and Nef to CD4 Down-Modulation and Resistance of Human Immunodeficiency Virus Type 1-Infected T Cells to Superinfection. J Virol, 80, 8047–8059.

Wu A.G., Pruijssers A.J., Brown J.J., Stencel-Baerenwald J.E., Sutherland D.M., Iskarpatyoti J.A., Dermody T.S. (2018) Age-dependent susceptibility to reovirus encephalitis in mice is influenced by maturation of the type-I interferon response. Pediatr Res, 83, 1057–1066.

Yang J.R., Lin Y.C., Huang Y.P., Su C.H., Lo J., Ho Y.L., Yao C.Y., Hsu L.C., Wu H.S., Liu M.T. (2011) Reassortment and mutations associated with emergence and spread of oseltamivir-resistant seasonal influenza A/H1N1 viruses in 2005-2009. PLoS One, 6, e18177.

Yu, G. Wang, L. G. Han, Y. He, Q. Y. (2012) clusterProfiler: an R package for comparing biological themes among gene clusters. OMICS J Integr Biol 16, 284-7.

Zamora P.F., Hu L., Knowlton J.J., Lahr R.M., Moreno R.A., Berman A.J., Prasad B.V.V., Dermody T.S. (2018) Reovirus Nonstructural Protein σNS Acts as an RNA Stability Factor Promoting Viral Genome Replication. J Virol, 92, e00563-18.

Zarbl H., Skup D., Millward S. (1980) Reovirus progeny subviral particles synthesize uncapped mRNA. J Virol, 34, 497-505.

Zhang X., Walker S.B., Chipman P.R., Nibert M.L., Baker T.S. (2003) Reovirus polymerase λ3 localized by cryo-electron microscopy of virions at a resolution of 7.6 Å. Nat Struct Biol, 10, 1011–1018.

Zhang Y., Liu Y., Lian H., Zhang F., Zhang S., Hu R. (2016) A natural reassortant and mutant serotype 3 reovirus from mink in China. Arch Virol, 161, 495–498.

Zhang, X. Walker, S. B. Chipman, P. R. Nibert, M. L. Baker, T. S. (2003) Reovirus polymerase lambda 3 localized by cryo-electron microscopy of virions at a resolution of 7.6 A. Nat Struct Biol, 10, 1011-8.

Zhu F.X., Sathish N., Yuan Y. (2010) Antagonism of host antiviral responses by Kaposi's sarcoma-associated herpesvirus tegument protein ORF45. PLoS One, 5, e10573.

Zou G., Zhang B., Lim P., Yuan Z., Bernard K.A., Shi P. (2009) Exclusion of West Nile virus superinfection through RNA replication. J Virol, 83, 11765–11776.

Zou, S. Brown, E. G. (1992) Identification of sequence elements containing signals for replication and encapsidation of the reovirus M1 genome segment. Virology, 186, 377-388.

Zurney J., Kobayashi T., Holm G.H., Dermody T.S., Sherry B. (2009) Reovirus μ2 protein inhibits interferon signaling through a novel mechanism involving nuclear accumulation of interferon regulatory factor 9. J Virol, 83, 2178-2187.

Zwart M.P., Elena S.F. (2015) Matters of Size: Genetic Bottlenecks in Virus Infection and Their Potential Impact on Evolution. Annu Rev Virol, 2, 161–179.